National Research Council Canada
Conseil national de recherches Canada

A STUDY OF TRANSONIC FLUTTER OF A TWO-DIMENSIONAL AIRFOIL USING THE U-g AND p-k METHODS

by

B.H.K. Lee
National Aeronautical Establishment

OTTAWA
NOVEMBER 1984

AERONAUTICAL REPORT
LR-615
NRC NO. 23959

Canada

NATIONAL AERONAUTICAL ESTABLISHMENT

SCIENTIFIC AND TECHNICAL PUBLICATIONS

AERONAUTICAL REPORTS:

Aeronautical Reports (LR): Scientific and technical information pertaining to aeronautics considered important, complete, and a lasting contribution to existing knowledge.

Mechanical Engineering Reports (MS): Scientific and technical information pertaining to investigations outside aeronautics considered important, complete, and a lasting contribution to existing knowledge.

AERONAUTICAL NOTES (AN): Information less broad in scope but nevertheless of importance as a contribution to existing knowledge.

LABORATORY TECHNICAL REPORTS (LTR): Information receiving limited distribution because of preliminary data, security classification, proprietary, or other reasons.

Details on the availability of these publications may be obtained from:

Publications Section,
National Research Council Canada,
National Aeronautical Establishment,
Bldg. M-16, Room 204,
Montreal Road,
Ottawa, Ontario
K1A 0R6

ÉTABLISSEMENT AÉRONAUTIQUE NATIONAL

PUBLICATIONS SCIENTIFIQUES ET TECHNIQUES

RAPPORTS D'AÉRONAUTIQUE

Rapports d'aéronautique (LR): Informations scientifiques et techniques touchant l'aéronautique jugées importantes, complètes et durables en termes de contribution aux connaissances actuelles.

Rapports de génie mécanique (MS): Informations scientifiques et techniques sur la recherche externe à l'aéronautique jugées importantes, complètes et durables en termes de contribution aux connaissances actuelles.

CAHIERS D'AÉRONAUTIQUE (AN): Informations de moindre portée mais importantes en termes d'accroissement des connaissances.

RAPPORTS TECHNIQUES DE LABORATOIRE (LTR): Informations peu disséminées pour des raisons d'usage secret, de droit de propriété ou autres ou parce qu'elles constituent des données préliminaires.

Les publications ci-dessus peuvent être obtenues à l'adresse suivante:

Section des publications
Conseil national de recherches Canada
Établissement aéronautique national
Im. M-16, pièce 204
Chemin de Montréal
Ottawa (Ontario)
K1A 0R6

A STUDY OF TRANSONIC FLUTTER OF A TWO-DIMENSIONAL AIRFOIL USING THE U-g AND p-k METHODS

UNE ÉTUDE SUR LES VIBRATIONS AÉROÉLASTIQUES EN RÉGIME TRANSSONIQUE D'UN PROFIL AÉRODYNAMIQUE BIDIMENSIONNEL AU MOYEN DES MÉTHODES U-g ET p-k

by/par

B.H.K. Lee

L.H. Ohman, Head/Chef
High Speed Aerodynamics Laboratory/
Laboratoire d'aérodynamique à hautes vitesses

G.M. Lindberg
Director/Directeur

SUMMARY

Transonic flutter of a NACA64A006 airfoil undergoing plunging and pitching oscillations is studied using the U-g and p-k methods. The aerodynamic coefficients are calculated using an improved version of an ONERA unsteady transonic aerodynamics code which include the second time derivative term of the velocity potential in the governing equation. Comparisons with LTRAN2-NLR show good agreement up to and in some cases exceeding $k_c = 0.4$, except for the pitching moment curves at the transonic dip Mach number of 0.85. All flutter results are presented for $M = 0.85$. The p-k method gives flutter speeds identical to those from the U-g method. Subcritical damping ratios using the U-g method with Frueh's and Miller's damping formula are quite close to those obtained from the p-k method, especially for large values of the airfoil-air mass ratio. Response of the airfoil to externally applied forces and moments is studied using the p-k method and a viscous damping model for coupled motions.

RÉSUMÉ

Il s'agit de l'étude des vibrations aéroélastiques en régime transsonique d'un profil NACA64A006 soumis à des oscillations dans le plan vertical au moyen des méthodes U-g et p-k. Les coefficients aérodynamiques sont calculés à partir d'une version améliorée du code des vitesses aérodynamiques instationnaires en régime transsonique de l'ONERA, laquelle a recours à la seconde dérivatif du temps du potentiel de la vitesse dans l'équation principale. Des comparaisons avec LTRAN2-NLR montrent que les valeurs obtenues sont conformes jusqu'à, et quelquefois surpassant, $k_c = 0.4$, sauf dans le cas des courbes de moment de tangage pour un nombre de Mach creux transsonic de 0.85. La méthode p-k fournit des vitesses de vibrations aéroélastiques identiques à celles de la méthode U-g. Des rapports d'amortissement moins critiques employés dans le cadre de la méthode U-g avec les formules d'amortissement de Frueh et de Miller sont très proches de ceux obtenus avec la méthode p-k, surtout pour les grandes valeurs de rapport de masse de profile-d'air. La réponse du profil à des forces et à des moments extérieurs est étudiée par la méthode p-k et un modèle d'amortissement visqueux pour les mouvements couplés.

CONTENTS

ILLUSTRATIONS

ILLUSTRATIONS (Cont'd)

ILLUSTRATIONS (Cont'd)

ILLUSTRATIONS (Cont'd)

SYMBOLS

Symbol	Definition
a_h	non-dimensional distance measured from midchord to elastic axis
b	semi-chord of airfoil
c	chord
C_p	pressure coefficient
C_{ℓ_h}	lift coefficient due to plunge
C_{ℓ_α}	lift coefficient due to pitch
C_{m_h}	moment coefficient due to plunge

SYMBOLS (Cont'd)

Symbol	Definition
C_{m_α}	moment coefficient due to pitch
g	structural damping coefficient
h	plunge displacement
k_c	reduced frequency $\omega c/U$
m	mass of airfoil per unit span
M	free stream Mach number
p	complex eigenvalue
$\bar{p}$	non-dimensional complex eigenvalue
q	dynamic pressure
Q_h	total forces
Q'_h	externally applied force
Q_α	total moment
Q'_α	externally applied moment
r_α	radius of gyration about elastic axis
t	time
U	free stream velocity
x_α	non-dimensional distance measured from elastic axis to center of mass
Z_h	defined in Equation 34
Z_α	defined in Equation 35
α	pitch angle
γ	damping ratio defined in Equation 18
ζ	damping ratio defined in Equation 31
ζ_h	viscous damping for plunging motion
ζ_α	viscous damping for pitching motion
λ	flutter eigenvalue defined in Equation 9

SYMBOLS (Cont'd)

Symbol	Definition
μ	airfoil-air mass ratio, $m/\pi\rho b^2$
ξ	non-dimensional displacement h/c
ρ	air density
ω	frequency
ω_h	uncoupled bending frequency
ω_α	uncoupled torsional frequency

A STUDY OF TRANSONIC FLUTTER OF A TWO-DIMENSIONAL AIRFOIL USING THE U-g AND p-k METHODS

1.0 INTRODUCTION

Two and three-degree-of-freedom transonic flutter of two-dimensional conventional and supercritical airfoils has been the subject of numerous investigations in recent years (Refs. 1-12). The drop in flutter velocity at transonic Mach number is an important factor in design of modern airfoils. In the past, before unsteady transonic computation codes were available, the flutter speed in the transonic range was estimated by extrapolating the subsonic and supersonic branches of the flutter curves. Among the methods for predicting unsteady transonic flow past oscillating airfoil (Refs. 13-19), those based on the transonic small disturbance equation are most efficient, and hence are widely used in flutter calculations of two-dimensional airfoils.

Two approaches have been employed in the analysis of transonic flutter. The first utilizes the conventional U-g method (Ref. 20). The aerodynamic lift and moment coefficients are determined from transonic flow calculations and the structural equations are solved for the flutter velocity (Refs. 1-5). Airfoils that have been studied include NACA64A006, NACA64A010 and MBB A-3 with variations in parameters such as mass ratio, center of mass location, frequency ratio, etc.

The second approach determines the aeroelastic responses by coupling aerodynamic computation codes with structural equations of motion using a variety of numerical integration techniques (Refs. 6-12). Such an approach was first taken by Ballhaus and Goorjian (Ref. 6) who carried out the aeroelastic response of a NACA64A006 airfoil with a single degree-of-freedom in pitch. Extensions of this procedure to two and three-degree-of-freedom and other airfoils such as NACA64A010 and MBB A-3 have been reported by Yang et al. (Refs. 8-10).

The original finite-difference scheme for solving the transonic small disturbance equation, called LTRAN2 by Ballhaus and Goorjian (Ref. 16), is accurate only at low reduced frequencies ($k_c < 0.075$). Houwink and van der Vooren (Ref. 17) improved this code by retaining the time-derivative terms in the boundary and auxiliary conditions. Their modified code called LTRAN2-NLR claimed accuracy up to $k_c = 0.4$. Similar modifications have also been carried out by Couston and Angelini (Ref. 18) at ONERA. Further improvements have been reported by Rizzetta and Chin (Ref. 19) who retained the second time-derivative term of the velocity potential in the governing equation and presented results for a NACA64A10 airfoil with flap oscillations up to reduced frequency of 5. Isogai (Ref. 5) developed a similar computation code, and claimed accuracy up to $k_c = 0.25$ for the entire transonic Mach number range (from subcritical Mach number to above Mach number 1). Similar improvements to the Couston's and Angelini's code (Ref. 18) have been carried out at ONERA, and this code has been made available to NAE. Minor modifications (Ref. 21) have been made and these included addition of some graphics for the output data. The use of these various modified or improved unsteady transonic aerodynamic codes in flutter analysis can be found in References 1-13.

The U-g method gives critical flutter speeds in agreement with other methods such as the traditional British approach with lined-up frequency parameters, but overestimates the relative damping ratio at other speeds (Ref. 22). The use of Frueh's and Miller's (Ref. 23) correction formula for damping gives useful values of the decay factors, but Woodcock and Lawrence (Ref. 24) found the U-g method is still inferior to the British method. Hassig (Ref. 25) developed a method which gives damping values in excellent agreement with the British method. The p-k method, as called by Hassig (Ref. 25), iterates for the zeros of the flutter determinant using values of the aerodynamics interpolated from given values at a set of frequency parameters. This method assumes that for sinusoidal motions with slowly varying amplitude, the aerodynamic forces can be approximated by those based on constant amplitude.

The use of time marching techniques which couple the aerodynamics with the structural equations of motion should give accurate results for the critical flutter speeds and damping ratios at other speeds. However, this method is time consuming and is not suited for flutter analysis where many parameters such as mass ratio, frequency ratio, etc. are varied.

The first part of this report presents aerodynamics data of a NACA64A006 airfoil oscillating in pitch and plunge using the high frequency version of ONERA unsteady transonic code. The results are compared with those obtained by Yang and Chen (Ref. 9) employing LTRAN2-NLR. To the best of the author's knowledge, data from the ONERA code have not been reported by ONERA in the open literature. They are, therefore, presented in somewhat detailed manner in this report. From the aerodynamics obtained from the ONERA code, the U-g method is used to compute critical flutter speeds and damping ratios for a two-degree-of-freedom NACA64A006 airfoil using Frueh's and Miller's formula (Ref. 23). The results using the p-k method are compared with those from the U-g method. Response curves from the p-k method and those using a viscous damping model for coupled motions are also included for forced sinusoidal motion.

2.0 FLUTTER ANALYSIS OF TWO-DEGREE-OF-FREEDOM AIRFOIL MOTION

Figure 1 shows the notations used in the analysis of a two-degree-of-freedom motion of an airfoil oscillating in pitch and in plunge. The bending deflection is denoted by h, positive in the downward direction. α is the pitch angle about the elastic axis, positive with the nose up. The elastic axis is located at a distance $a_h b$ from the midchord, while the mass center is located at a distance $x_\alpha b$ from the elastic axis. Both distances are positive when measured towards the trailing edge of the airfoil. The aeroelastic equations of motion have been derived by Fung (Ref. 20) and can be written as:

$$\ddot{\xi} + x_\alpha \ddot{\alpha} + \omega_h^2 \xi = \frac{Q_h}{mb} \tag{1}$$

$$x_\alpha \ddot{\xi} + r_\alpha^2 \ddot{\alpha} + r_\alpha^2 \omega_\alpha^2 \alpha = \frac{Q_\alpha}{mb^2} \tag{2}$$

where $\xi = h/b$ is the non-dimensional displacement, m is the mass per unit span of the airfoil, ω_h, ω_α are the uncoupled plunging and pitching frequency respectively, r_α is the radius of gyration about the elastic axis, and Q_h and Q_α are the total forces and moments acting about the elastic axis respectively. In the absence of externally applied forces and moments, Q_h and Q_α can be written as:

$$Q_h = -qc \left(C_{\ell_h} \frac{\xi}{2} + C_{\ell_\alpha} \alpha \right) \tag{3}$$

$$Q_\alpha = qc^2 \left(C_{m_h} \frac{\xi}{2} + C_{m_\alpha} \alpha \right) \tag{4}$$

where q is the dynamic pressure, C_ℓ and C_m are the lift and moment coefficients with the subscripts h and α denoting unit plunging and pitching motions respectively.

2.1 The U-g Method

In the U-g method, a structural damping coefficient g is introduced into Equations (1) and (2) by multiplying the third term of the two equations by the factor (1 + ig). For harmonic oscillations, ξ and α can be written in the following form:

$$\xi = \xi_o e^{i\omega t} \tag{5}$$

$$\alpha = \alpha_o e^{i\omega t} \tag{6}$$

Equations (1) and (2) can be expressed as:

$$\left[\frac{1}{4}\mu k_c^2 - \frac{C_{\ell_h}}{2\pi} - \lambda\left(\frac{\omega_h}{\omega_\alpha}\right)^2\right]\xi_o + \left[\frac{1}{4}\mu k_c^2 x_\alpha - \frac{C_{\ell_\alpha}}{\pi}\right]\alpha_o = 0 \tag{7}$$

$$\left[\frac{1}{4}\mu k_c^2 x_\alpha + \frac{C_{m_h}}{\pi}\right]\xi_o + \left[\frac{1}{4}\mu k_c^2 r_\alpha^2 + \frac{2C_{m_\alpha}}{\pi} - \lambda r_\alpha^2\right]\alpha_o = 0 \tag{8}$$

where $\mu = m/\pi b^2\rho$ is the airfoil-air mass ratio, $k_c = \omega c/U$ is the reduced frequency and

$$\lambda = \mu(1 + ig)\frac{\omega_\alpha^2 b^2}{U^2} \tag{9}$$

The complex eigenvalue λ can be solved from the following quadratic equation

$$A\lambda^2 + B\lambda + C = 0 \tag{10}$$

where

$$A = r_\alpha^2\left(\frac{\omega_h}{\omega_\alpha}\right)^2 \tag{11}$$

$$B = -\left(\frac{\omega_h}{\omega_\alpha}\right)^2 d - r_\alpha^2 a \tag{12}$$

$$C = ad - bc \tag{13}$$

$$a = \frac{1}{4}\mu k_c^2 - \frac{C_{\ell_h}}{2\pi} \tag{14}$$

$$b = \frac{1}{4}\mu k_c^2 x_\alpha - \frac{C_{\ell_\alpha}}{\pi} \tag{15}$$

$$c = \frac{1}{4}\mu k_c^2 x_\alpha + \frac{C_{m_h}}{\pi} \tag{16}$$

$$d = \frac{1}{4}\mu k_c^2 r_\alpha^2 + \frac{2C_{m_\alpha}}{\pi} \tag{17}$$

Hassig (Ref. 25), quoting from Frueh and Miller (Ref. 23), gives an expression for the damping ratio which is written in the present notations as:

$$\gamma = \frac{g}{2}\left[1 - \frac{2}{k_c}\frac{d\left(\frac{\omega}{\omega_\alpha}\right)}{d\left(\frac{U}{b\omega_\alpha}\right)}\right] \tag{18}$$

2.2 The p-k Method

Equations (5) and (6) can be written in the following form:

$$\xi = \xi_o e^{pt} \tag{19}$$

$$\alpha = \alpha_o e^{pt} \tag{20}$$

where $p = \beta + i\omega$, and β is the damping factor. Substituting into Equations (1) to (4) gives:

$$\left\{\bar{p}^2 + 4\left(\frac{\omega_h}{\omega_\alpha}\right)^2\left(\frac{b\omega_\alpha}{U}\right)^2 + \frac{2}{\pi\mu}C_{\ell_h}\right\}\xi_o + \left\{\bar{p}^2 x_\alpha + \frac{4}{\pi\mu}C_{\ell_\alpha}\right\}\alpha_o = 0 \tag{21}$$

$$\left\{\bar{p}^2 x_\alpha - \frac{4}{\pi\mu}C_{m_h}\right\}\xi_o + \left\{r_\alpha^2\bar{p}^2 + 4r_\alpha^2\left(\frac{b\omega_\alpha}{U}\right)^2 - \frac{8}{\pi\mu}C_{m_\alpha}\right\}\alpha_o = 0 \tag{22}$$

where $\bar{p} = \frac{c}{U} \cdot p$, and can be solved from the following:

$$D\bar{p}^4 + E\bar{p}^2 + F = 0 \tag{23}$$

where

$$D = r_\alpha^2 - x_\alpha^2 \tag{24}$$

$$E = \bar{d} + \bar{a}r_\alpha^2 - x_\alpha (\bar{c} + \bar{b}) \tag{25}$$

$$F = \bar{a}\bar{d} - \bar{b}\bar{c} \tag{26}$$

$$\bar{a} = 4\left(\frac{\omega_h}{\omega_\alpha}\right)^2 \left(\frac{b\omega_\alpha}{U}\right)^2 + \frac{2}{\pi\mu} C_{\ell_h} \tag{27}$$

$$\bar{b} = \frac{4}{\pi\mu} C_{\ell_\alpha} \tag{28}$$

$$\bar{c} = -\frac{4}{\pi\mu} C_{m_h} \tag{29}$$

$$\bar{d} = 4r_\alpha^2\left(\frac{b\omega_\alpha}{U}\right)^2 - \frac{8}{\pi\mu} C_{m_\alpha} \tag{30}$$

The damping ratio ζ is given as:

$$\zeta = -\frac{\beta}{\sqrt{\beta^2 + \omega^2}} \tag{31}$$

2.3 Viscous Damping Model for Coupled Motions

In the study of the dynamic response of a wing to random loads or buffeting, a viscous damping force is often used in the structural equations of motion in place of the aerodynamic damping force, and the damping ratio is obtained from flutter calculations (see, for example, Ref. 26). Introducing a viscous damping term in Equations (1) and (2), and assuming harmonic motion of the form given in Equations (5) and (6), the structural equations of motion are:

$$Z_h(\omega)\,\xi_o - \omega^2\, x_\alpha\, \alpha_o = \frac{Q_h}{mb} \tag{32}$$

$$-\omega^2 x_\alpha \xi_0 + r_\alpha^2 Z_\alpha(\omega)\alpha_0 = \frac{Q_\alpha}{mb^2} \tag{33}$$

where

$$Z_h(\omega) = \omega_h^2 - \omega^2 + i\,2\zeta_h \omega_h \omega \tag{34}$$

$$Z_\alpha(\omega) = \omega_\alpha^2 - \omega^2 + i\,2\xi_\alpha \omega_\alpha \omega \tag{35}$$

ζ_h and ζ_α are the damping ratios for plunging and pitching motions. Equations (32) and (33) can be used to study the response of the airfoil to external loads.

3.0 RESULTS AND DISCUSSIONS

3.1 Aerodynamic Coefficients

In this study only two-degree-of-freedom motions in pitch and plunge are considered. The aerodynamic coefficients presented are those for lift and moment due to unit plunge displacement and pitch rotation respectively, namely, C_{ℓ_h}, C_{m_h}, C_{ℓ_α}, and C_{m_α}. The computations are performed using the ONERA improved version of Couston's and Angelini's (Ref. 18) unsteady transonic aerodynamics code. The results for a NACA64A006 airfoil are presented herein in a somewhat detailed manner since it does not appear that computations using this computer code have been compared with other transonic codes and reported in the open literature.

In Figures 2 to 13, C_{ℓ_h}, C_{m_h}, C_{ℓ_α}, and C_{m_α} are plotted versus k_c for Mach numbers M = 0.8, 0.85 and 0.875. The amplitudes for the plunging and pitching motions are h/c = 0.04 and α = 0.1 deg. respectively, and the pitch axis is located at the 1/4 chord point. The results are computed up to a value of k_c = 2. Shown also in the figures are computations by Yang and Chen (Ref. 9) using LTRAN2-NLR which is claimed to be accurate up to k_c = 0.4. The results from the ONERA code agree quite well with LTRAN2-NLR up to and in some cases exceeding k_c = 0.4, except for the C_{m_α} curves (especially the imaginary part) at M = 0.85. At higher frequencies, LTRAN2-NLR is not accurate since, unlike the ONERA code, the second time derivative of the velocity potential term has not been included in the governing equation.

The four aerodynamic coefficients are plotted versus Mach number in Figures 14 to 17 for reduced frequency k_c = 0.1 and 0.2. It is seen that at M = 0.85 there are large changes in the aerodynamic coefficients, especially the moment coefficients. This Mach number coincides with the transonic dip observed for the NACA64A006 airfoil by Yang et al. (Refs. 1, 2). At M = 0.7 and 0.8 the flow past the airfoil contains no shock waves. At M = 0.85, Fig. 18 shows that a shock wave is present for part of a plunge cycle at k_c = 0.5. The results are typical up to a value of k_c approximately 1.4, above which a shock wave is present for the full cycle as shown in Figure 19 for k_c = 2. The shock positions* for the third and fourth cycles of computations are shown in Figure 20 for k_c = 0.5 and 2.0. It is seen that at low frequencies, the shock movements are much larger than those at higher frequencies.

For plunging motions, C_p plots for the upper surface of the airfoil at M = 0.85 for the third and fourth cycles of computations are shown in Figure 21 for k_c = 0.5 and 2.0. The numbers from 3 to 29 marked on the curves represent computation grid points, and their distances from the leading edge non-dimensionalized w.r.t. the chord are given in Table 1. Because of the interrupted shock wave

*The shock positions are determined, according to Reference 21, from grid points where $\Delta Cp/\Delta x$ is a maximum, while also satisfying the criterion $\Delta Cp/\Delta x > 2$.

motions at low frequencies, shown for example in Figure 21 ($k_c = 0.5$), the pressures in the region behind the shock show irregular oscillations. At higher frequencies, when shock waves are presented at all times in a plunge cycle (Fig. 21, $k_c = 2.0$), the pressures behind the shock oscillates sinusoidally.

Results for pitch oscillations similar to those presented in Figures 18 to 21 are not reported in this report. For a NACA64A010 airfoil, Isogai (Ref. 5) gives some quite detailed results for pitching motion.

3.2 Flutter Analysis of NACA64A006 Airfoil

Flutter calculations using the ONERA unsteady transonic aerodynamics code are compared in Figure 22 with those obtained by Yang et al. (Ref. 1) using an implicit scheme (Ref. 6) and a relaxation approach (Refs. 14, 15) for the aerodynamic coefficients. In this figure, the U-g method is used and the flutter speed $U/b\omega_\alpha$, reduced frequency k_c and frequency ratio ω/ω_α are plotted against airfoil-air mass ratio μ. The Mach number is 0.85, and the following parameters are used: $x_\alpha = 0.25$, $r_\alpha = 0.5$, $\omega_h/\omega_\alpha = 0.2$, pitch axis = 0.25 ($a_h = -0.5$), which are the ones used by Yang et al. (Ref. 1). This figure shows lower flutter speeds using ONERA code than those from Reference 6, except at a mass ratio of 50. The present results can be taken to be more accurate than Reference 1 since the aerodynamics are improved by taking the second time derivative of the velocity potential in the governing equation. The aerodynamic coefficients are in good agreement with LTRAN2-NLR (see Figs. 6 to 9) in the range of values for k_c between 0.1 and 0.2 where flutter speeds are calculated. Comparisons of the aerodynamics from the indicial and relaxation methods given in Reference 2 with either the LTRAN2-NLR or the present results show the relaxation approach yields closer agreement than the indicial method which gives much poorer results especially for the C_{ℓ_α} and C_{m_α} coefficients.

The effect of μ on the damping and frequency ratios are shown in Figures 23 to 27 for $M = 0.85$. The results for ζ and γ of the two modes are computed using Equations (18) and (31). The critical flutter speeds and frequencies obtained from both methods are identical. For the bending mode, the differences in subcritical damping and frequency ratios between the p-k and U-g methods decrease for increasing μ. At $\mu = 250$, these two methods give almost identical results. For the torsion mode, the differences between ζ and γ increase with μ while the differences in ω_2/ω_α decrease. The fairly good agreement between the two methods may be a special case for a two-degree-of-freedom two-dimensional airfoil motion. Results for subcritical damping from Reference 24 show poor comparison between the U-g and the British method with lined-up frequency parameter, which has in turn been demonstrated by Hassig (Ref. 25) to be in good agreement with the p-k method.

3.3 Response of Airfoil to External Excitations

To investigate the response of the airfoil as the flutter speed is approached, ξ and α are solved from Equations (1) and (2) for two cases: $Q'_\alpha = 0$ and $Q'_h = 0$, where Q'_α and Q'_h are the externally applied sinusoidal excitation moment and force at the airfoil's elastic axis respectively. Using the p-k method, the amplitude and phase of $\xi_o \dfrac{mb\omega_\alpha^2}{Q'_h}$ and $\alpha_o \dfrac{mb\omega_\alpha^2}{Q'_h}$ for $Q'_\alpha = 0$ and $\xi_o \dfrac{mb^2\omega_\alpha^2}{Q'_\alpha}$ and $\alpha_o \dfrac{mb^2\omega_\alpha^2}{Q'_\alpha}$ for $Q'_h = 0$ are plotted against $\dfrac{\omega}{\omega_\alpha}$ and $U/b\omega_\alpha$ for $M = 0.85$ and $\mu = 100$ in Figures 28 to 35. For a purely translational excitation force, the displacement amplitude (Fig. 28) decreases with increasing values of $U/b\omega_\alpha$ until a minimum is reached around $U/b\omega_\alpha = 2.5$ to 3.0. Further increase in $U/b\omega_\alpha$ results in a rapid growth of the amplitude. The pitch amplitude (Fig. 30), shows a similar behaviour for ω/ω_α in the vicinity of the uncoupled bending frequency. The amplitude near the uncoupled torsional frequency decays as the flutter speed is approached. Figures 29 and 31 show the corresponding phase angles for displacement and pitch rotation respectively.

When a moment is applied at the elastic axis, the displacement increases rather gradually initially until $U/b\omega_\alpha$ approaches tne flutter speed (Fig. 32). Similar behaviour of the pitch amplitude near the uncoupled bending frequency is shown in Figure 34. The peak response near $\omega/\omega_\alpha = 1$ decays from large values at small $U/b\omega_\alpha$ to very small values as $U/b\omega_\alpha$ approaches the critical value. The phase angles for the displacement and pitch response are shown in Figures 33 and 35.

In Section 2.3 a viscous damping model for the airfoil motion is given. In the study of dynamic response of wing to external loads, such as buffeting, often the aerodynamic damping is combined with the structural damping to yield a total damping proportional to the velocity (see, for example, Ref. 27). The damping values can be determined either experimentally or from flutter calculations, such as the p-k method. Figures 36 to 43 show the displacement and pitch response of a NACA64A006 airfoil at M = 0.85 and $\mu = 100$. The values of ζ_h, ζ_α and ω_h/ω_α are obtained for $U/b\omega_\alpha = 4$ using the p-k method. Curves for other values of $U/b\omega_\alpha$ are quite similar to those shown in these figures. For a translational excitation force ($Q'_\alpha = 0$), Figures 36 to 39 show the viscous damping and p-k methods give quite similar response curves. However, when the external excitation is a moment applied at the elastic axis ($Q'_h = 0$), Figures 40 and 42 show the large response obtained near the uncoupled bending frequency from the p-k method cannot be duplicated using the viscous damping model, even though the response for pitching motion near the uncoupled torsional frequency agrees fairly well. The phase curves for the displacement show a difference of nearly 180 degrees between the two methods, while those for the pitch rotation are reasonably good except near the uncoupled bending frequency.

4.0 CONCLUSIONS

The improved version of ONERA unsteady transonic aerodynamics code, which include the second time derivative term of the velocity potential in the governing equation, has been used to compute aerodynamic coefficients for plunging and pitching motions of a NACA64A006 airfoil at various Mach numbers. The results agree quite well with LTRAN2-NLR up to and in some cases exceeding $k_c = 0.4$, except for the C_{m_α} curves (especially the imaginary part) at M = 0.85. This Mach number coincides with the transonic dip and large changes in the aerodynamic coefficients, especially the moment coefficients, are observed. Results of shock motions are given for the airfoil oscillating in plunge. At M = 0.85 and k_c below 1.4, computations show that a shock wave is present only for part of a plunge cycle. The shock motions are fairly large and the pressures in the region behind the shock show irregular oscillations.

Flutter speeds for a NACA64A006 airfoil using the U-g method and aerodynamic coefficients from ONERA code are lower than those reported by Yang et al. using LTRAN2. The comparisons are made at M = 0.85 for various airfoil-air mass ratios. The p-k method gives flutter speeds and k_c values identical to those from the U-g method. The computed subcritical damping ratios at M = 0.85 for different μ show the U-g method using Frueh's and Miller's formula gives results quite close to the p-k method, especially for large values of μ. The comparison is always very close for small values of $U/b\omega_\alpha$ irrespect of μ. The fairly good agreement between these two methods may be a special case for a two-degree-of-freedom two-dimensional airfoil performing plunging and pitching oscillations. Results for more complicated cases show that subcritical damping ratios obtained from the U-g method agree poorly with the British method with lined-up frequency parameters, which has in turn been demonstrated to be in good agreement with the p-k method.

The p-k method can be used to study the response of an airfoil to externally applied excitation forces and moments. Two examples are given for either a translational force or a moment applied at the elastic axis. Using the computed values of damping ratios ζ_h and ζ_α for the bending and torsion modes together with the ratio ω/ω_α, the response using a viscous damping model has been determined and compared with the p-k method. It is shown that for translational excitation force, the response curves for the two methods are in good agreement. However, when the external excitation is a moment applied at the elastic axis, the large response obtained near the uncoupled bending frequency from the p-k method cannot be duplicated using the viscous damping model, even though the response for pitching motion near the uncoupled torsional frequency agrees fairly well.

5.0 REFERENCES

1. Yang, T.Y.
   Guruswamy, P.
   Striz, A.G.
   Olsen, J.J.
   Flutter Analysis of a NACA64A006 Airfoil in Small Disturbance Transonic Flow.
   J. Aircraft, Vol. 17, No. 4, April 1980, pp. 225-232.

2. Yang, T.Y.
   Striz, A.G.
   Guruswamy, P.
   Flutter Analysis of Two-Dimensional and Two-Degree-of-Freedom Airfoils in Small-Disturbance Unsteady Transonic Flow.
   Flight Dynamics Laboratory, WPAFB, Ohio, AFFDL-TR-78-202, December 1978.

3. Traci, R.M.
   Albano, E.D.
   Farr, J.L.
   Small Disturbance Transonic Flows About Oscillating Airfoils and Planar Wings.
   Flight Dynamics Laboratory, WPAFB, Ohio, AFFDL-TR-75-100. June 1975.

4. Rizzetta, D.P.
   Transonic Flutter Analysis of a Two-Dimensional Airfoil.
   Flight Dynamics Laboratory, WPAFB, Ohio, AFFDL-TM-77-64-FBR, July 1977.

5. Isogai, K.
   Numerical Study of Transonic Flutter of a Two-Dimensional Airfoil.
   National Aerospace Laboratory, Chōfu, Tokyo, Japan, NAL-TR-617T, July 1980.

6. Ballhaus, W.F.
   Goorjian, P.M.
   Computation of Unsteady Transonic Flows by the Indicial Method.
   AIAA Journal, Vol. 16, Feb. 1978, pp. 117-124.

7. Rizzetta, D.P.
   Time-Dependent Response of a Two-Dimensional Airfoil in Transonic Flow.
   AIAA Journal, Vol. 17, Jan. 1979, pp. 26-32.

8. Yang, T.Y.
   Chen, C.H.
   Transonic Flutter and Response Analyses of Two 3-Degree-of-Freedom Airfoils.
   J. Aircraft, Vol. 19, Oct. 1982, pp. 875-884.

9. Yang, T.Y.
   Chen, C.H.
   Flutter and Time Response Analyses of Three Degrees of Freedom Airfoils in Transonic Flow.
   Flight Dynamics Laboratory, WPAFB, Ohio, AFWAL-TR-81-3103, Aug. 1981.

10. Yang, T.Y.
    Batina, J.T.
    Transonic Time-Response Analysis of 3-Degree-of-Freedom Conventional and Supercritical Airfoils.
    J. Aircraft, Vol. 20, Aug. 1983, pp. 703-710.

11. Carretta, C.
    Couston, M.
    Angelini, J.J.
    Simultaneous Resolution of Aerodynamic and Aeroelastic Equations of Motion for Transonic Two-Dimensional Airfoils.
    International Conf. on Numerical Methods for Coupled Problems, Swansea, 7-11 Sept. 1981.

12. Edwards, J.W.
    Bennett, R.M.
    Whitlow, Jr., W.
    Seidel, D.A.
    Time-Marching Transonic Flutter Solutions Including Angle-of-Attack Effects.
    J. Aircraft, Vol 20, Nov. 1983, pp. 899-906.

13. Magnus, R.
Yoshihara, H.
Unsteady Transonic Flows Over an Airfoil.
AIAA Journal, Vol. 13, Dec. 1975, pp. 1622-1628.

14. Farr, J.L.
Traci, R.M.
Albano, E.D
Computer Programs for Calculating Small Disturbance Transonic Flows About Oscillating Airfoils.
Flight Dynamics Laboratory, WPAFB, Ohio, AFFDL-TR-74-135, Nov. 1974.

15. Traci, R.M.
Albano, E.D.
Farr, J.L.
Perturbation Method for Transonic Flows About Oscillating Airfoils.
AIAA Journal, Vol. 14, Sept. 1976, pp. 1258-1265.

16. Ballhaus, W.F.
Goorjian, P.M.
Implicit Finite-Difference Computations of Unsteady Transonic Flow About Airfoils.
AIAA Journal, Vol. 15. Dec. 1977, pp. 1728-1735.

17. Houwink, R.
van der Vooren, J.
Improved Version of LTRAN2 for Unsteady Transonic Flow Computations.
AIAA Journal, Vol. 18, Aug. 1980, pp. 1008-1010.

18. Couston, M.
Angelini, J.J.
Numerical Solutions of Nonsteady Two-Dimensional Transonic Flows.
J. Fluids Engineering, Vol. 101, Sept. 1979, pp. 341-347.

19. Rizzetta, D.P.
Chin, W.C.
Effect of Frequency in Unsteady Transonic Flow.
AIAA Journal, Vol. 17, July 1979, pp. 779-781.

20. Fung, Y.C.
An Introduction to The Theory of Aeroelasticity, John Wiley & Sons, N.Y., 1955.

21. Jones, D.J.
Private Communication.

22. Lawrence, A.J.
Jackson, P.
Comparison of Different Methods of Assessing the Free Oscillatory Characteristics of Aeroelastic Systems.
RAE Technical Report 68296 (ARC CP 1084), 1968.

23. Frueh, F.J.
Miller, J.M.
Prediction of Damping Response from Flutter Analysis Solutions.
Air Force Office of Scientific Research, Arlington, Va., Rept. 65-0952, June 1965.

24. Woodcock, D.L.
Lawrence, A.J.
Further Comparisons of Different Methods of Assessing the Free Oscillatory Characteristics of Aeroelastic Systems.
RAE Technical Rept. 72188, Dec. 1972.

25. Hassig, H.J.
An Approximate True Damping Solution of the Flutter Equation by Determinant Iteration.
J. Aircraft, Vol. 8, Nov. 1971, pp. 885-889.

26. Mullans, R.E.
Lemley, C.E.
Buffet Dynamic Loads During Transonic Maneuvers.
Flight Dynamics Laboratory, WPAFB, Ohio, AFFDL-TR-72-46, Sept. 1972.

27. Jones, J.G.
A Survey of the Dynamic Analysis of Buffeting and Related Phenomena.
Royal Aircraft Establishment, RAE TR72197, Feb. 1973.

TABLE 1

DISTANCES FROM LEADING EDGE FOR C_p PLOTTED IN FIGURE 21

Position	x/c	Position	x/c
3	0.04029	17	0.5769
5	0.08516	19	0.6712
7	0.1410	21	0.7546
9	0.2079	23	0.8269
11	0.2857	25	0.8883
13	0.3745	27	0.9386
15	0.4744	29	0.9780

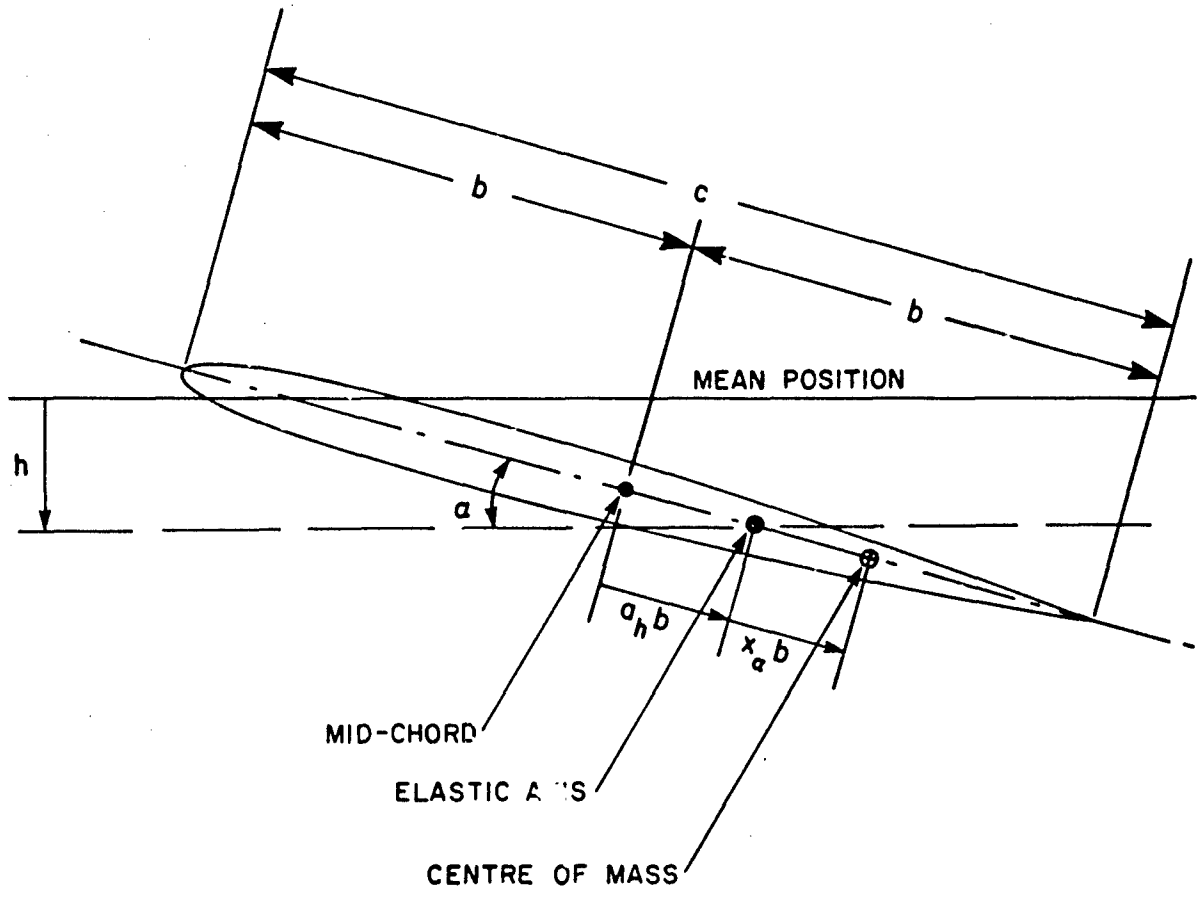

FIG. 1: TWO-DEGREE-OF-FREEDOM AIRFOIL MOTION

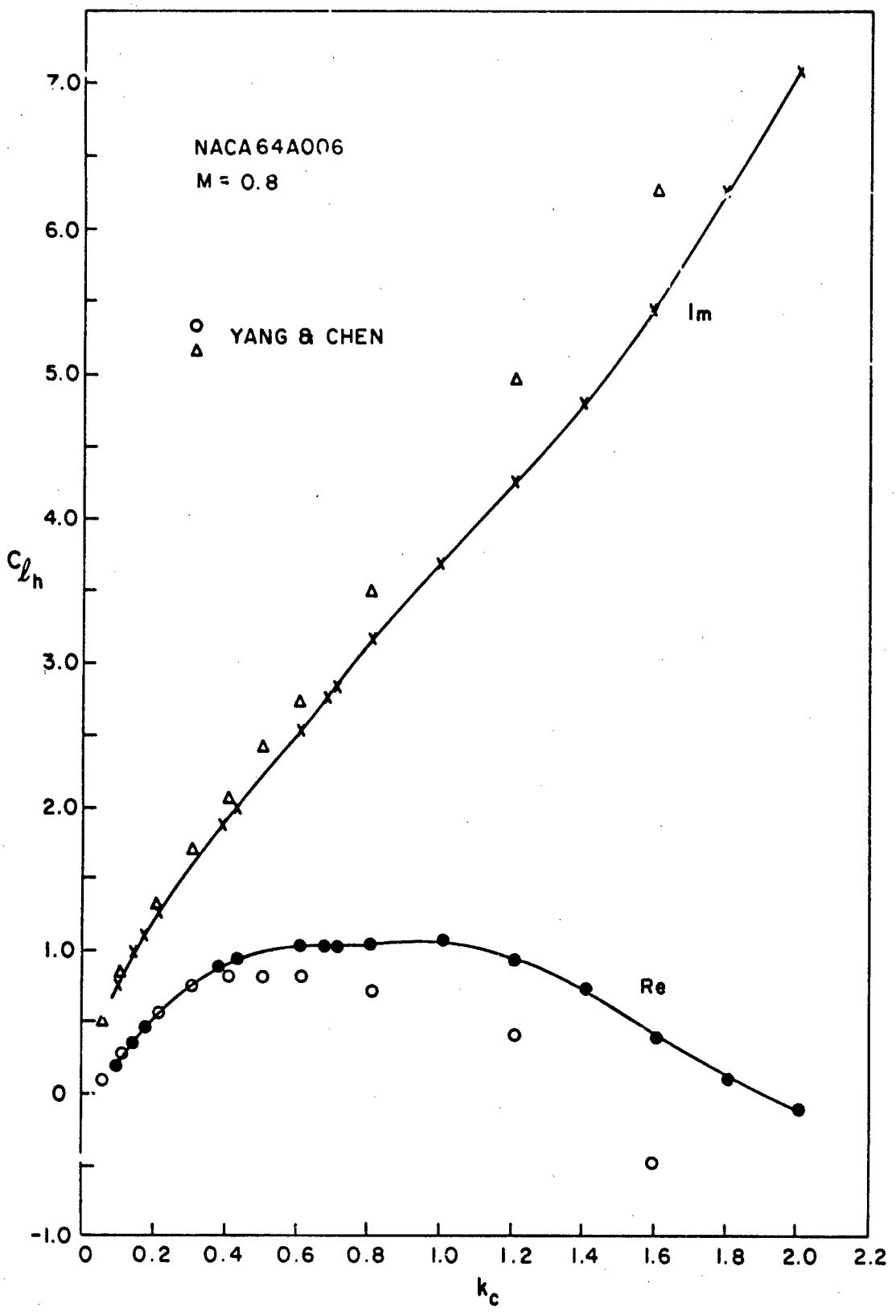

FIG. 2: VARIATION OF LIFT COEFFICIENT DUE TO PLUNGE WITH REDUCED FREQUENCY FOR A NACA64A006 AIRFOIL AT M = 0.8

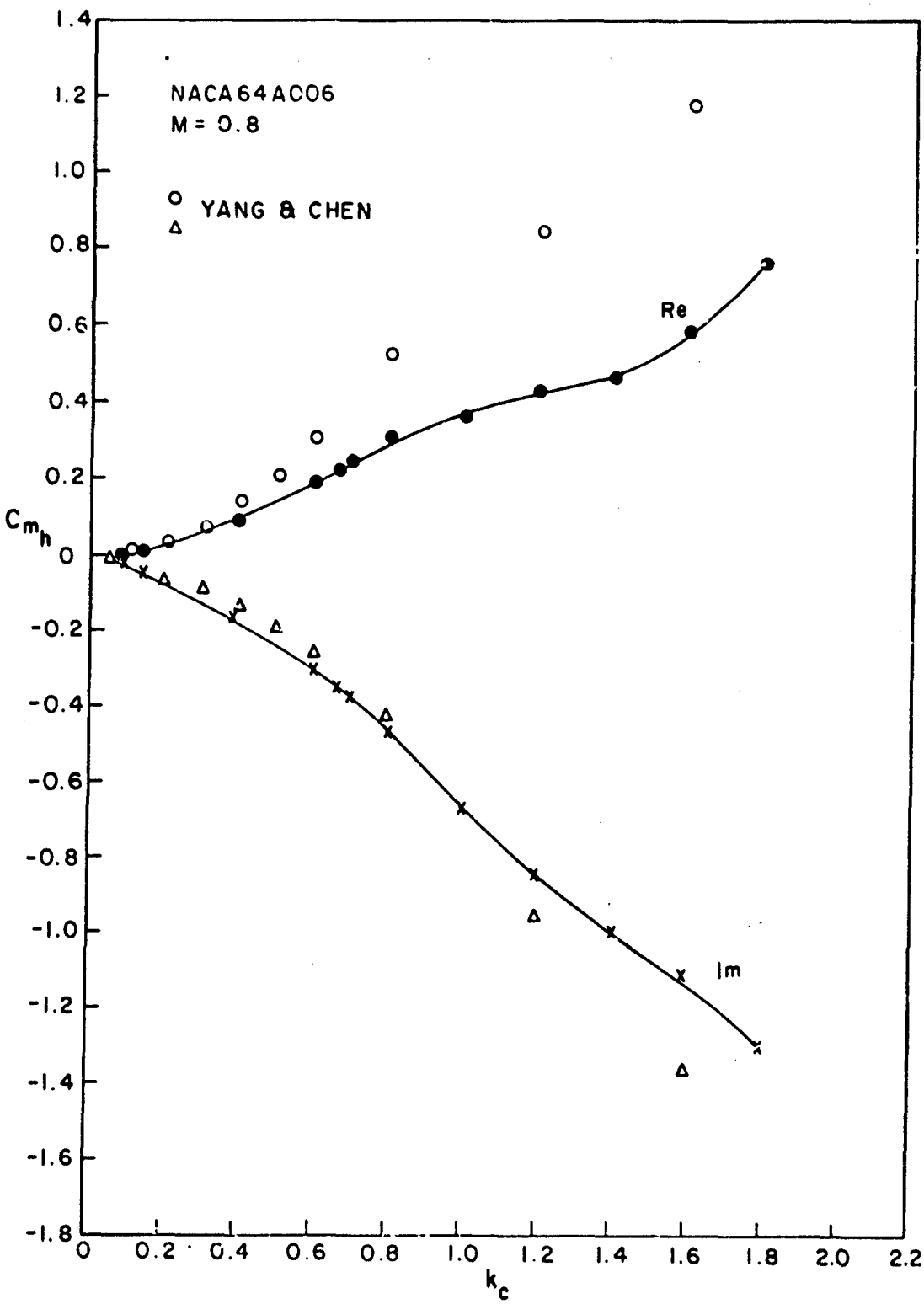

FIG. 3: VARIATION OF MOMENT COEFFICIENT DUE TO PLUNGE WITH REDUCED FREQUENCY FOR A NACA64A006 AIRFOIL AT M = 0.8

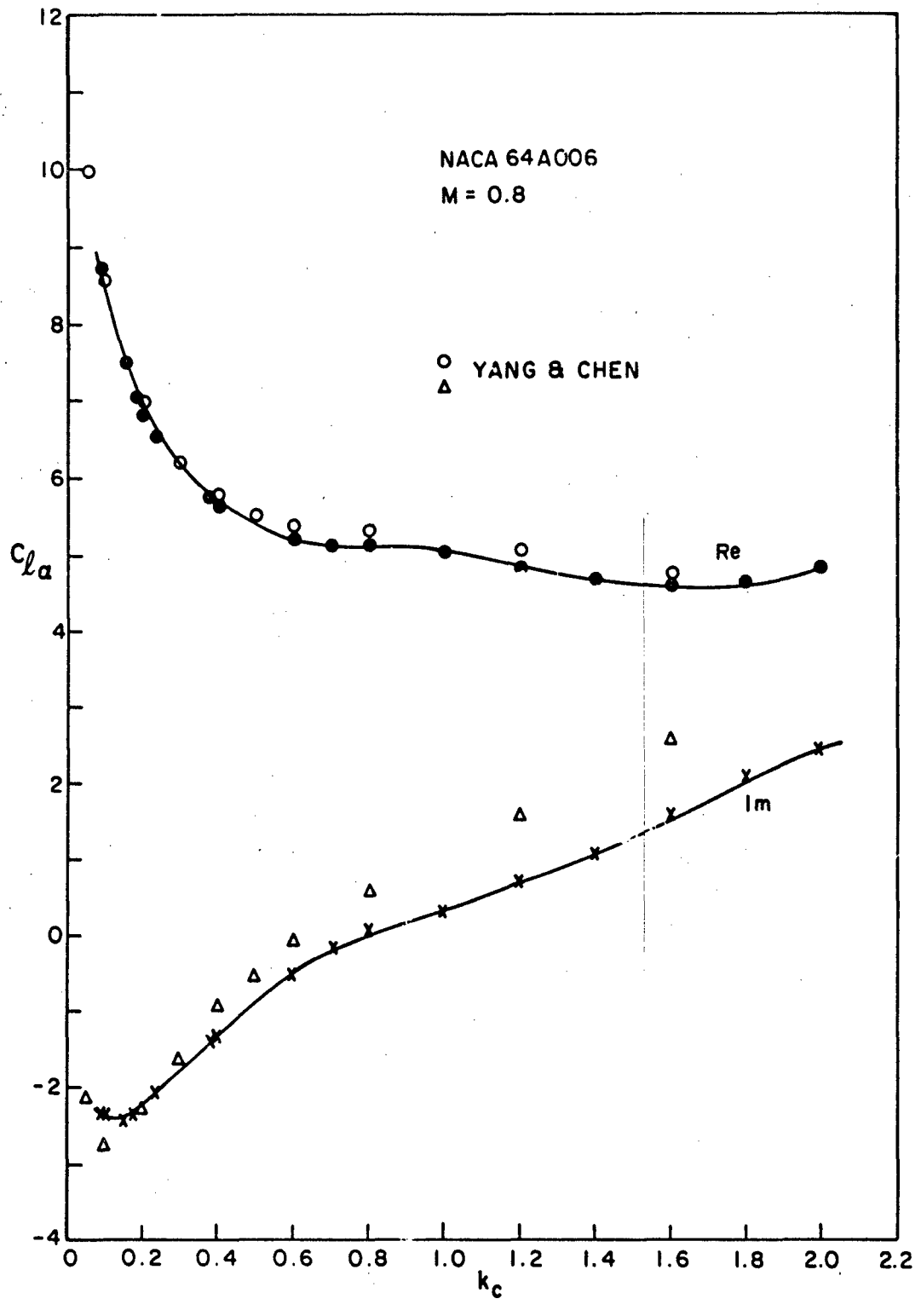

FIG. 4: VARIATION OF LIFT COEFFICIENT DUE TO PITCH WITH REDUCED FREQUENCY FOR A NACA64A006 AIRFOIL AT M = 0.8

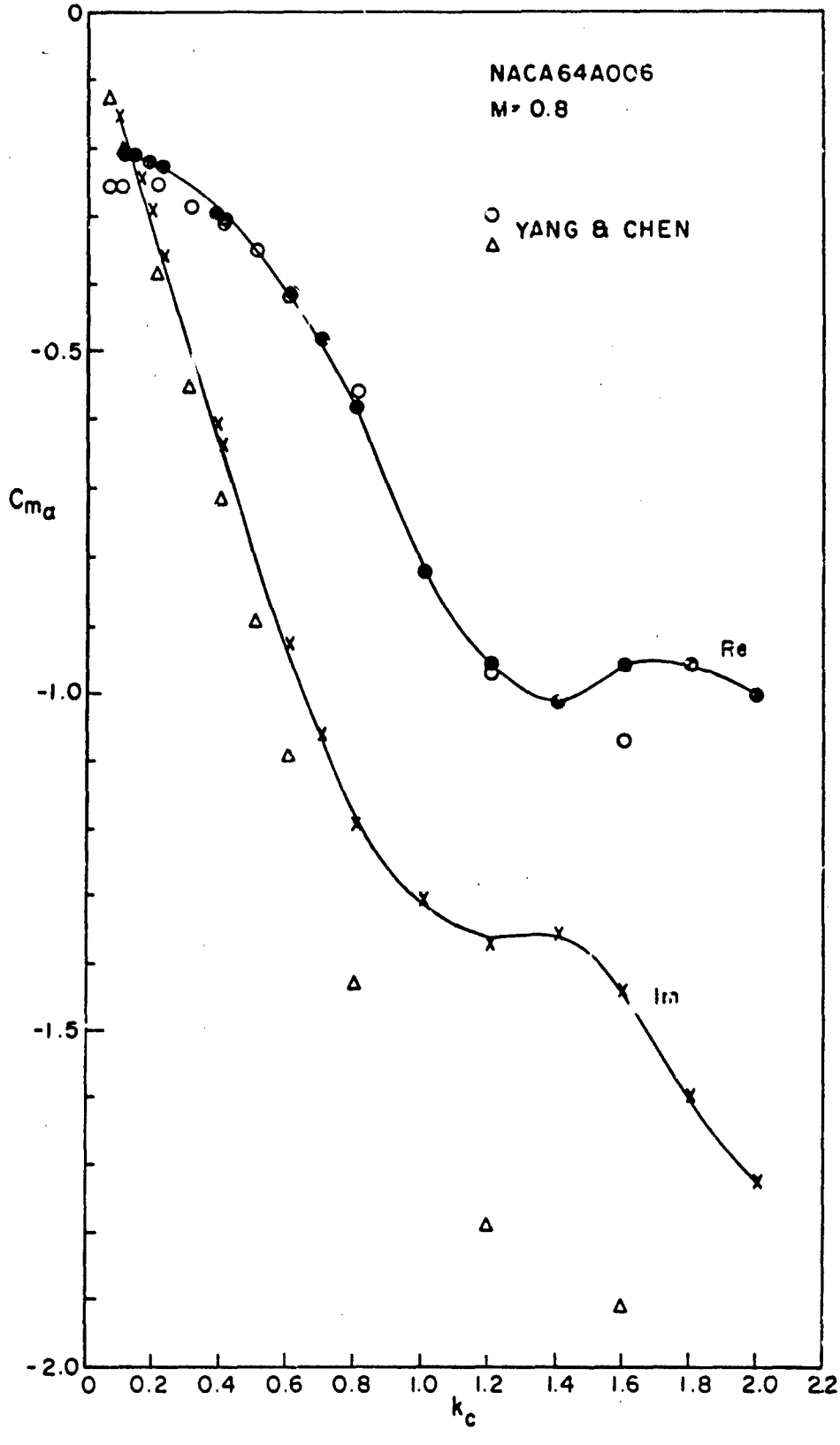

FIG. 5: VARIATION OF MOMENT COEFFICIENT DUE TO PITCH WITH REDUCED FREQUENCY FOR A NACA64A006 AIRFOIL AT M = 0.8

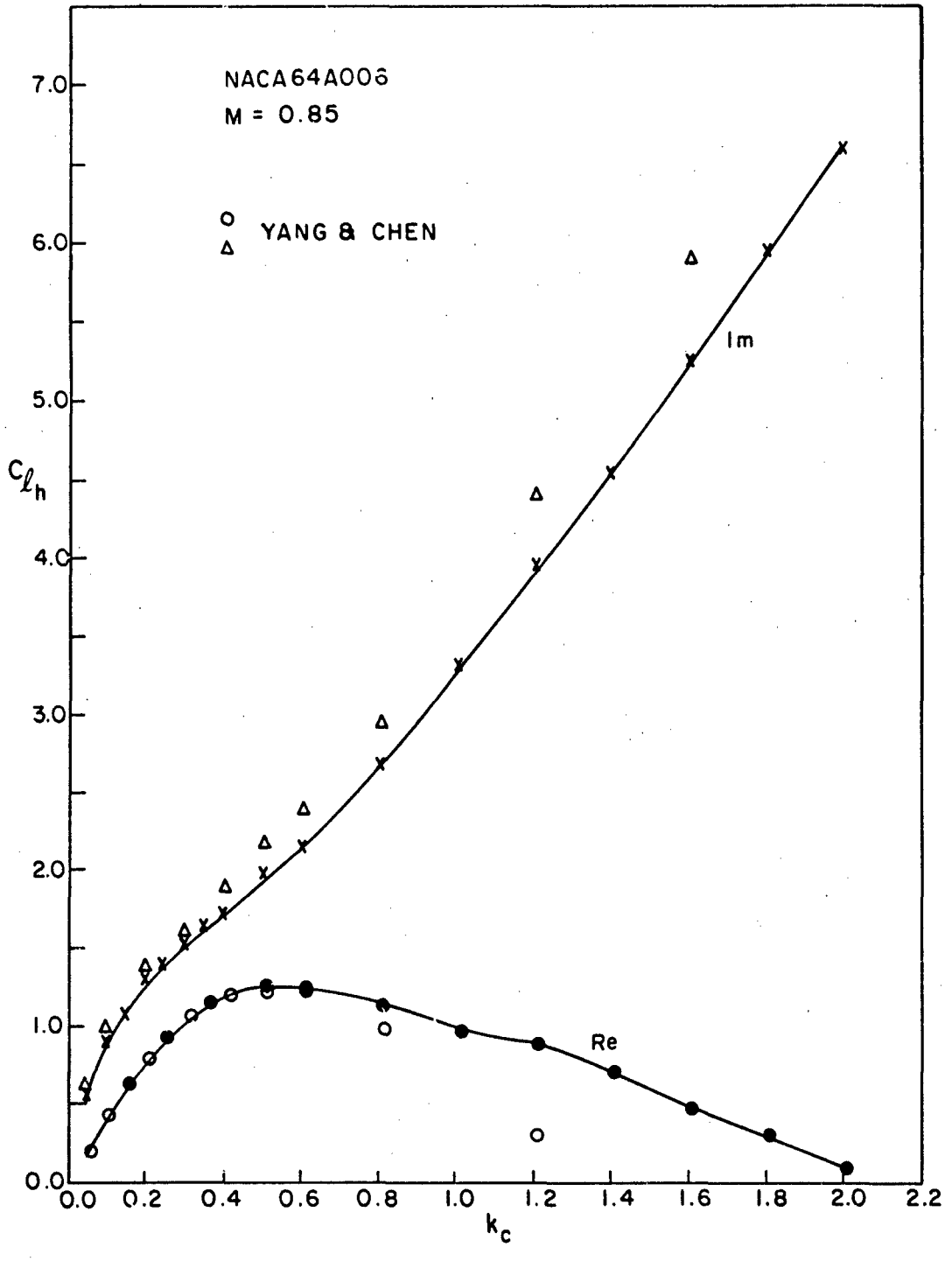

FIG. 6: VARIATION OF LIFT COEFFICIENT DUE TO PLUNGE WITH REDUCED FREQUENCY FOR A NACA64A006 AIRFOIL AT M = 0.85

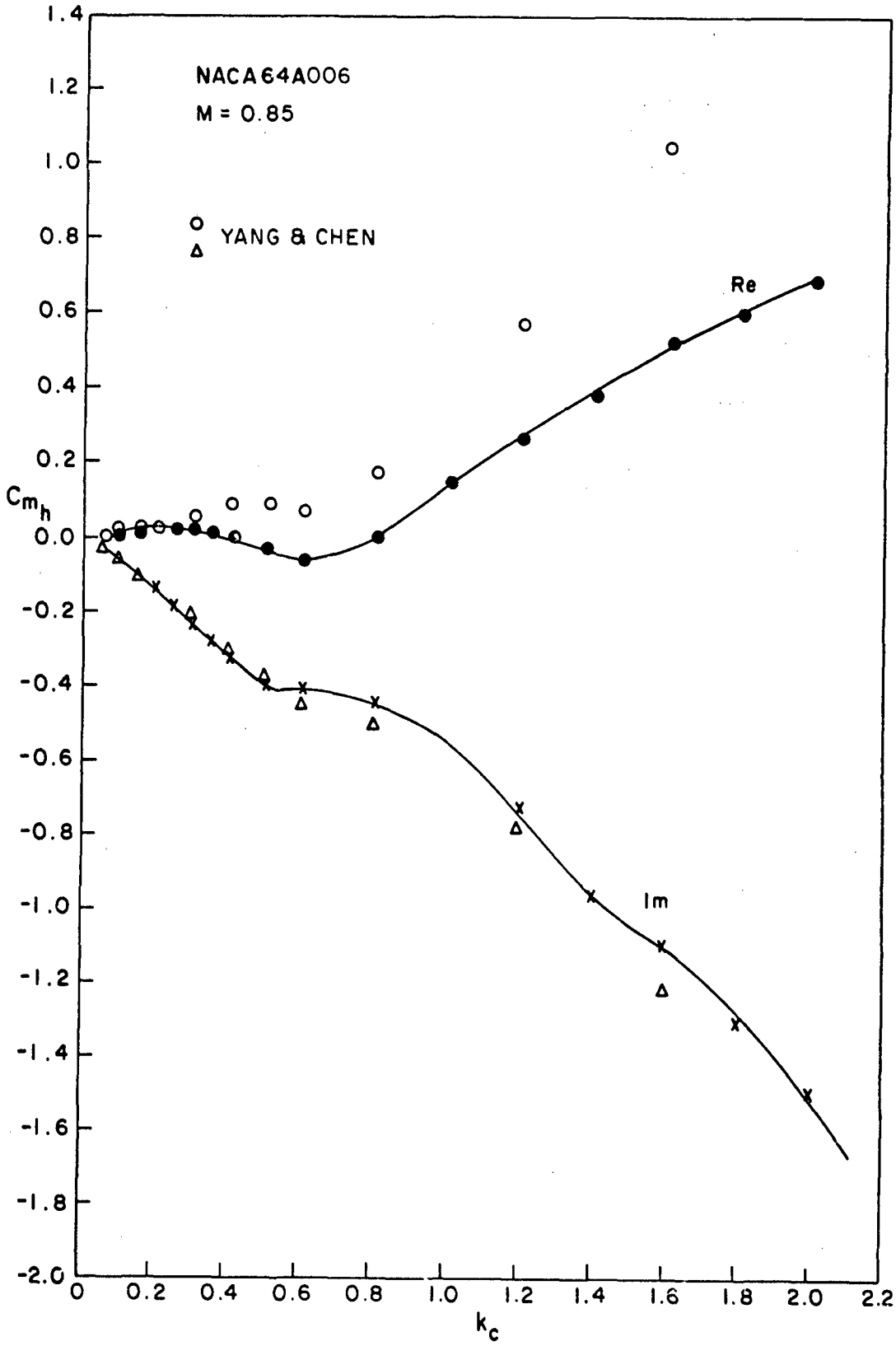

FIG. 7: VARIATION OF MOMENT COEFFICIENT DUE TO PLUNGE WITH REDUCED FREQUENCY FOR A NACA64A006 AIRFOIL AT M = 0.85

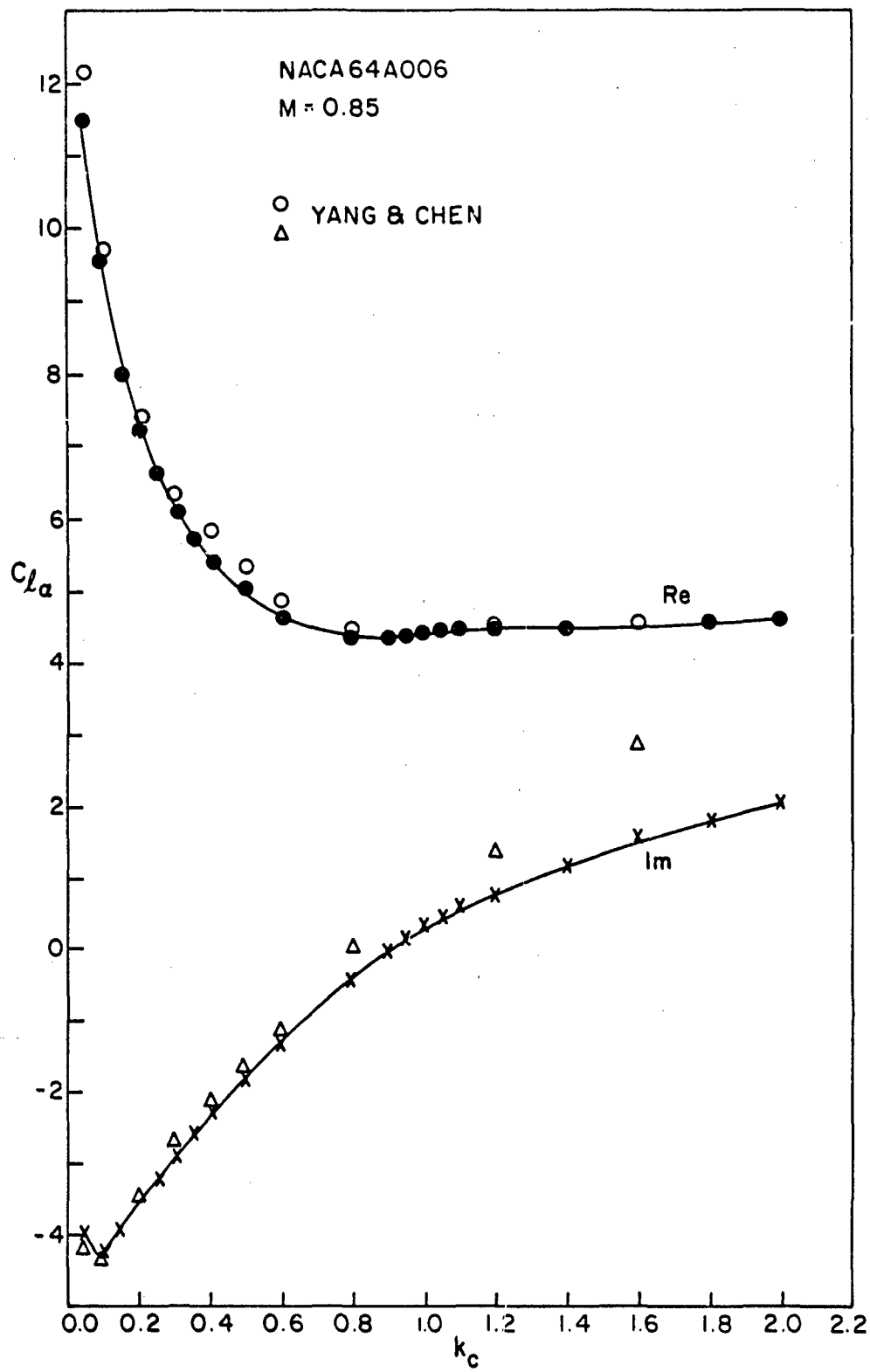

FIG. 8: VARIATION OF LIFT COEFFICIENT DUE TO PITCH WITH REDUCED FREQUENCY FOR A NACA64A006 AIRFOIL AT M = 0.85

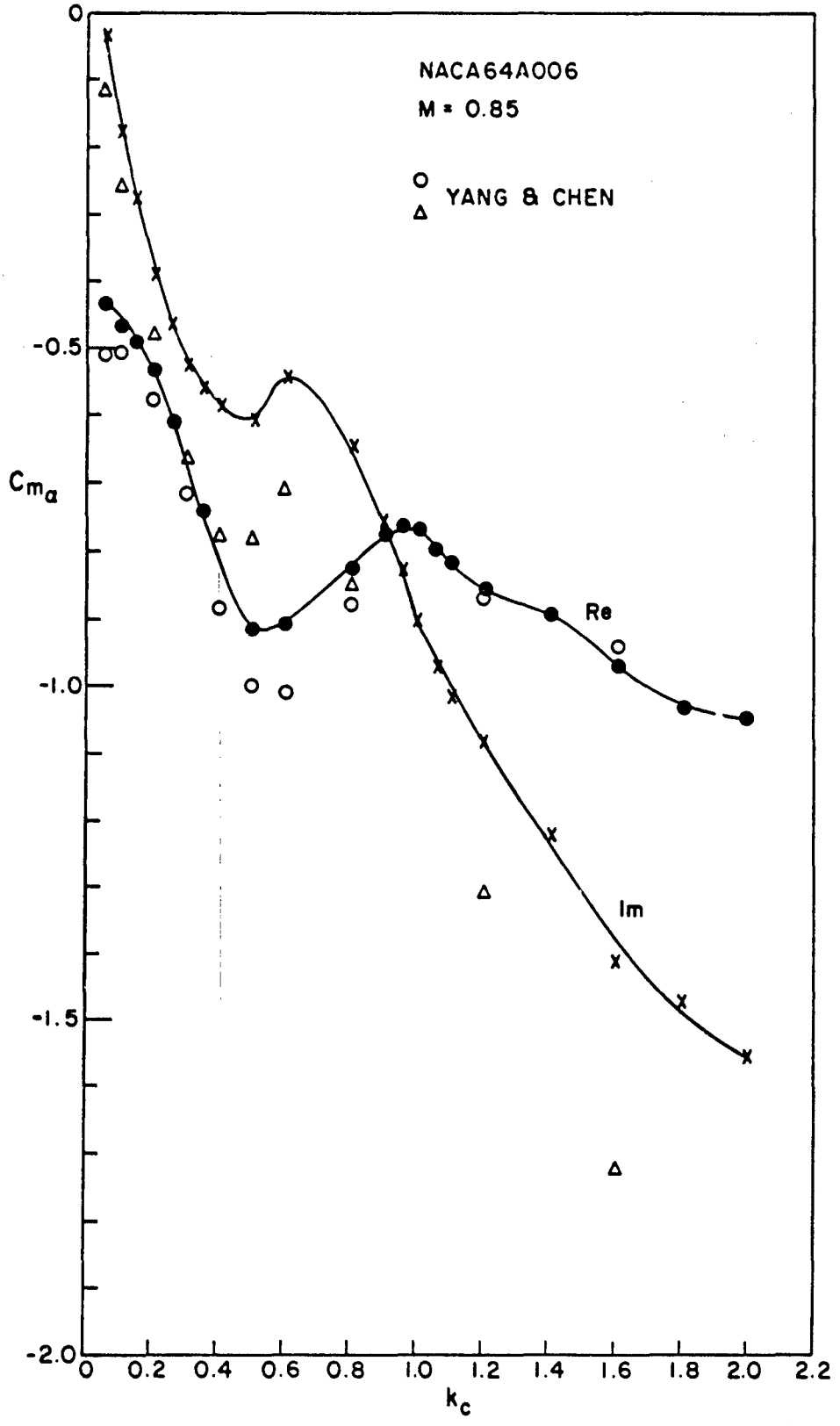

FIG. 9: VARIATION OF MOMENT COEFFICIENT DUE TO PITCH WITH REDUCED FREQUENCY FOR A NACA64A006 AIRFOIL AT M = 0.85

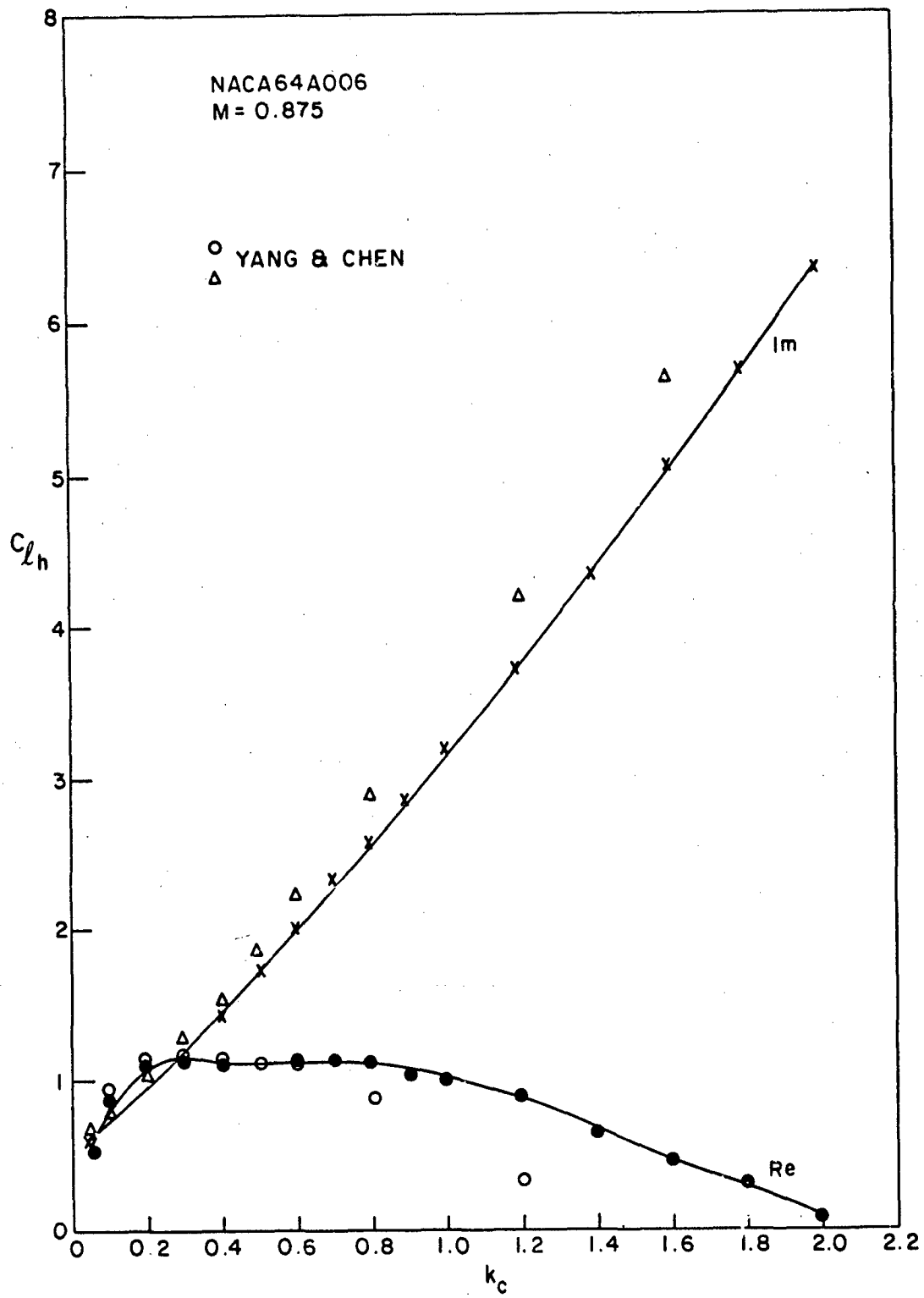

FIG. 10: VARIATION OF LIFT COEFFICIENT DUE TO PLUNGE WITH REDUCED FREQUENCY FOR A NACA64A006 AIRFOIL AT M = 0.875

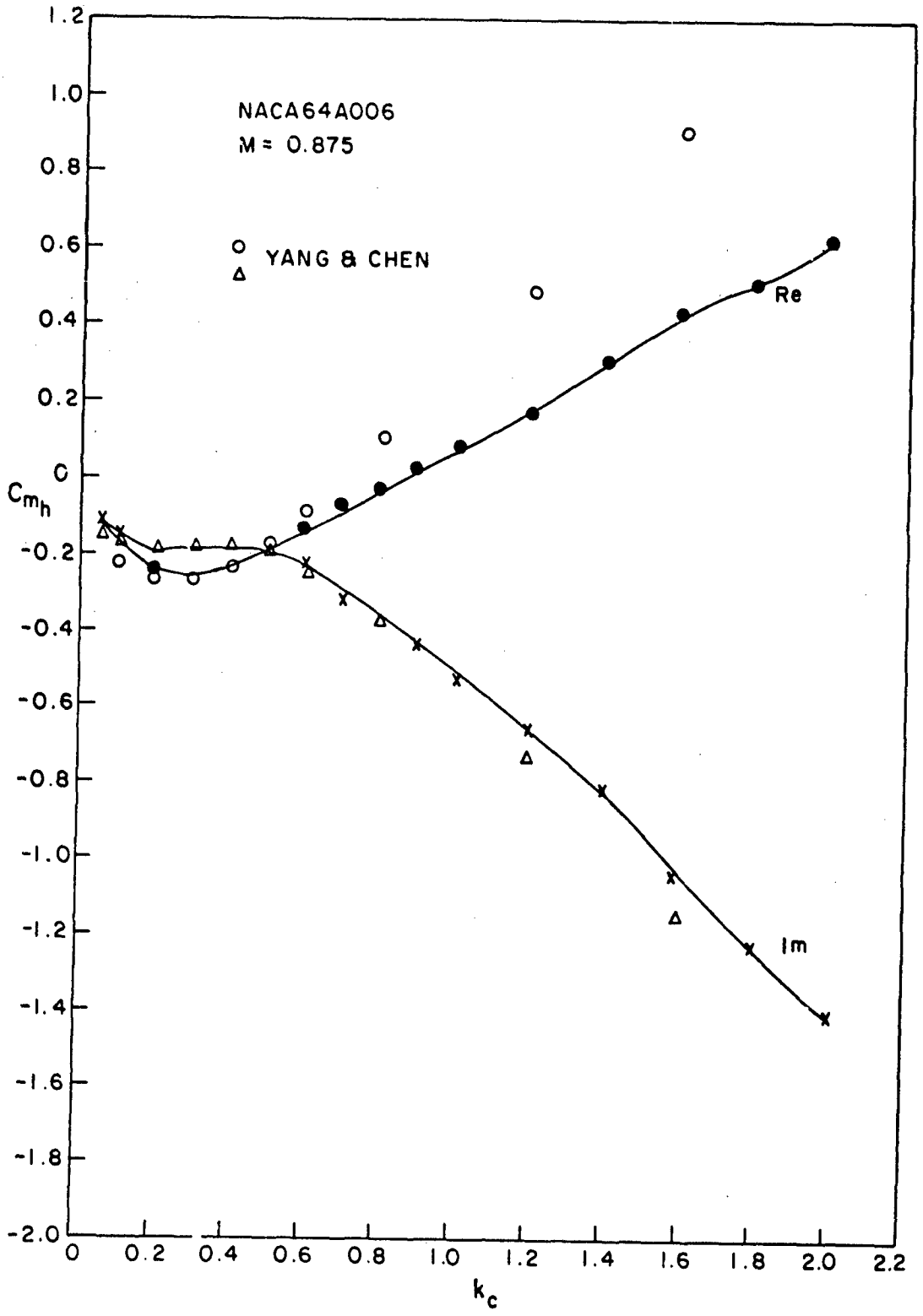

FIG. 11: VARIATION OF MOMENT COEFFICIENT DUE TO PLUNGE WITH REDUCED FREQUENCY FOR A NACA64A006 AIRFOIL AT M = 0.875

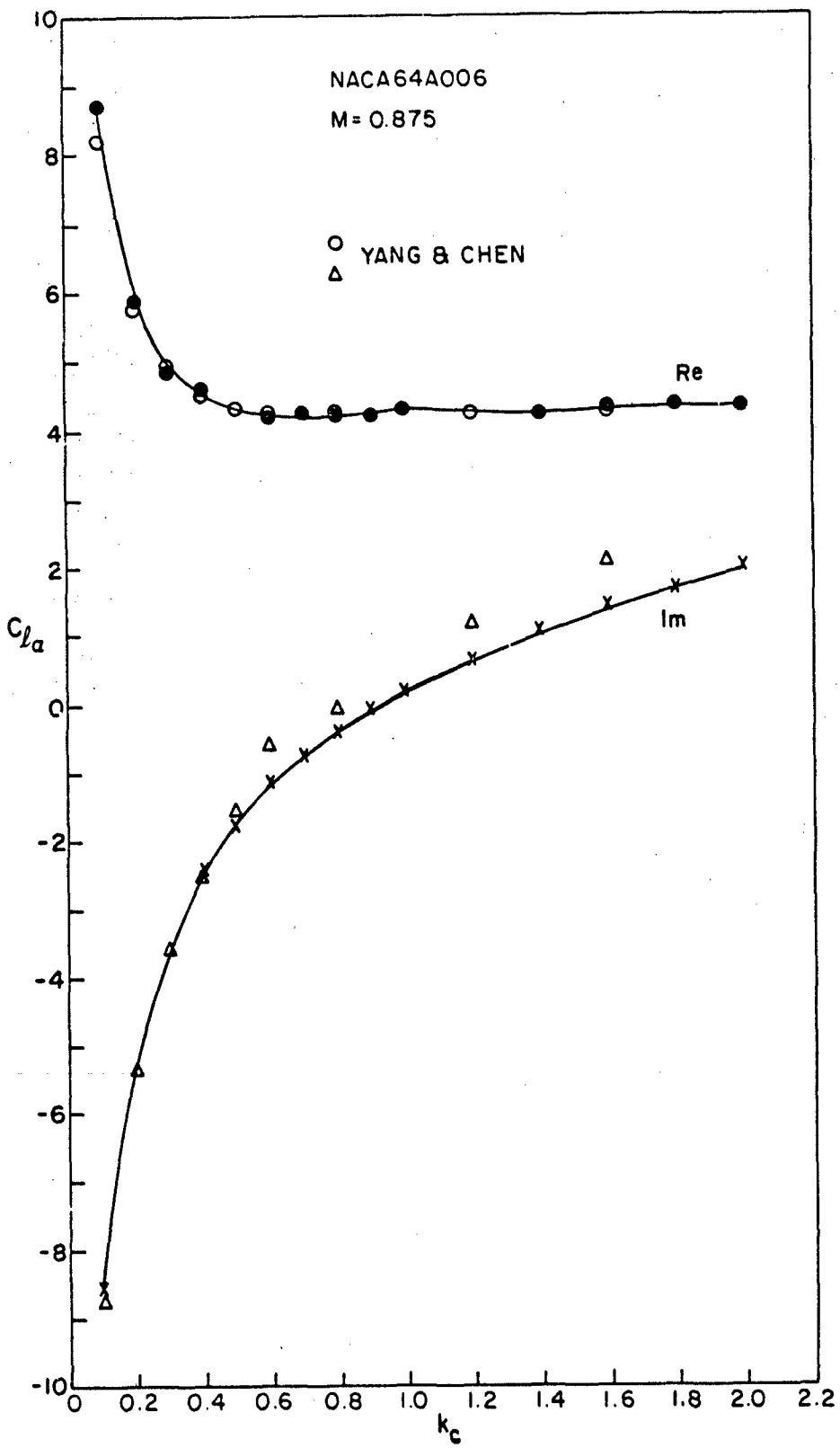

FIG. 12: VARIATION OF LIFT COEFFICIENT DUE TO PITCH WITH REDUCED FREQUENCY FOR A NACA64A006 AIRFOIL AT M = 0.875

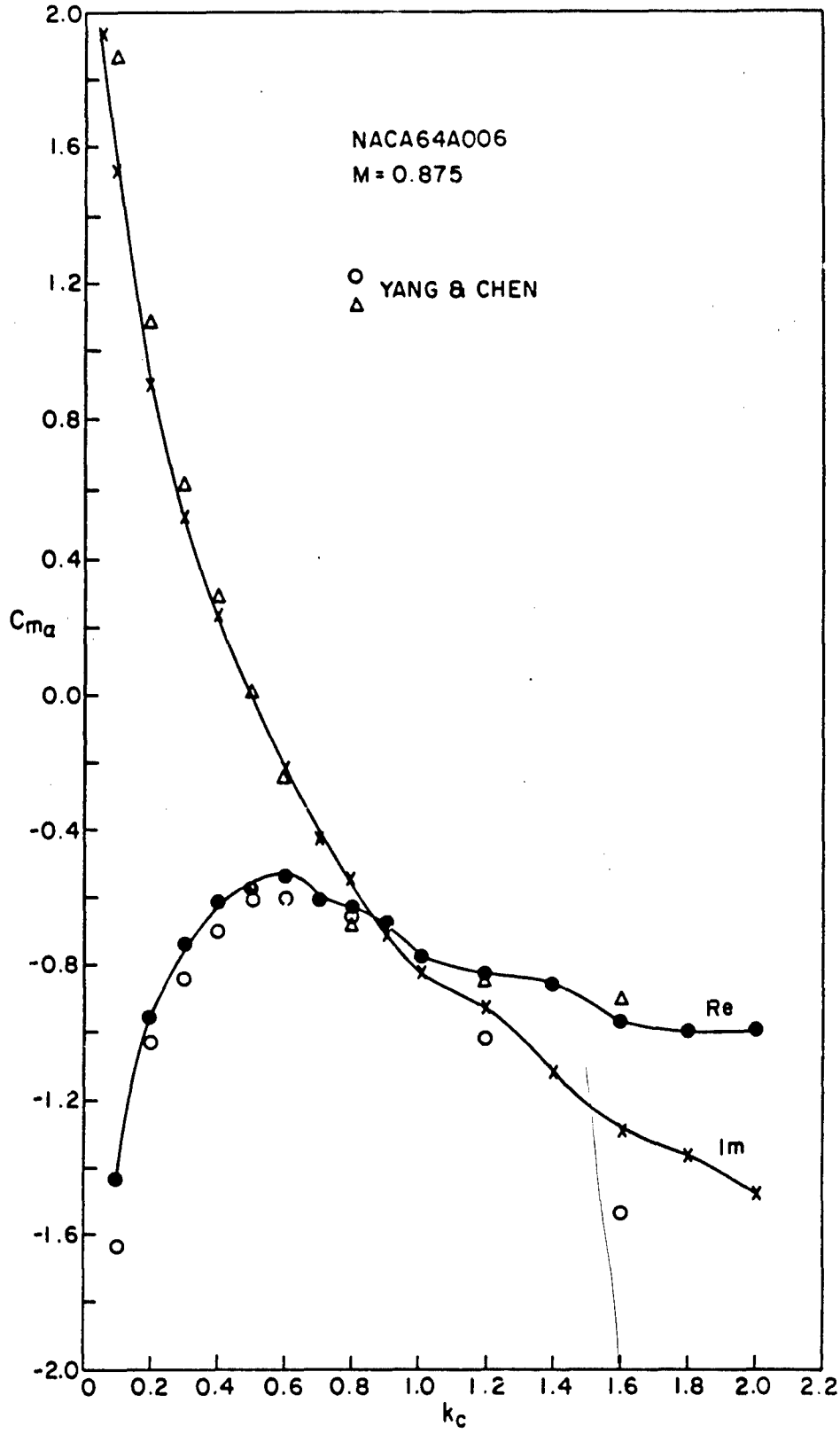

FIG. 13: VARIATION OF MOMENT COEFFICIENT DUE TO PITCH WITH REDUCED FREQUENCY FOR A NACA64A006 AIRFOIL AT M = 0.875

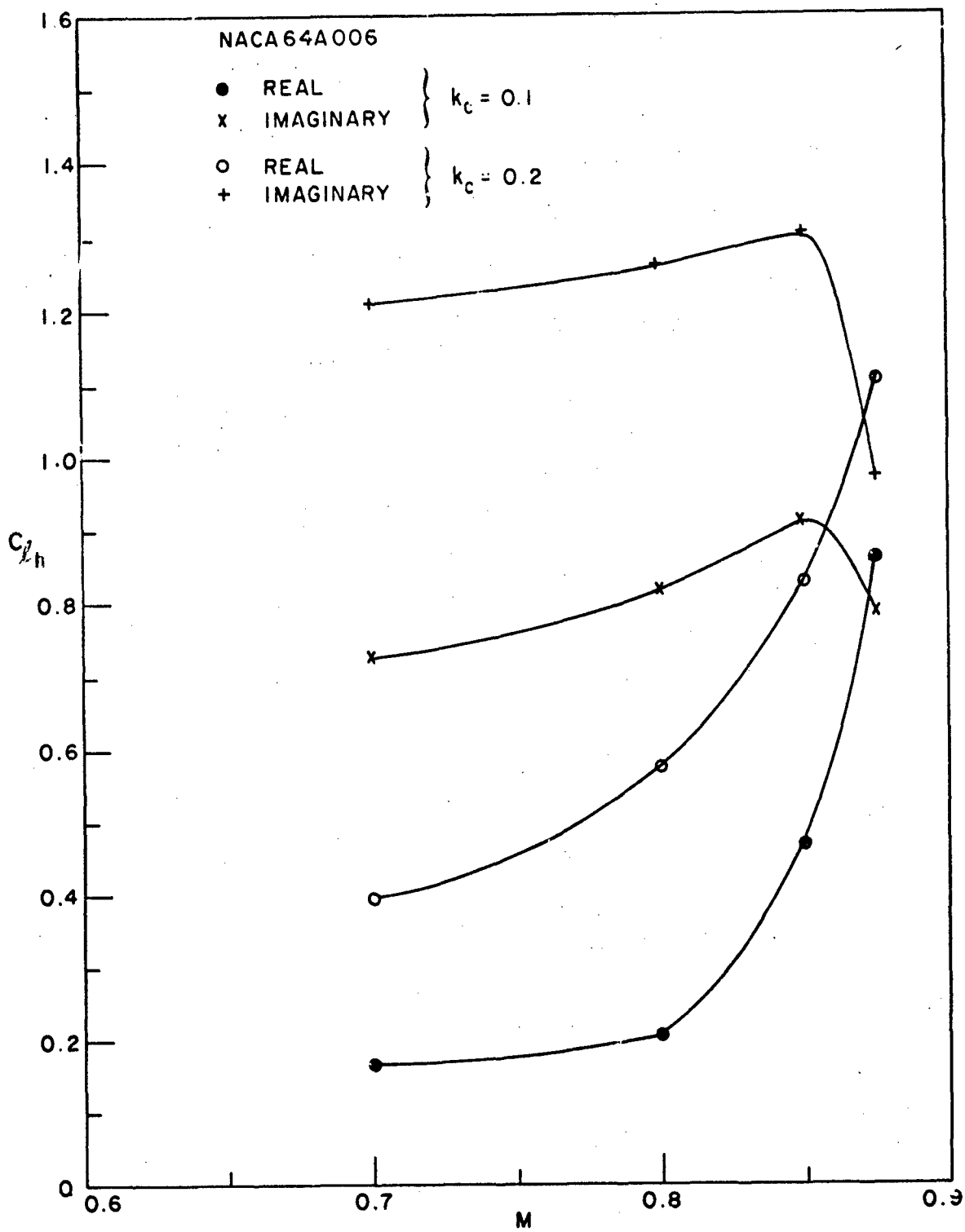

FIG. 14: VARIATION OF LIFT COEFFICIENT DUE TO PLUNGE WITH MACH NUMBER FOR A NACA64A006 AIRFOIL AT k_c = 0.1 AND 0.2

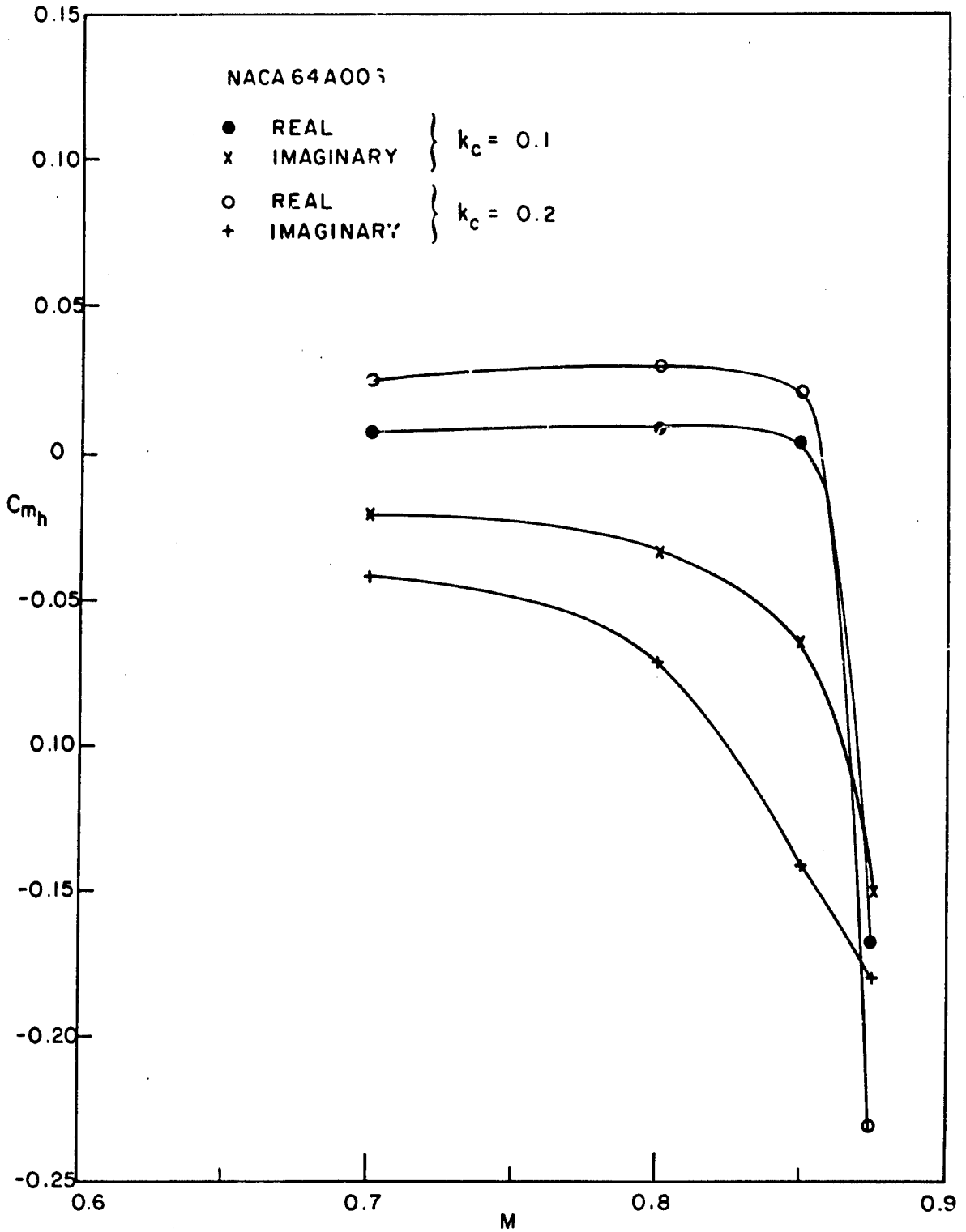

FIG. 15: VARIATION OF MOMENT COEFFICIENT DUE TO PLUNGE WITH MACH NUMBER FOR A NACA64A006 AIRFOIL AT k_c = 0.1 AND 0.2

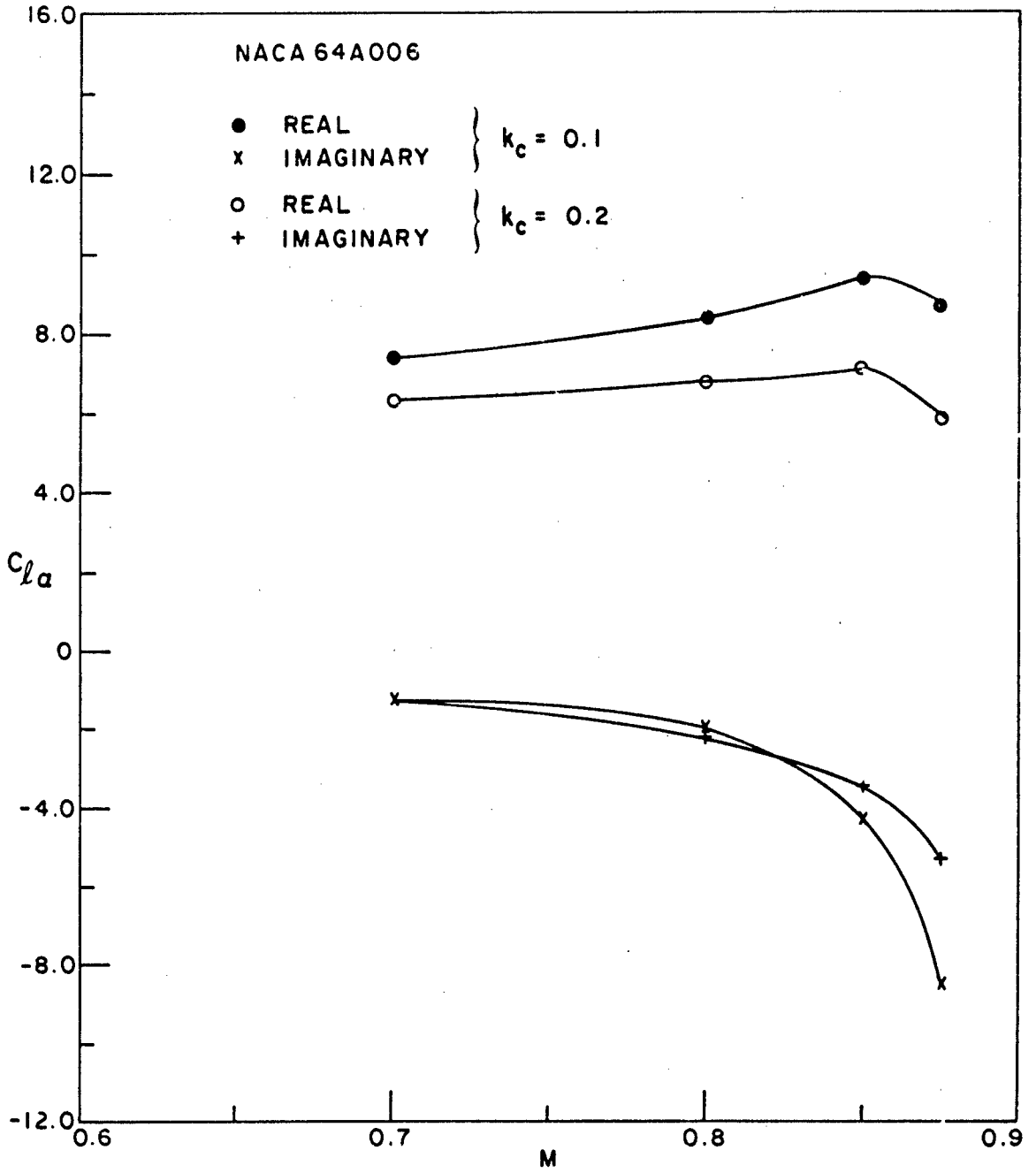

FIG. 16: VARIATION OF LIFT COEFFICIENT DUE TO PITCH WITH MACH NUMBER FOR A NACA64A006 AIRFOIL AT k_c = 0.1 AND 0.2

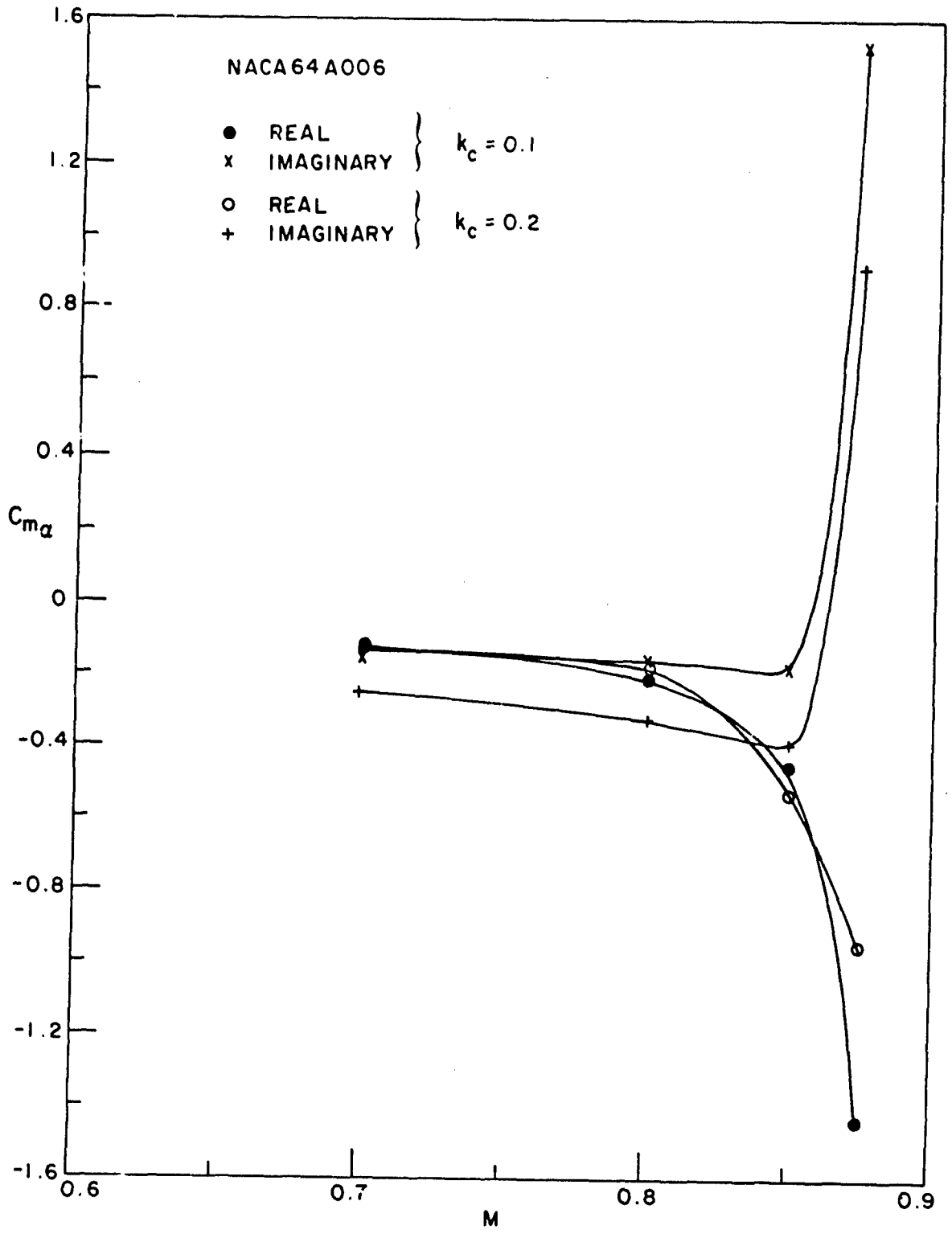

FIG. 17: VARIATION OF MOMENT COEFFICIENT DUE TO PITCH WITH MACH NUMBER FOR A NACA64A006 AIRFOIL AT k_c = 0.1 AND 0.2

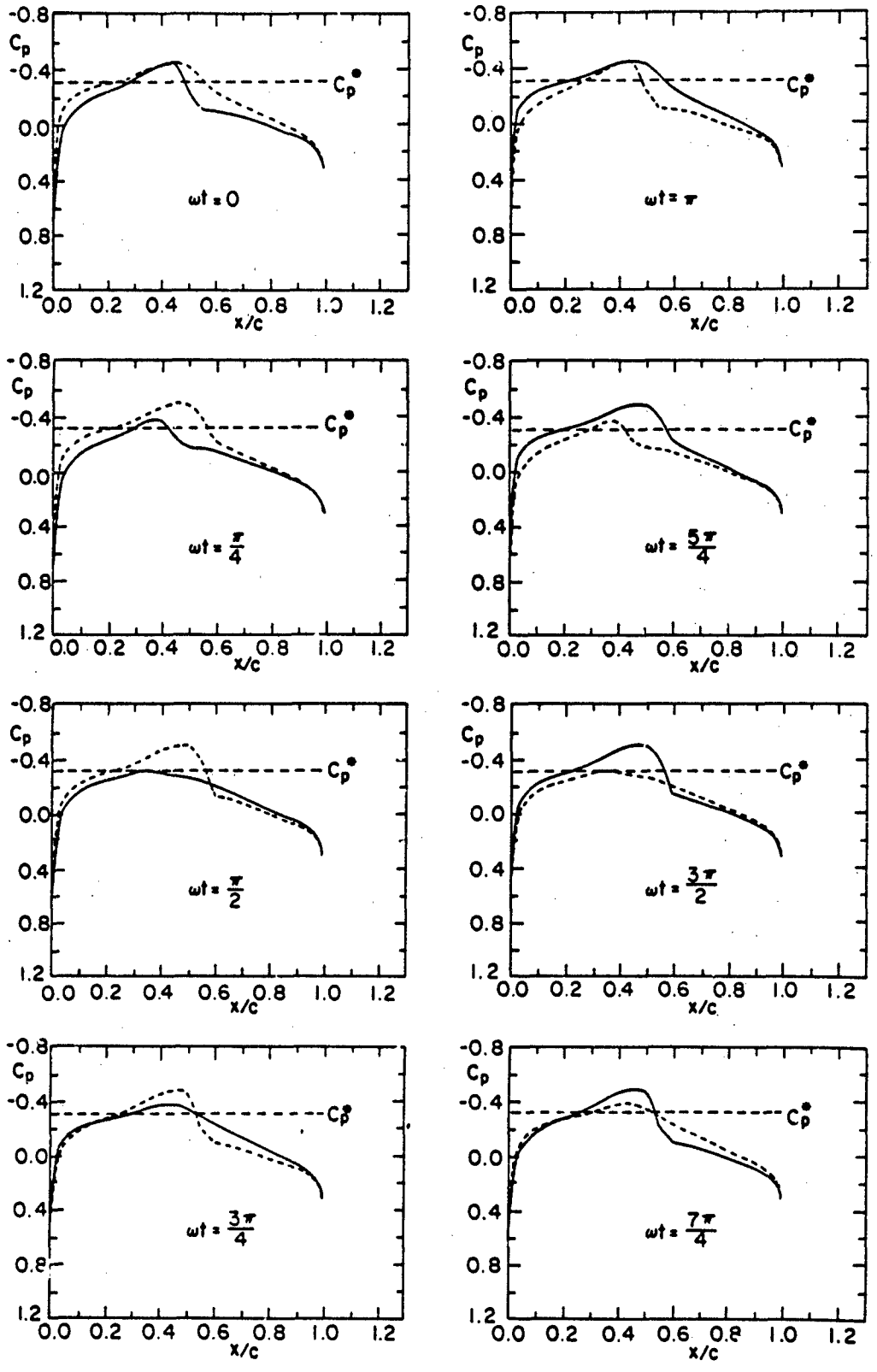

FIG. 18: C_p DISTRIBUTION FOR PLUNGING MOTION ON THE UPPER (————) AND LOWER (– – – – –) SURFACES OF A NACA64A006 AIRFOIL AT M = 0.85 AND k_c = 0.5

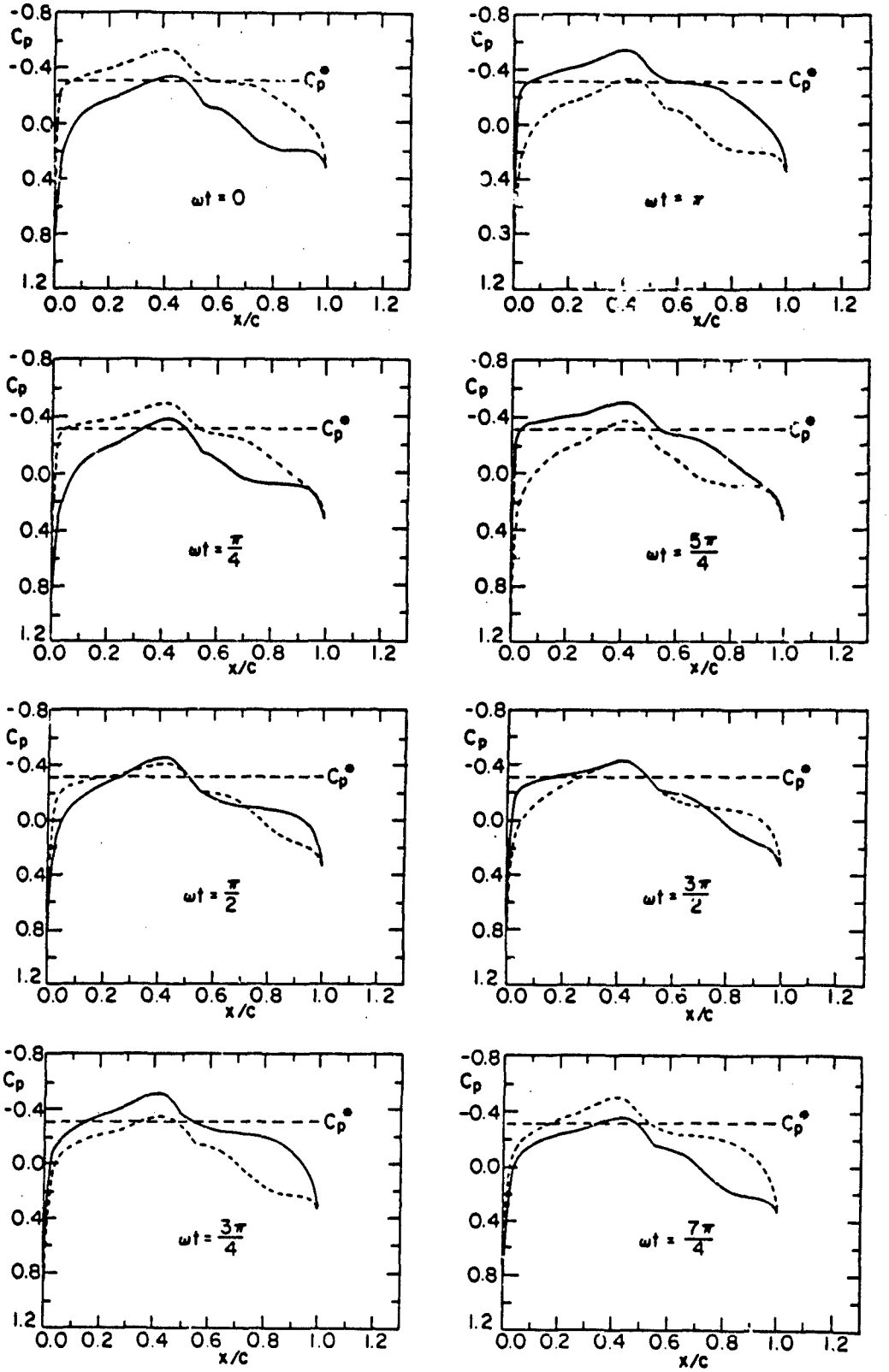

FIG. 19: C_p DISTRIBUTION FOR PLUNGING MOTION ON THE UPPER (————) AND LOWER (– – – –) SURFACES OF A NACA64A006 AIRFOIL AT M = 0.85 AND k_c = 2

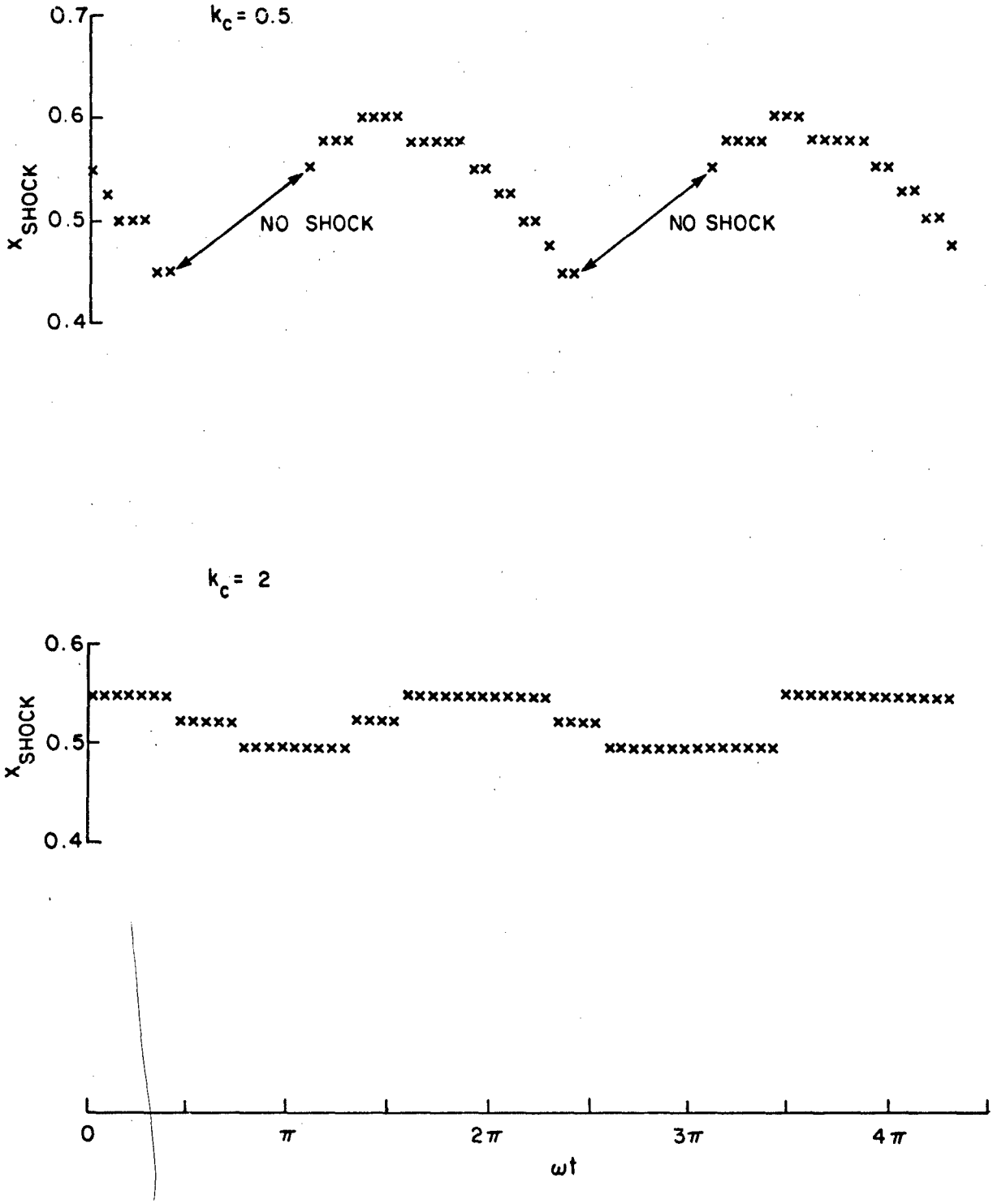

FIG. 20: SHOCK WAVE POSITION FOR PLUNGING OSCILLATION OF A NACA64A006 AIRFOIL AT M = 0.85, k_c = 0.5 AND 2

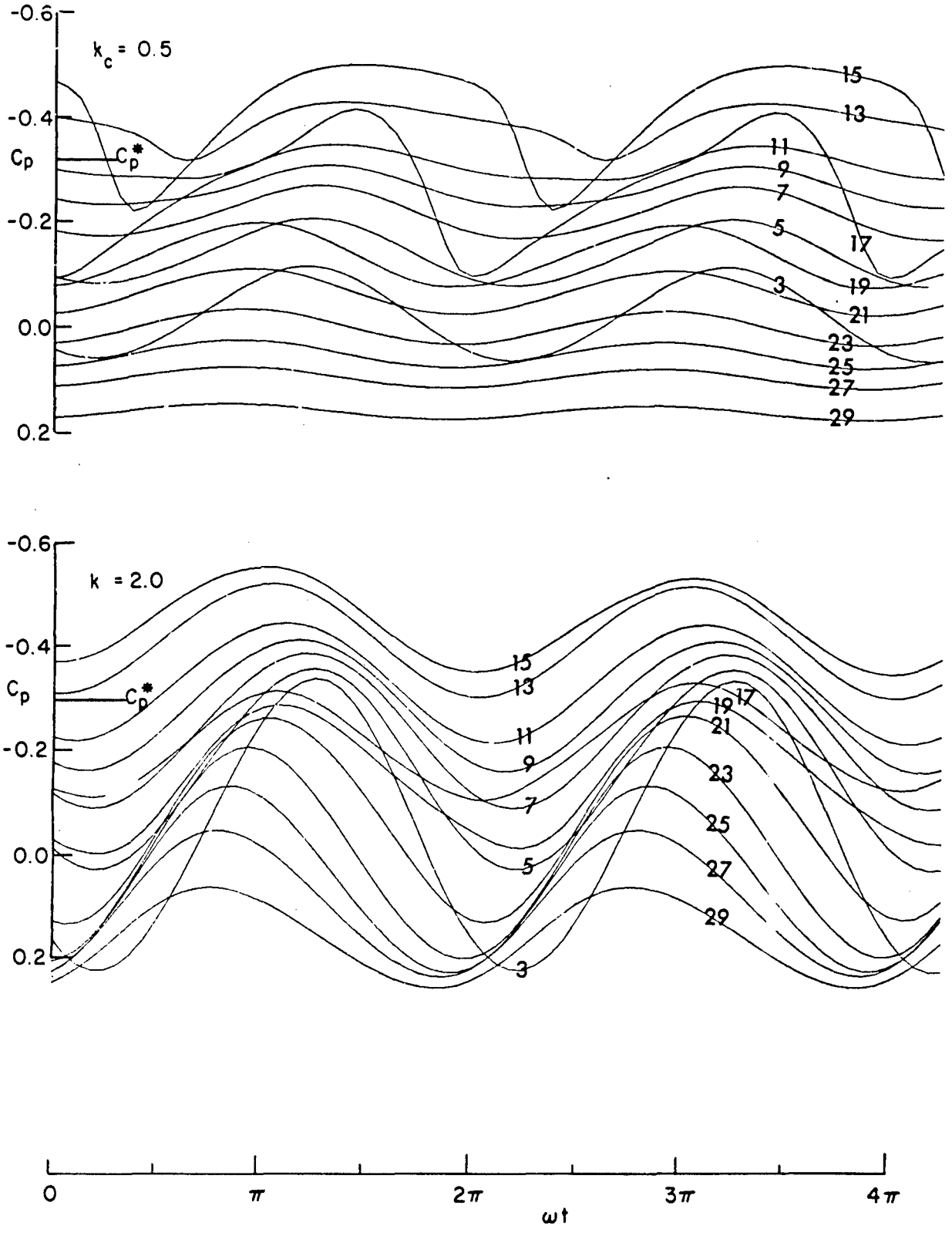

FIG. 21: C_p VARIATION WITH TIME ON UPPER SURFACE OF A NACA64A006 AIRFOIL AT M = 0.85, k_c = 0.5 AND 2. (THE DISTANCES FROM LEADING EDGE WHERE C_p ARE COMPUTED ARE GIVEN IN TABLE 1.)

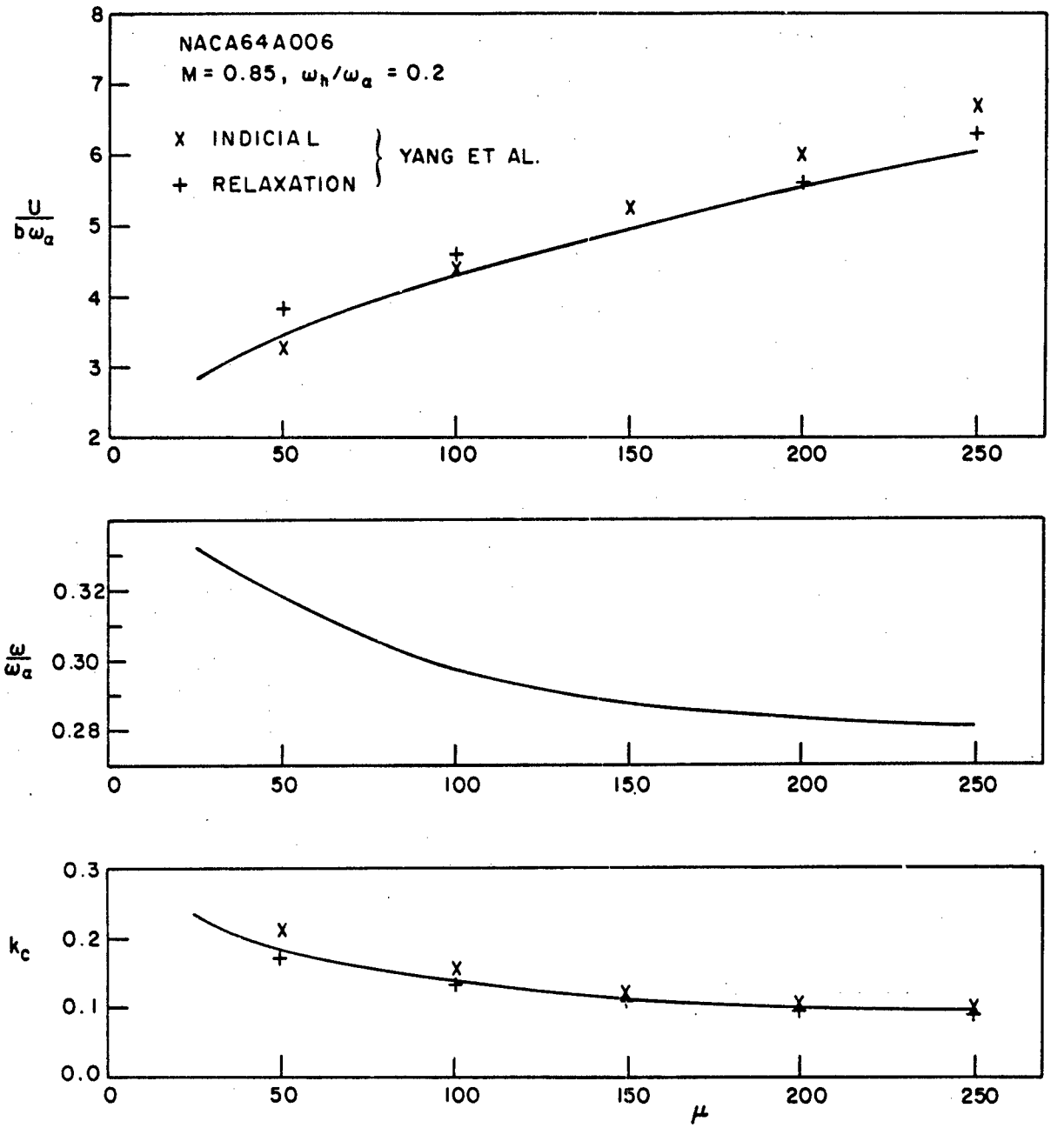

FIG. 22: VARIATION OF $U/b\omega_\alpha$, ω/ω_α AND k_c WITH μ FOR A NACA64A006 AIRFOIL AT M = 0.85

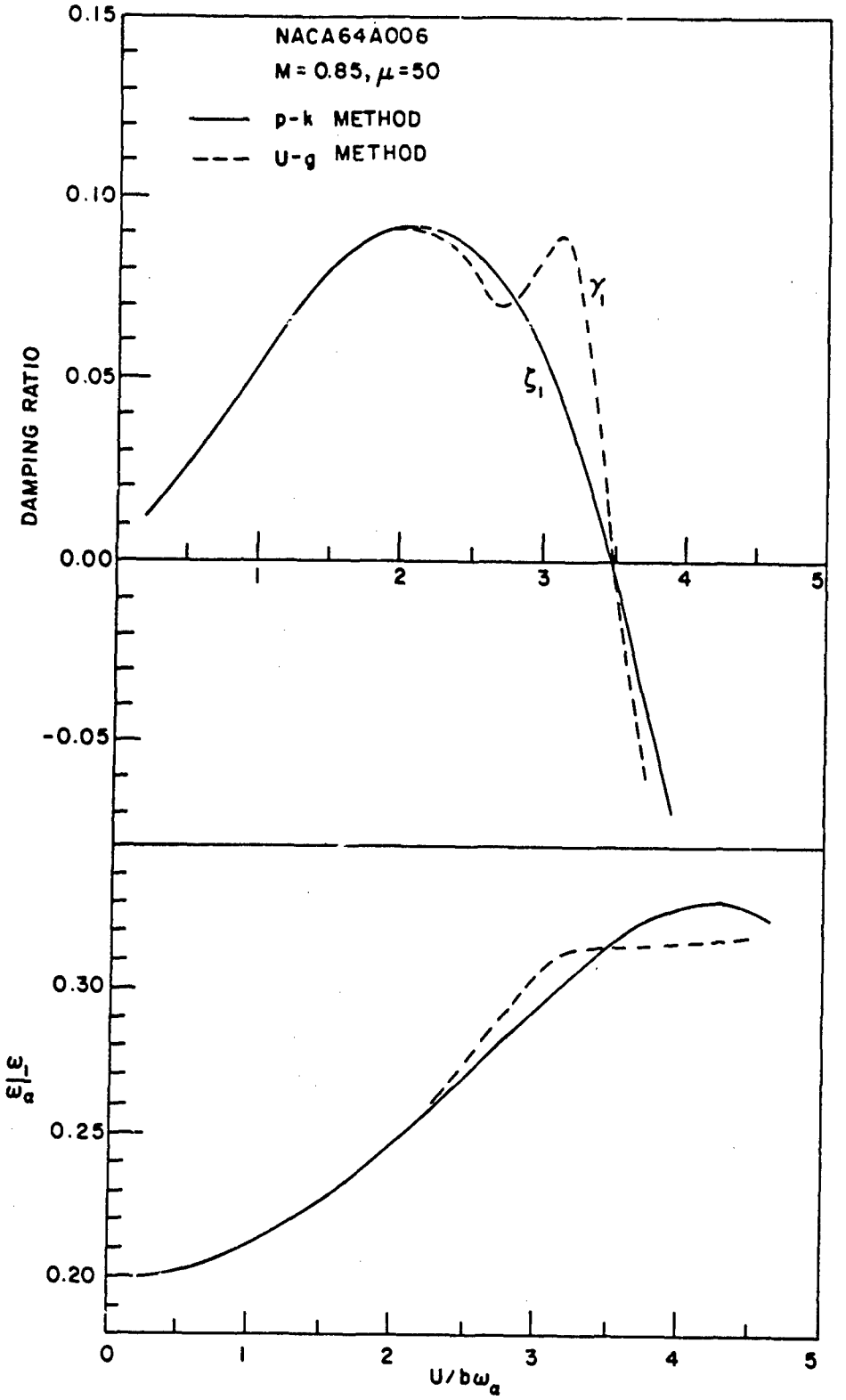

FIG. 23(a): COMPARISON OF DAMPING RATIO AND ω_1/ω_α WITH $U/b\omega_\alpha$ BETWEEN U-g AND p-k METHODS FOR A NACA64A006 AIRFOIL AT M = 0.85 AND μ = 50

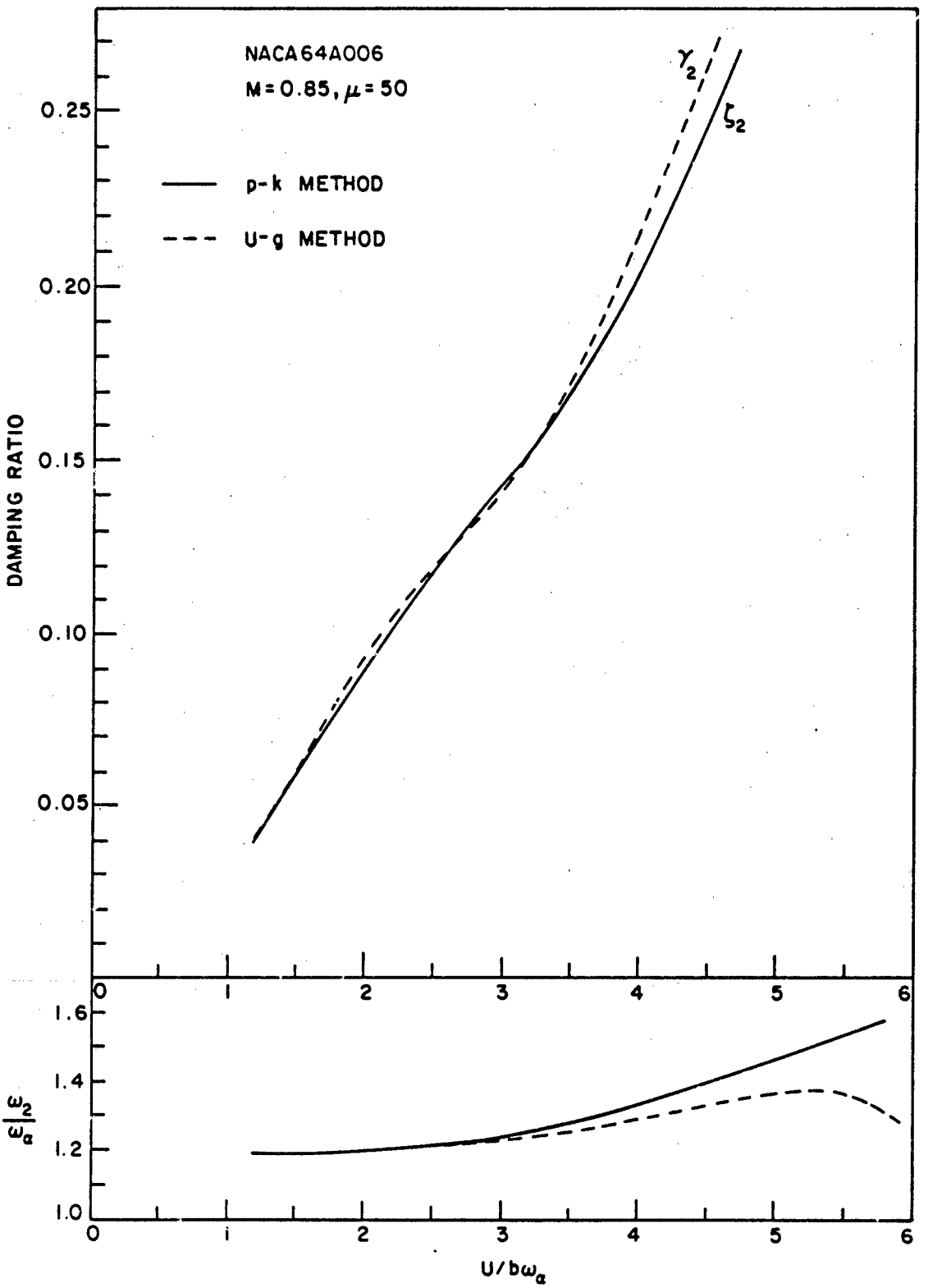

FIG. 23(b): COMPARISON OF DAMPING RATIO AND ω_2/ω_α WITH $U/b\omega_\alpha$ BETWEEN U-g AND p-k METHODS FOR A NACA64A006 AIRFOIL AT M = 0.85 AND μ = 50

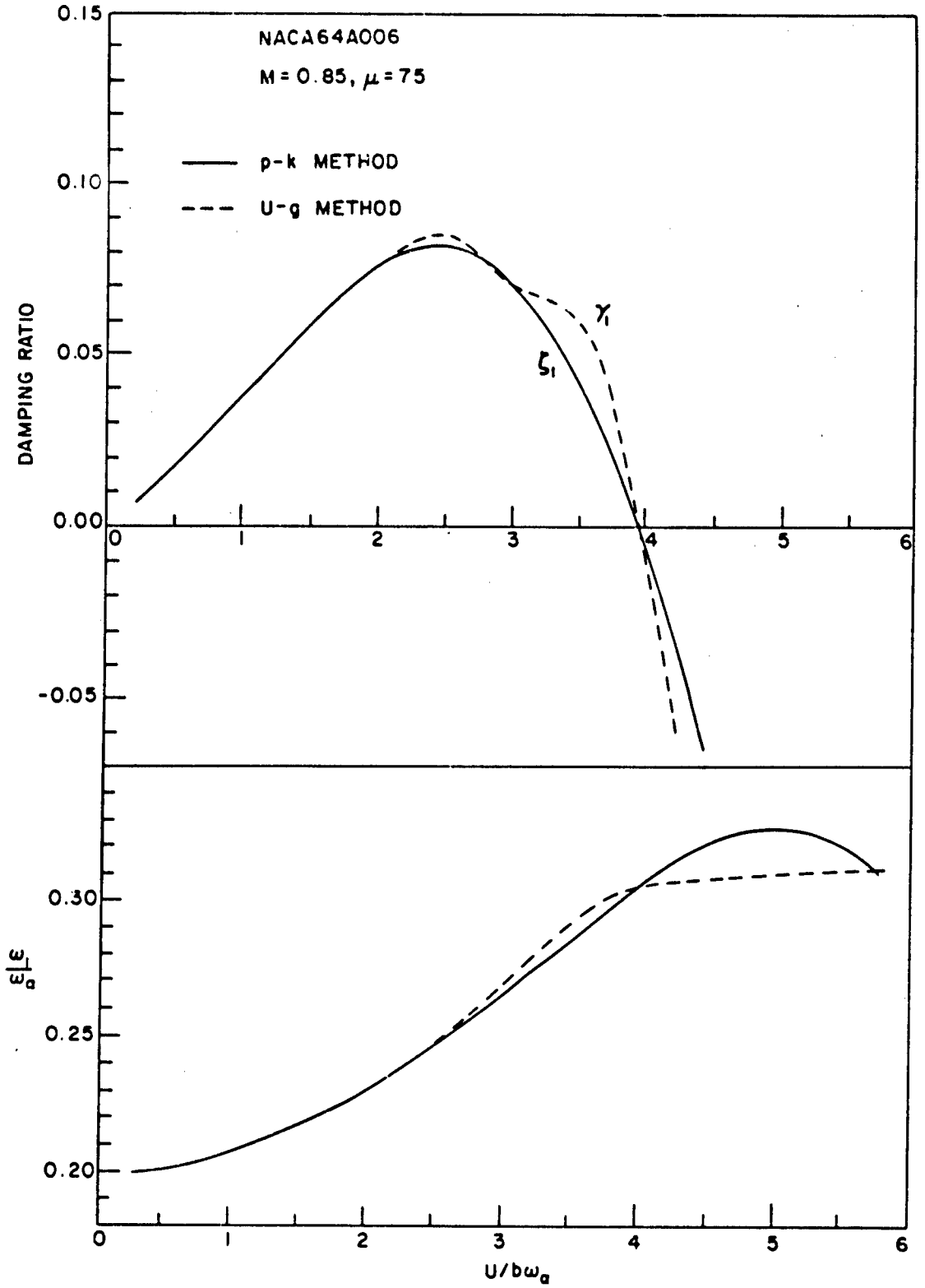

FIG. 24(a): COMPARISON OF DAMPING RATIO AND ω_1/ω_a WITH $U/b\omega_a$ BETWEEN U-g AND p-k METHODS FOR A NACA64A006 AIRFOIL AT M = 0.85 AND μ = 75

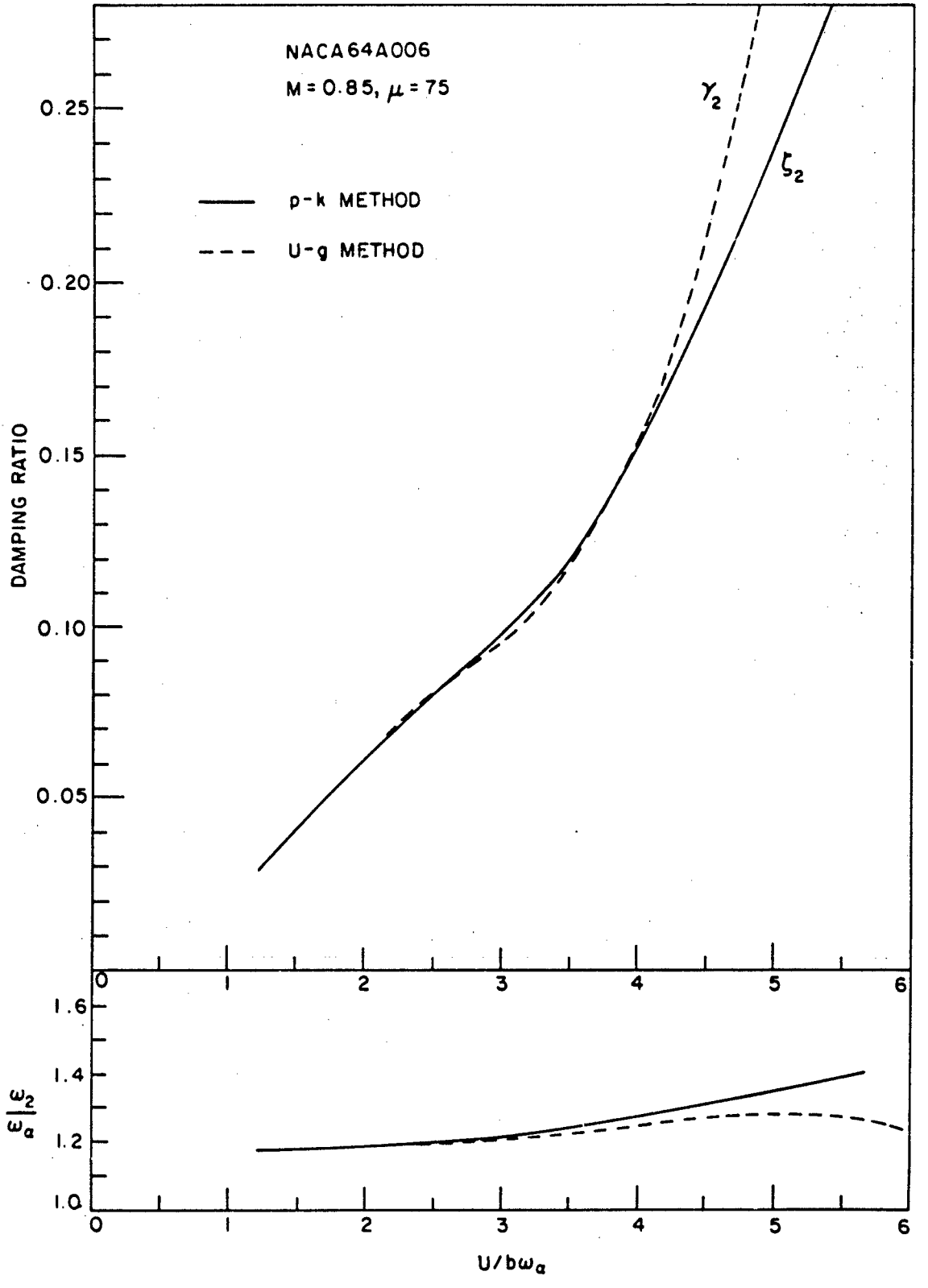

FIG. 24(b): COMPARISON OF DAMPING RATIO AND ω_2/ω_α WITH $U/b\omega_\alpha$ BETWEEN U-g AND p-k METHODS FOR A NACA64A006 AIRFOIL AT M = 0.85 AND μ = 75

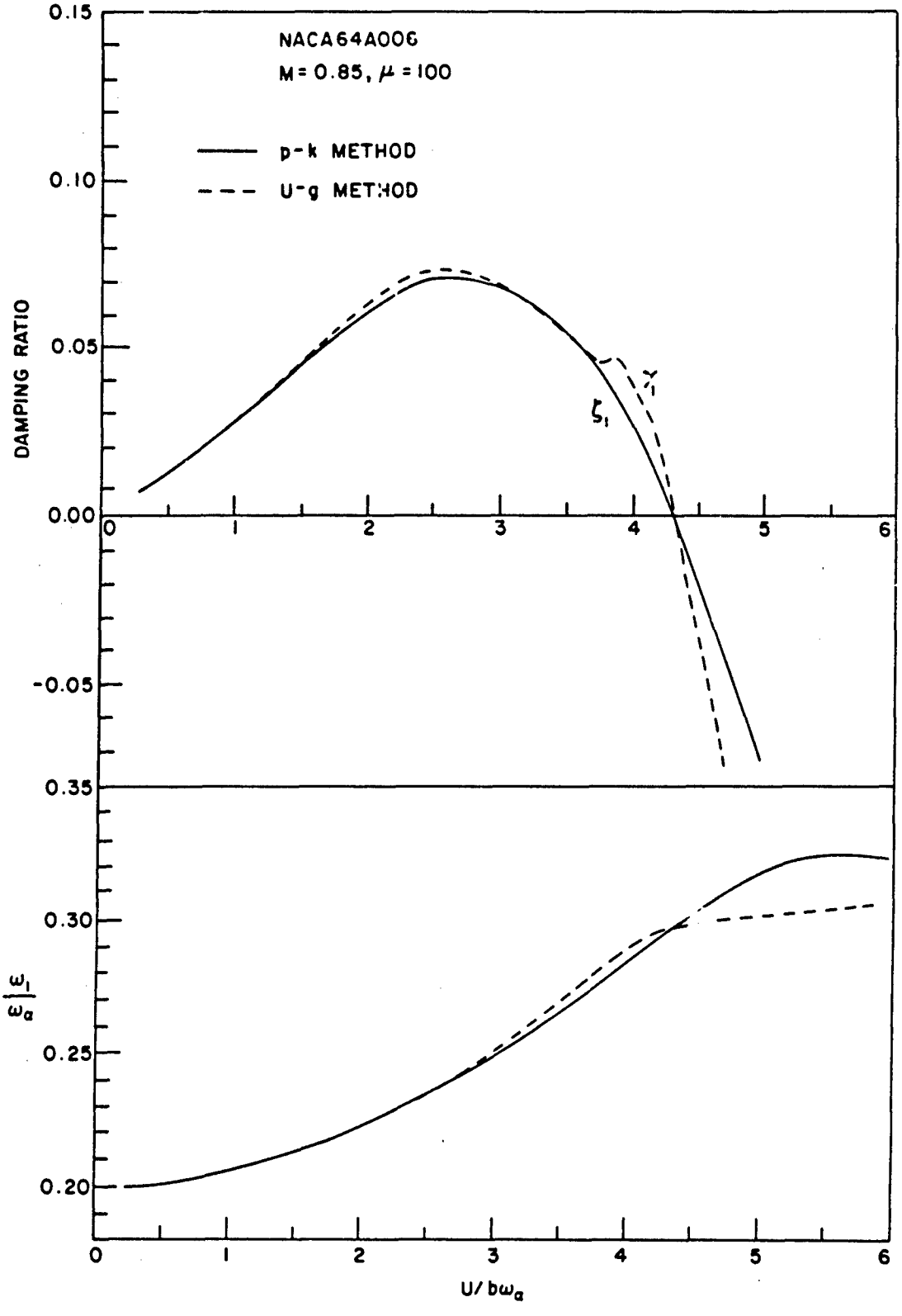

FIG. 25(a): COMPARISON OF DAMPING RATIO AND ω_1/ω_α WITH $U/b\omega_\alpha$ BETWEEN U-g AND p-k METHODS FOR A NACA64A006 AIRFOIL AT M = 0.85 AND μ = 100

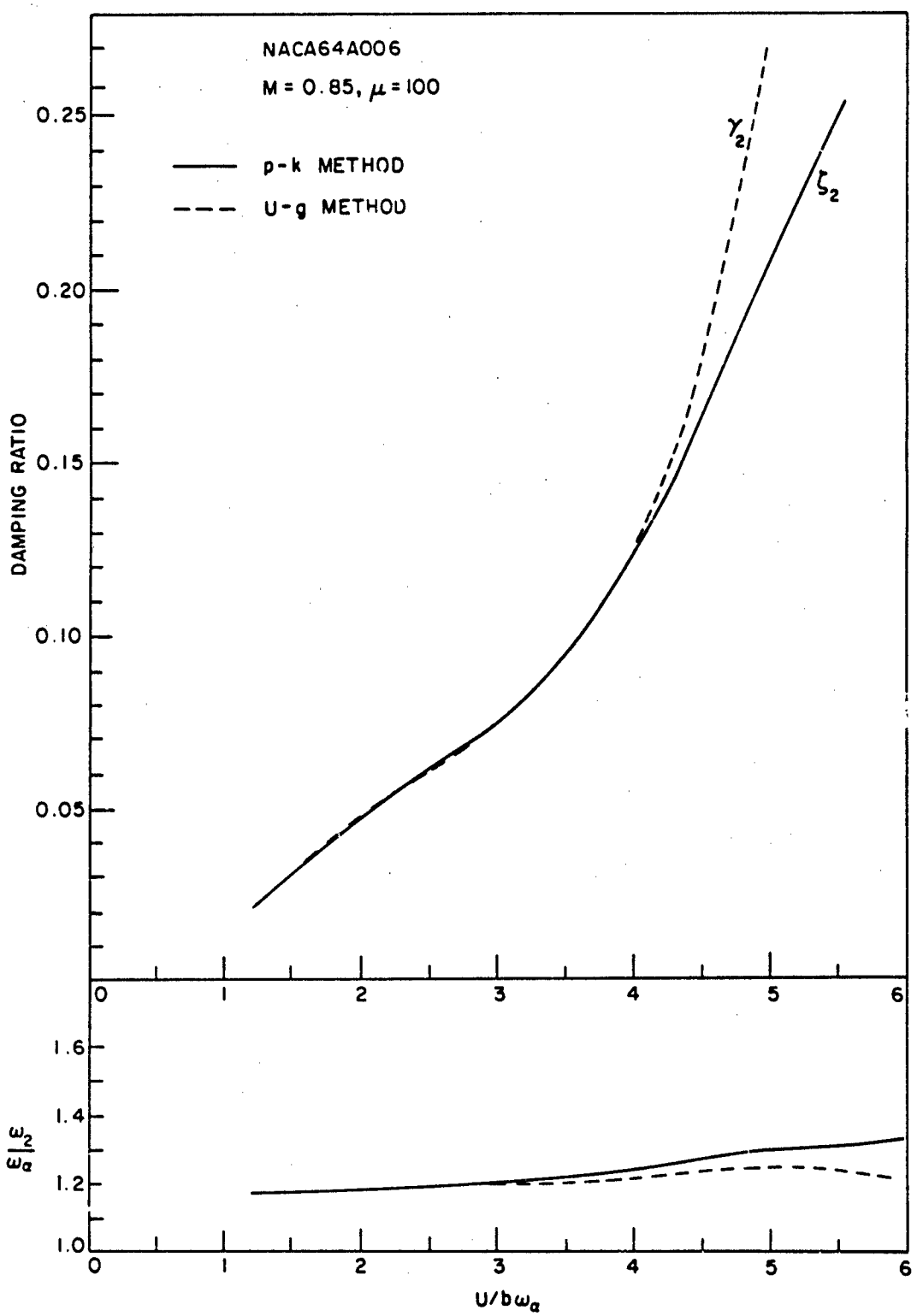

FIG. 25(b): COMPARISON OF DAMPING RATIO AND ω_2/ω_α WITH $U/b\omega_\alpha$ BETWEEN U-g AND p-k METHODS FOR A NACA64A006 AIRFOIL AT M = 0.85 AND μ = 100

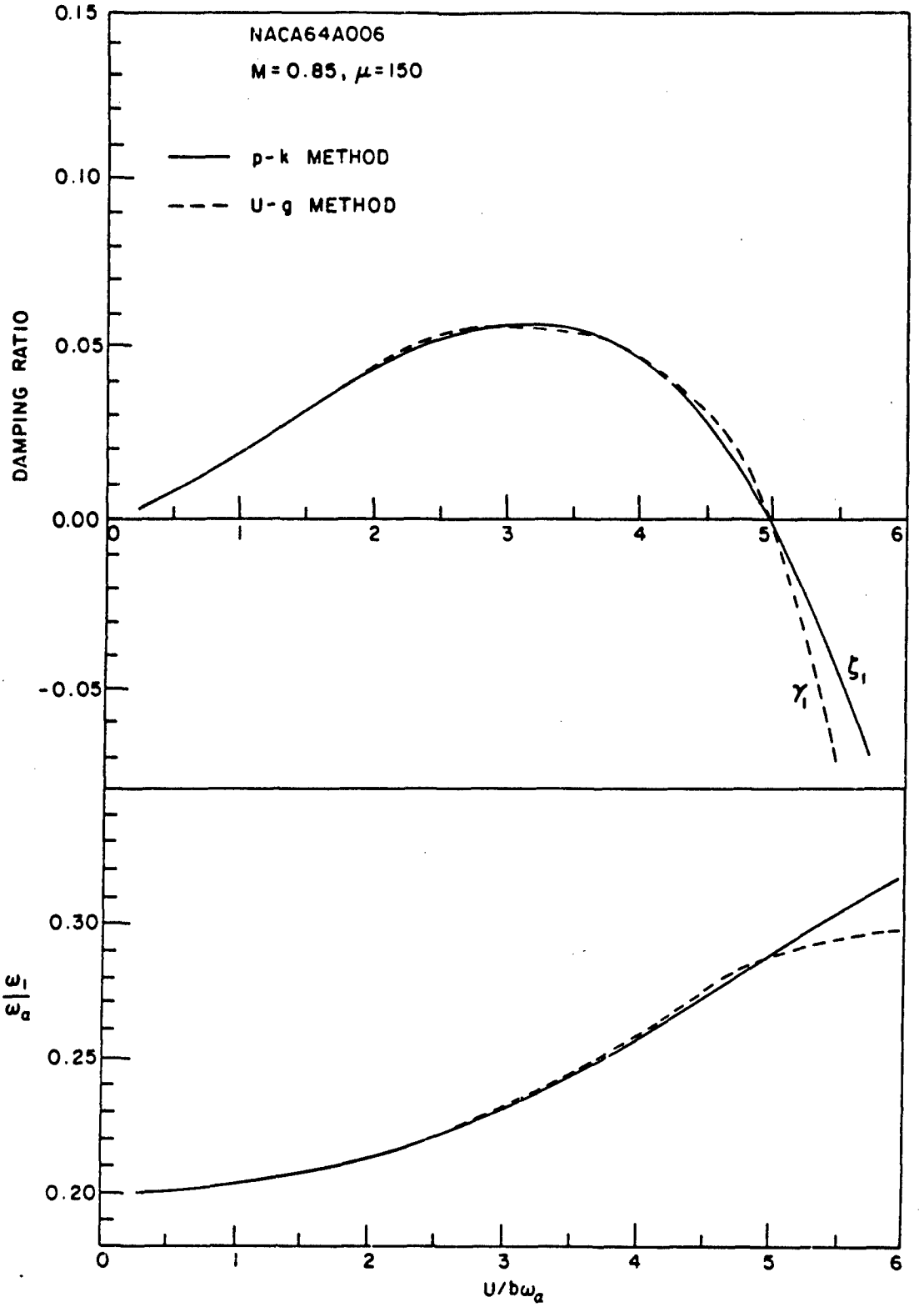

FIG. 26(a): COMPARISON OF DAMPING RATIO AND ω_1/ω_α WITH $U/b\omega_\alpha$ BETWEEN U-g AND p-k METHODS FOR A NACA64A006 AIRFOIL AT M = 0.85 AND μ = 150

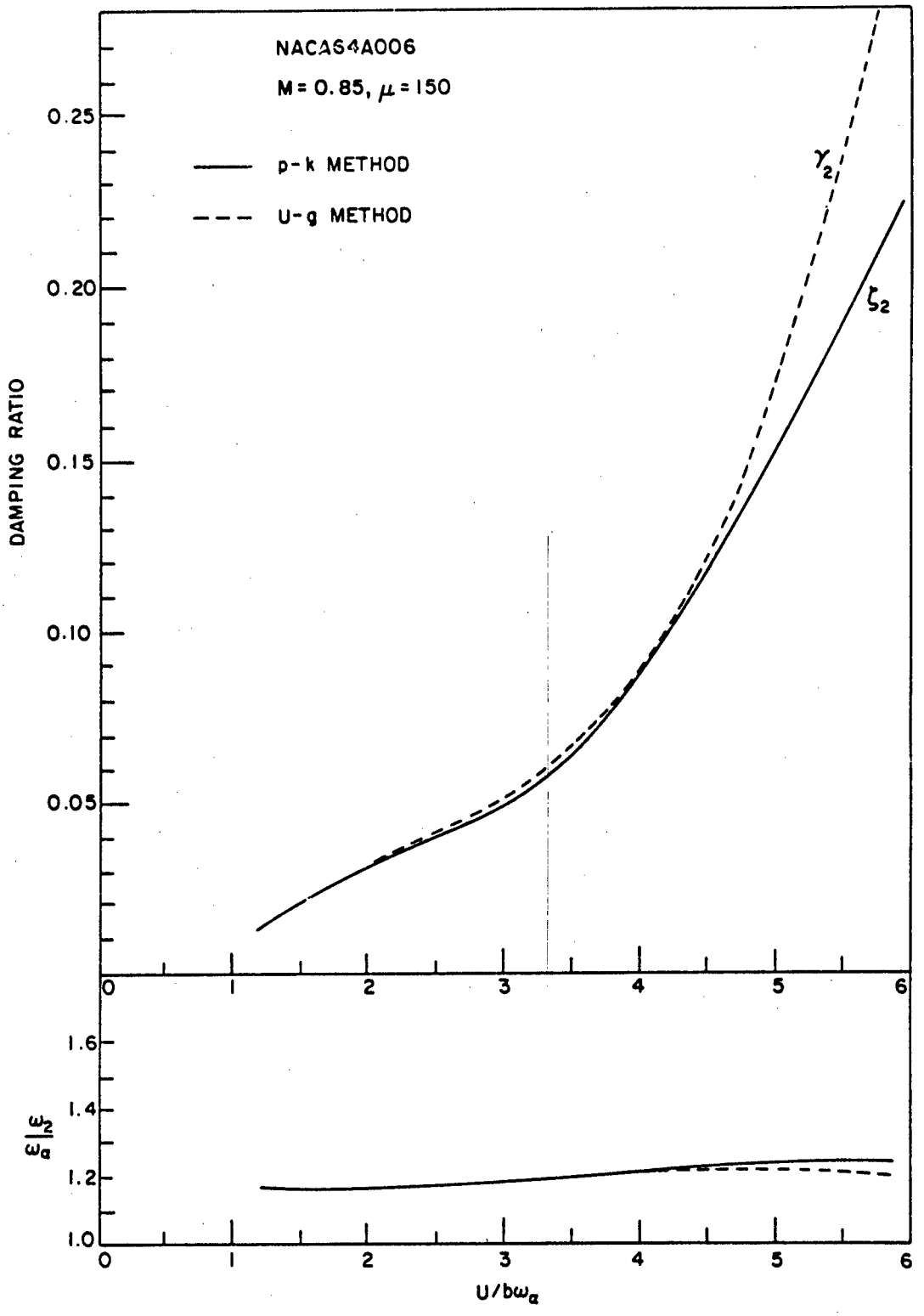

FIG. 26(b): COMPARISON OF DAMPING RATIO AND ω_2/ω_α WITH $U/b\omega_\alpha$ BETWEEN U-g AND p-k METHODS FOR A NACA64A006 AIRFOIL AT M = 0.85 AND μ = 150

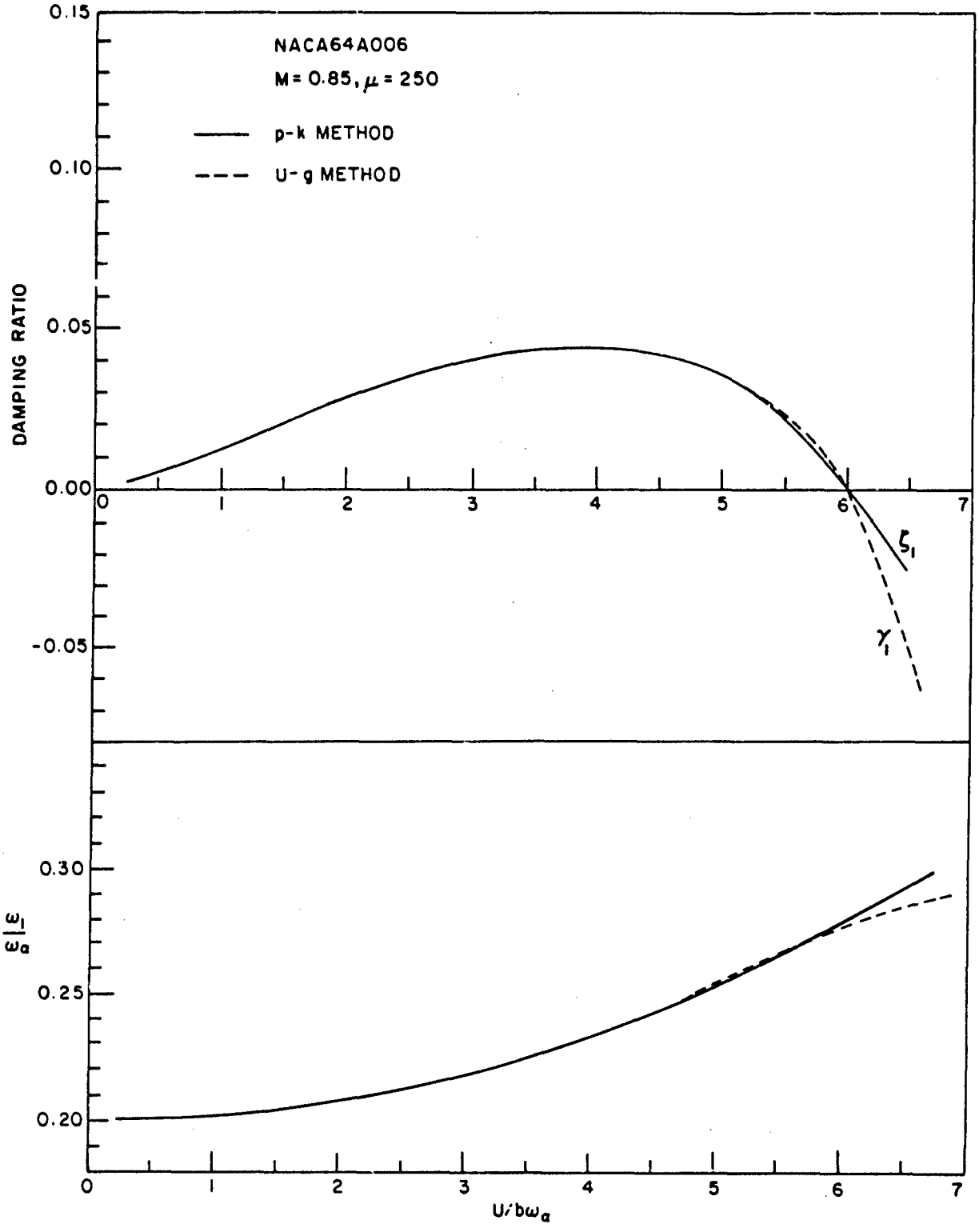

FIG. 27(a): COMPARISON OF DAMPING RATIO AND ω_1/ω_α WITH $U/b\omega_\alpha$ BETWEEN U-g AND p-k METHODS FOR A NACA64A006 AIRFOIL AT M = 0.85 AND μ = 250

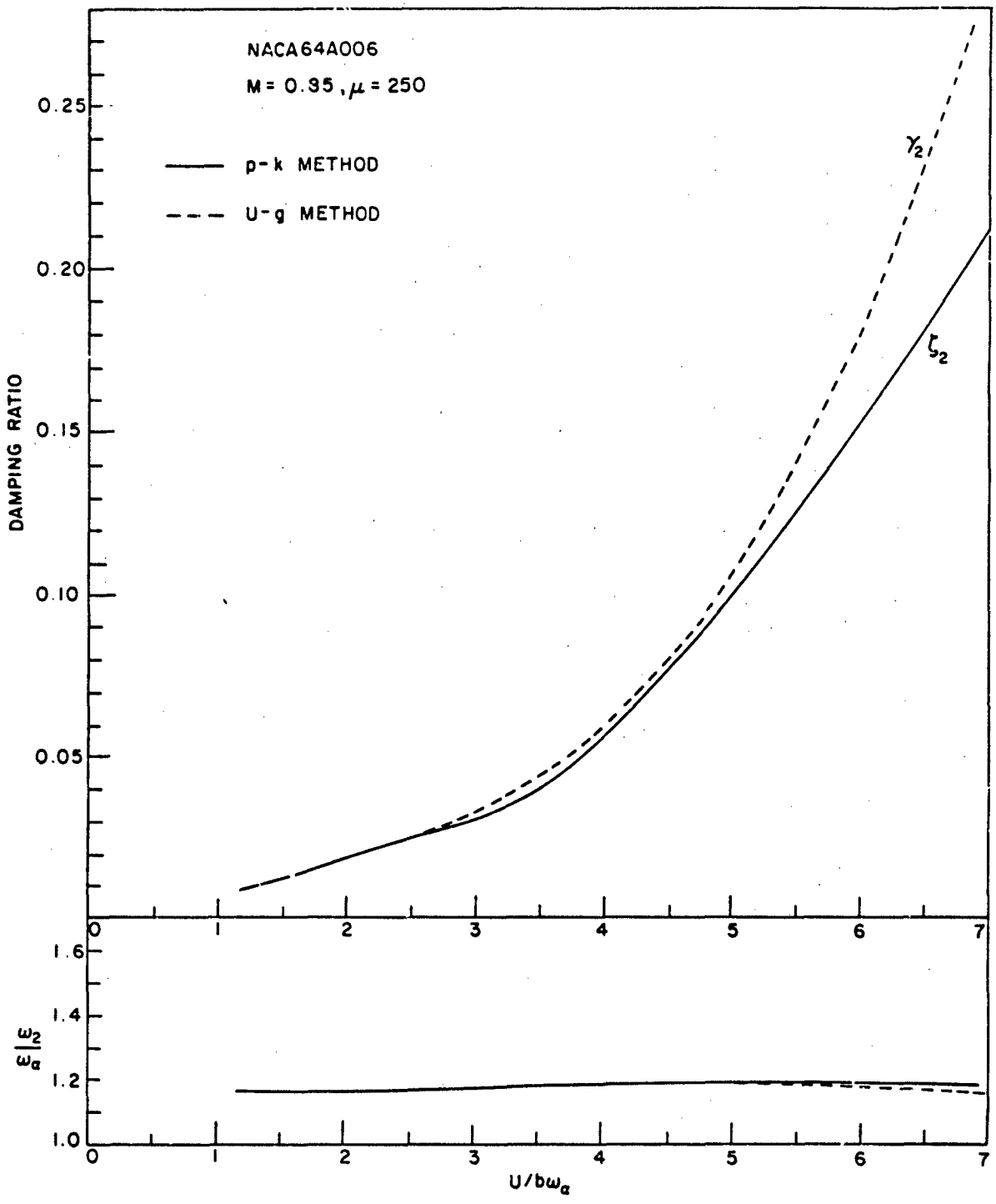

FIG. 27(b): COMPARISON OF DAMPING RATIO AND ω_2/ω_α WITH $U/b\omega_\alpha$ BETWEEN U-g AND p-k METHODS FOR A NACA64A006 AIRFOIL AT M = 0.85 AND μ = 250

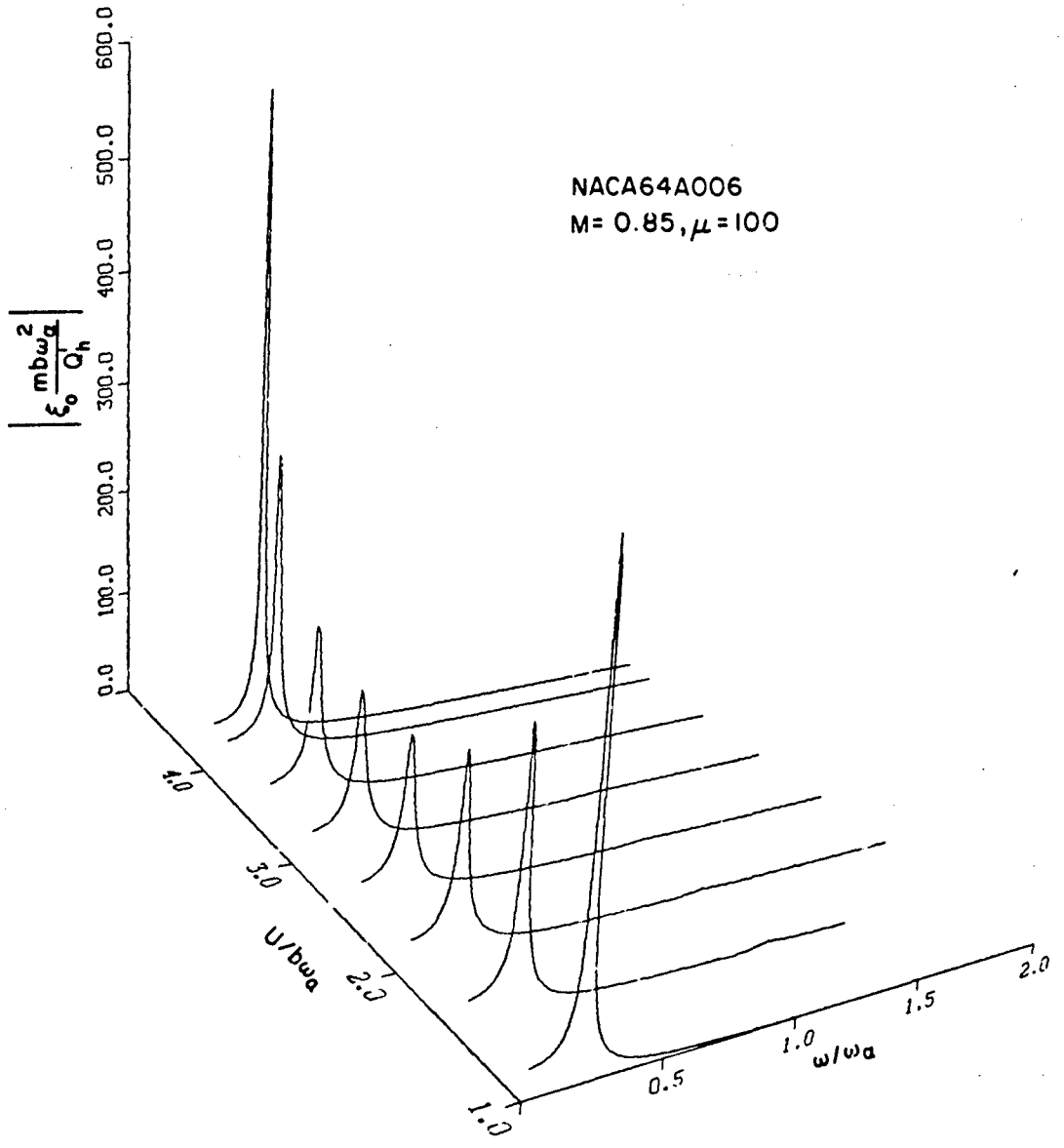

FIG. 28: VARIATION OF AMPLITUDE OF DISPLACEMENT RESPONSE WITH $U/b\omega_\alpha$ AND ω/ω_α FOR AN EXTERNALLY APPLIED SINUSOIDAL FORCE

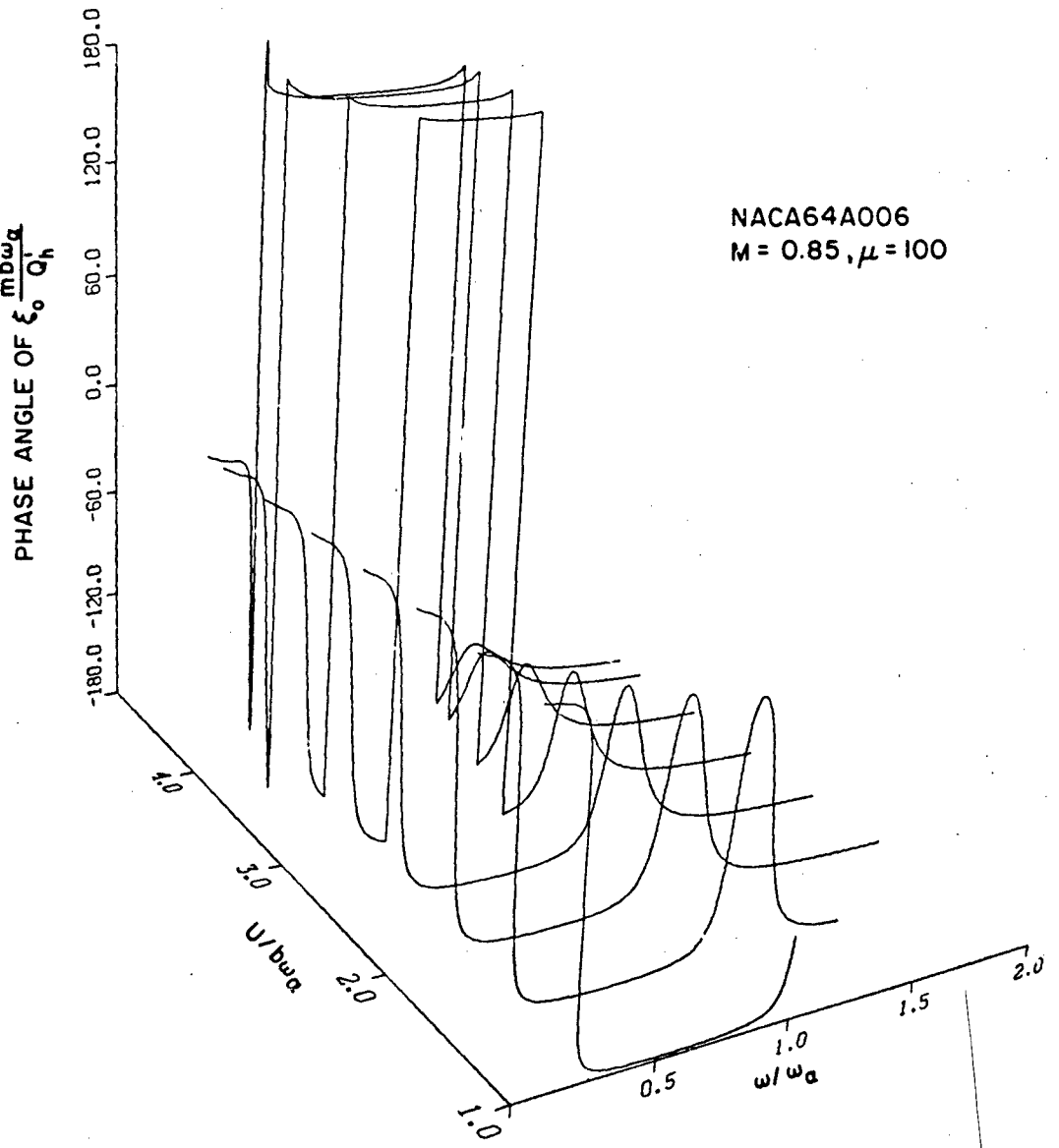

FIG. 29: VARIATION OF PHASE ANGLE OF DISPLACEMENT RESPONSE WITH $U/b\omega_\alpha$ AND ω/ω_α FOR AN EXTERNALLY APPLIED SINUSOIDAL FORCE

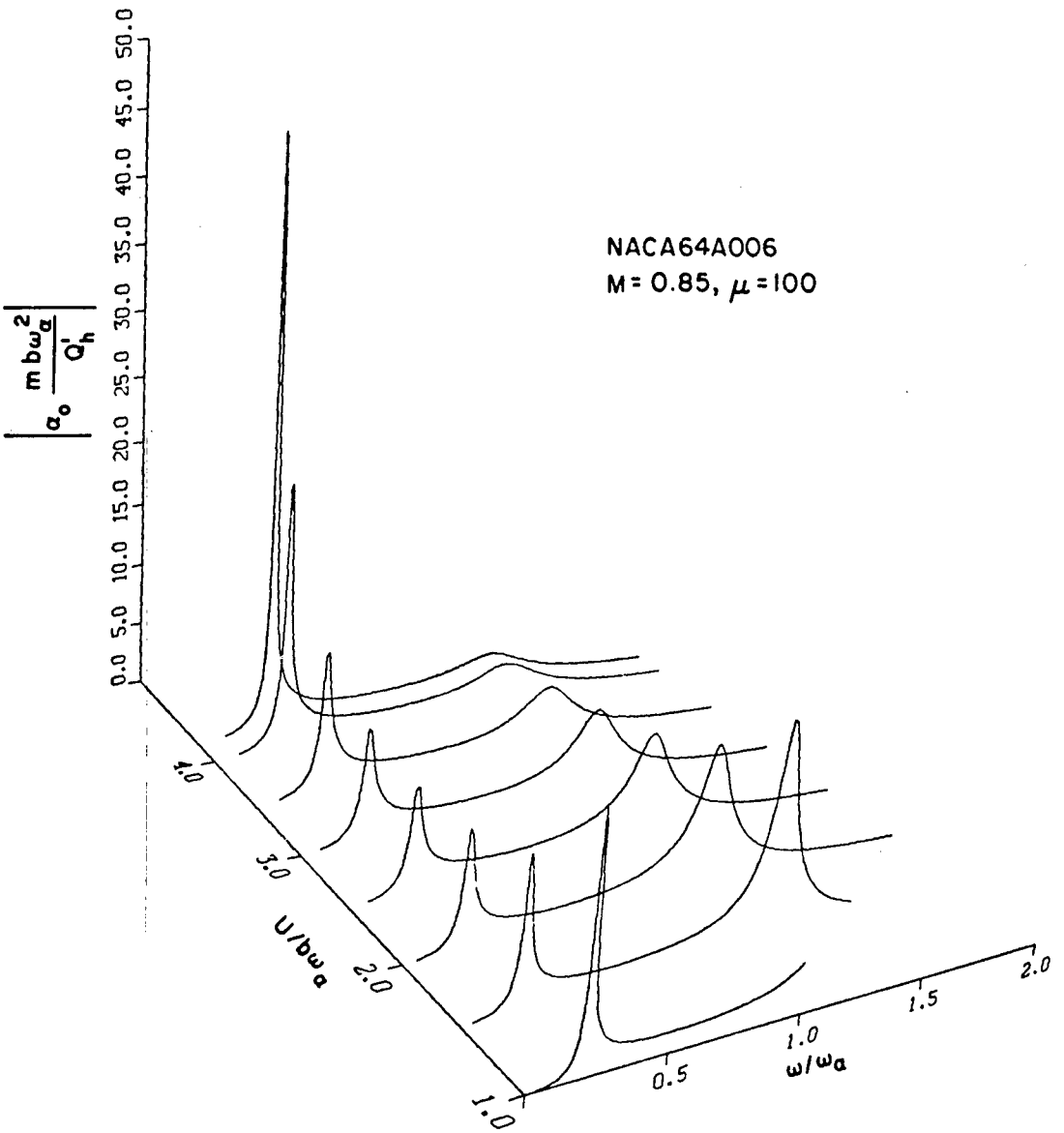

FIG. 30: VARIATION OF AMPLITUDE OF PITCH RESPONSE WITH $U/b\omega_\alpha$ AND ω/ω_α FOR AN EXTERNALLY APPLIED SINUSOIDAL FORCE

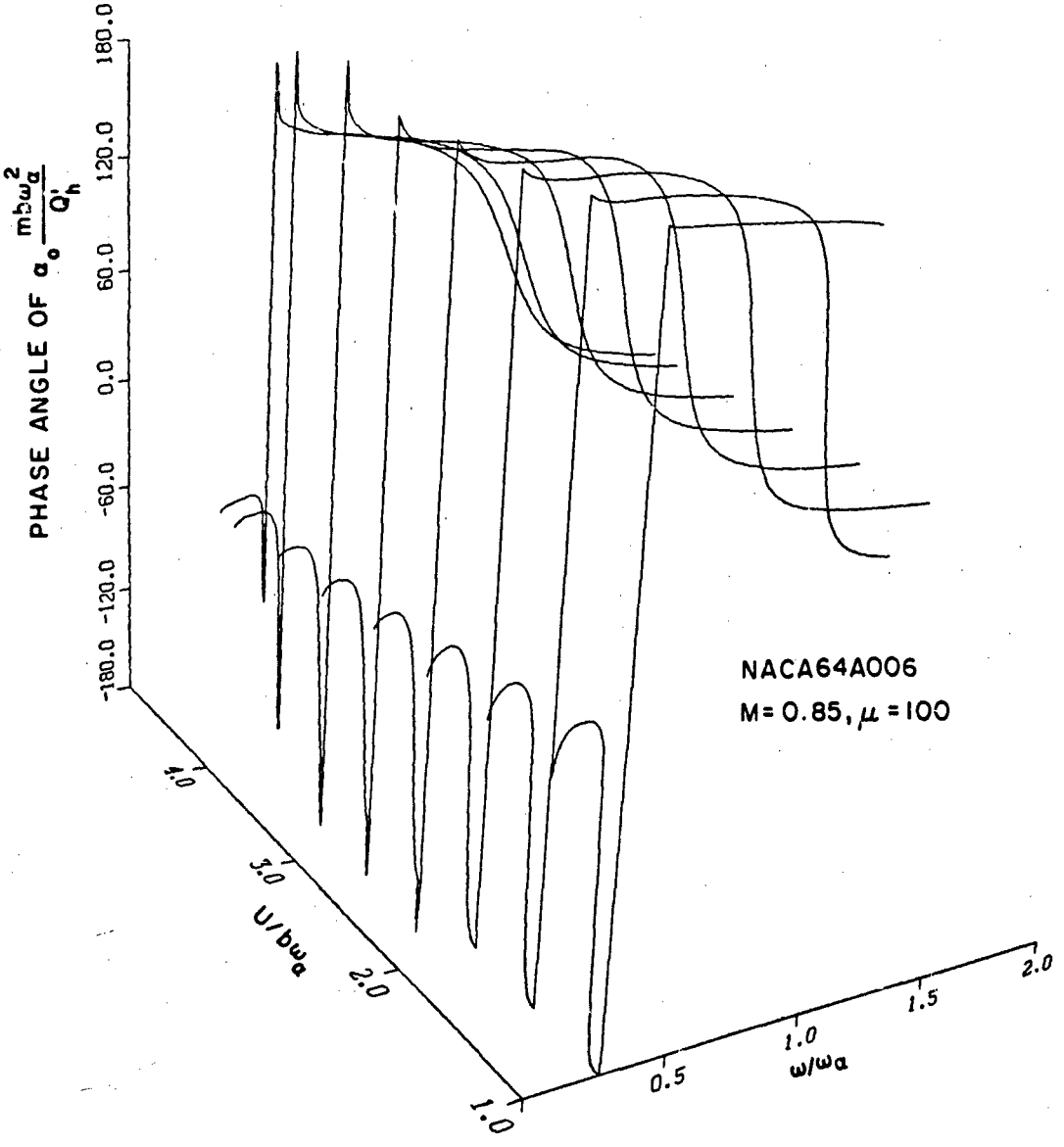

FIG. 31: VARIATION OF PHASE ANGLE OF PITCH RESPONSE WITH $U/b\omega_\alpha$ AND ω/ω_α FOR AN EXTERNALLY APPLIED SINUSOIDAL FORCE

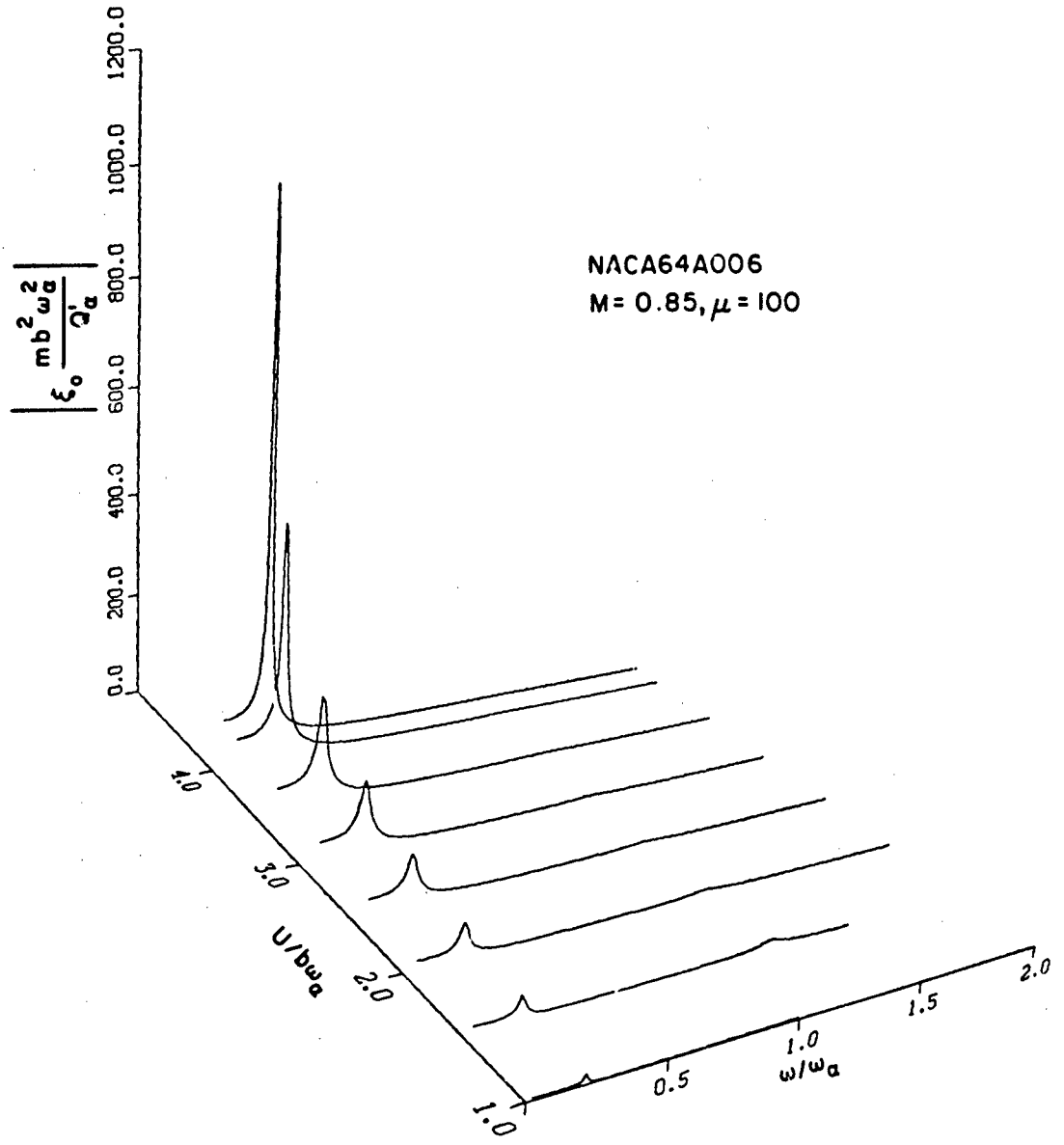

FIG. 32: VARIATION OF AMPLITUDE OF DISPLACEMENT RESPONSE WITH $U/b\omega_\alpha$ AND ω/ω_α FOR AN EXTERNALLY APPLIED SINUSOIDAL MOMENT AT ELASTIC AXIS

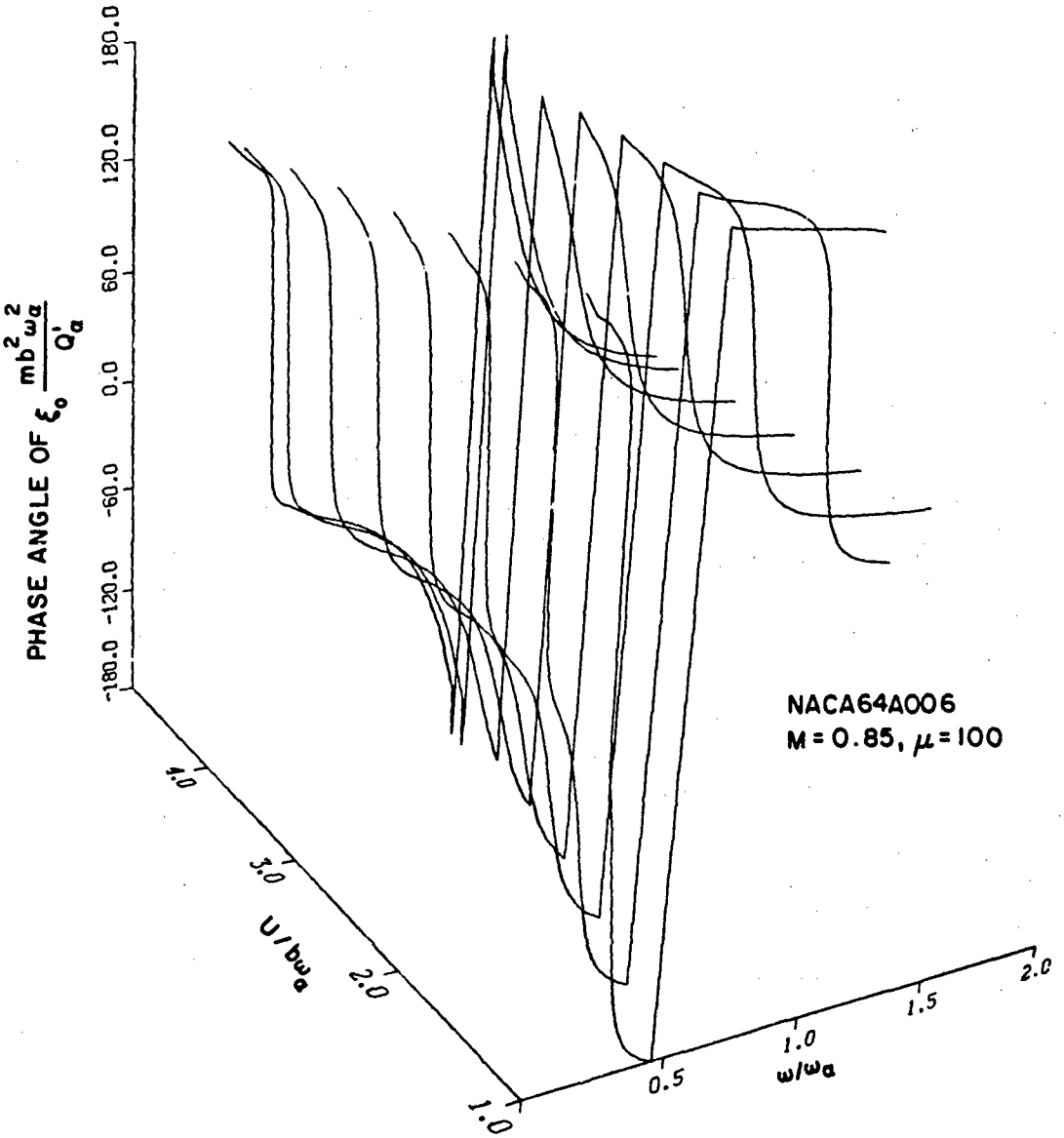

FIG. 33: VARIATION OF PHASE ANGLE OF DISPLACEMENT RESPONSE WITH $U/b\omega_\alpha$ AND ω/ω_α FOR AN EXTERNALLY APPLIED SINUSOIDAL MOMENT AT ELASTIC AXIS

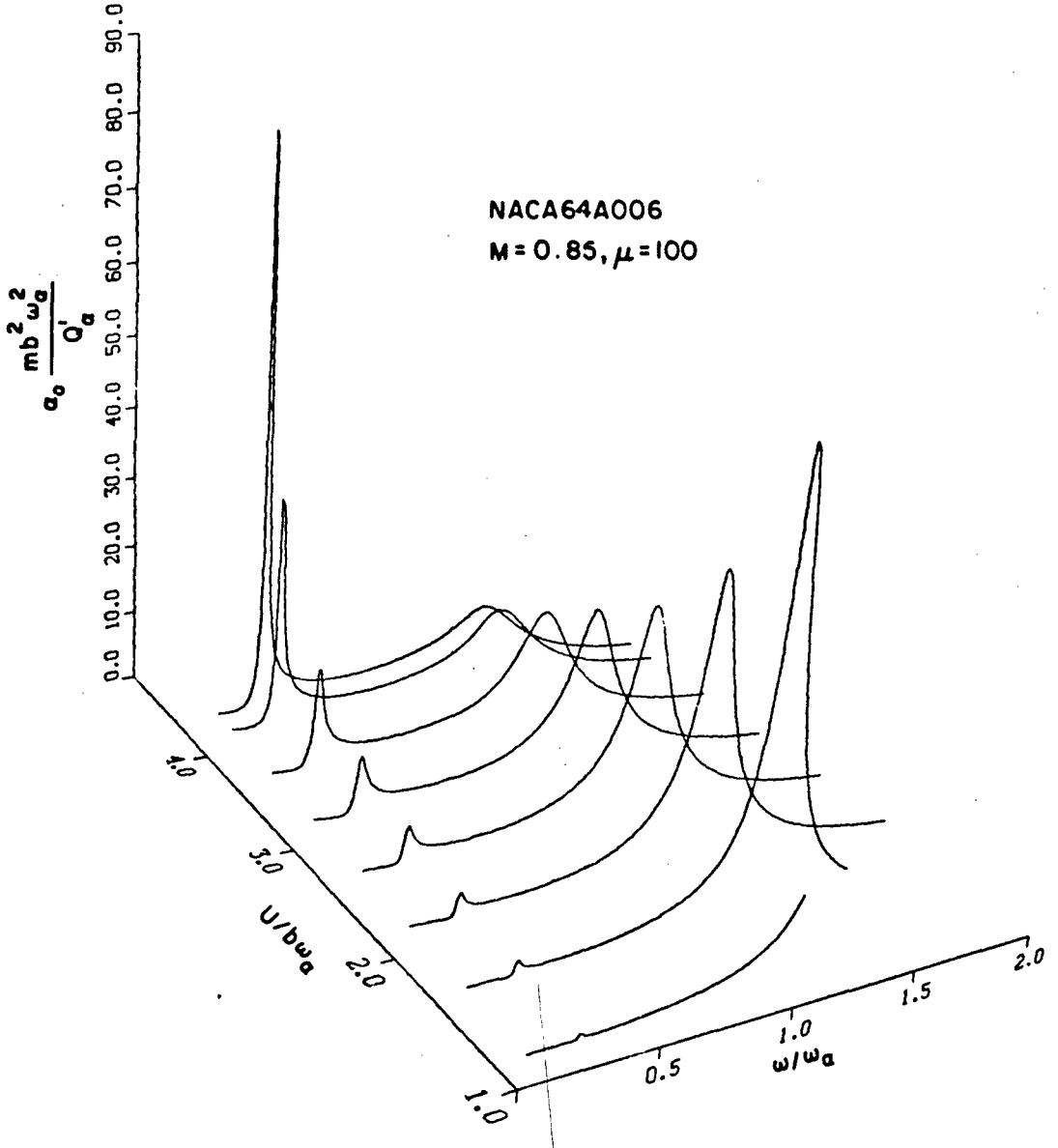

FIG. 34: VARIATION OF AMPLITUDE OF PITCH RESPONSE WITH $U/b\omega_\alpha$ AND ω/ω_α FOR AN EXTERNALLY APPLIED SINUSOIDAL MOMENT AT ELASTIC AXIS

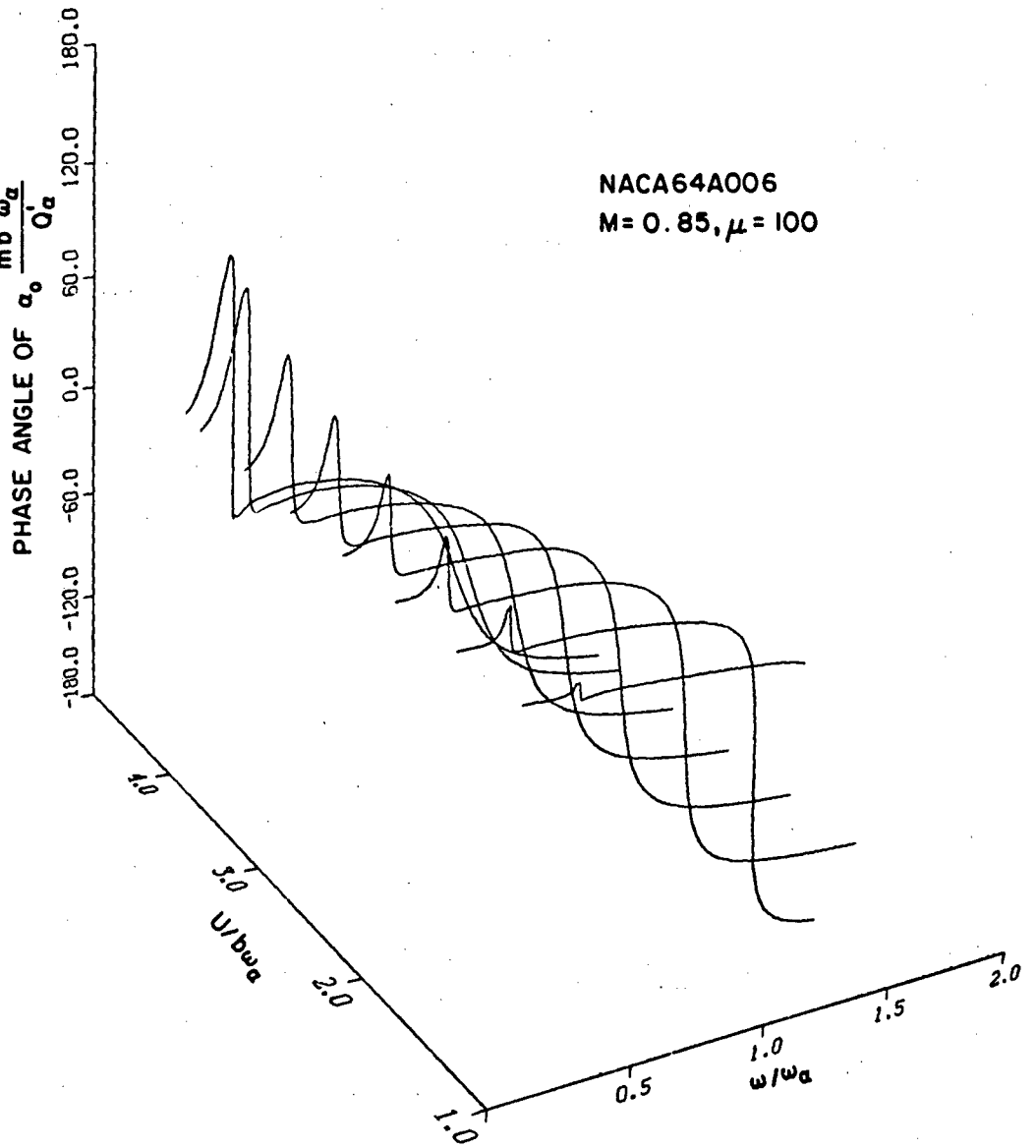

FIG. 35: VARIATION OF PHASE ANGLE OF PITCH RESPONSE WITH $U/b\omega_\alpha$ AND ω/ω_α FOR AN EXTERNALLY APPLIED SINUSOIDAL MOMENT AT ELASTIC AXIS

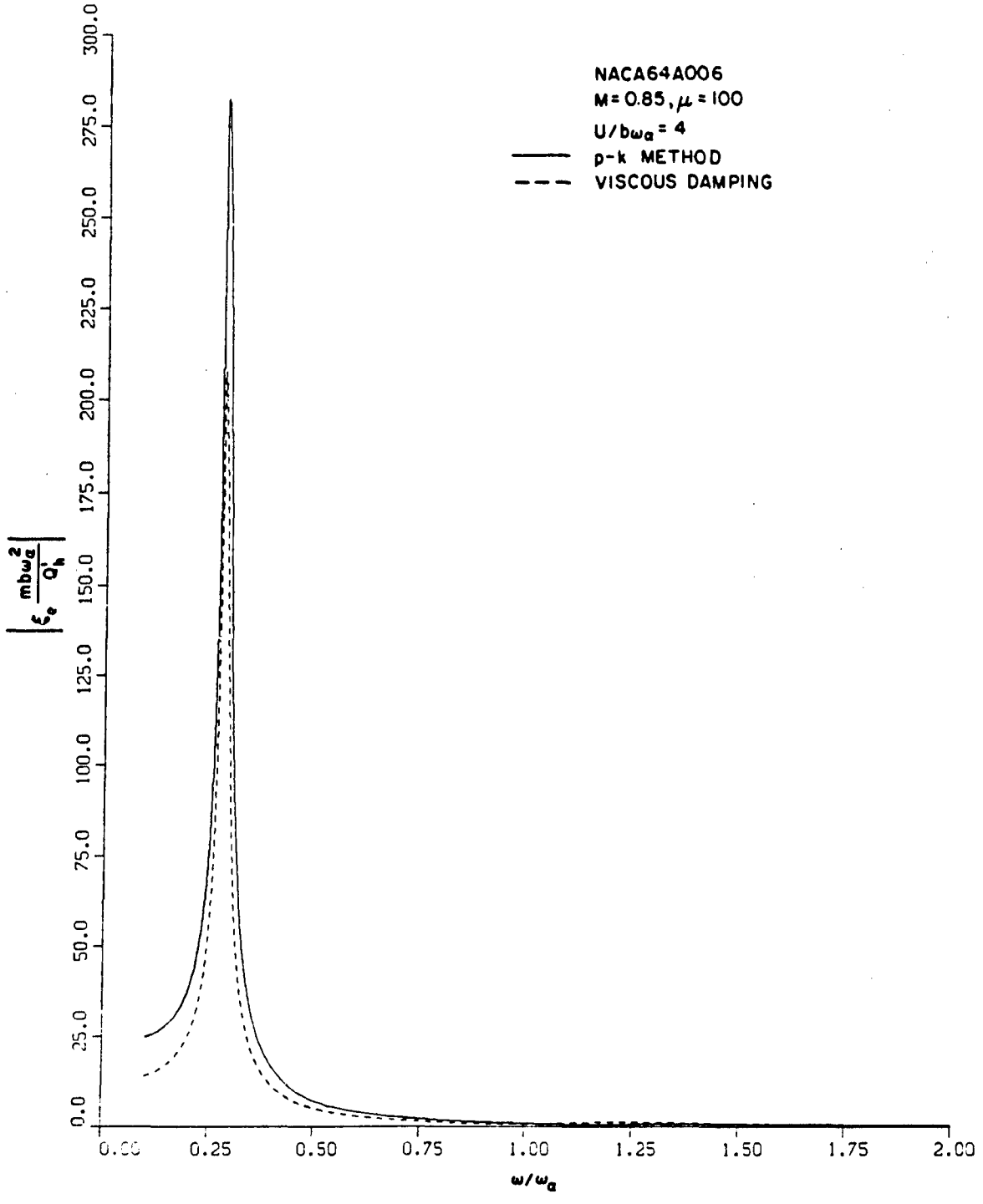

FIG. 36: COMPARISON OF AMPLITUDE OF DISPLACEMENT RESPONSE BETWEEN VISCOUS DAMPING AND p-k METHODS FOR AN EXTERNALLY APPLIED SINUSOIDAL FORCE

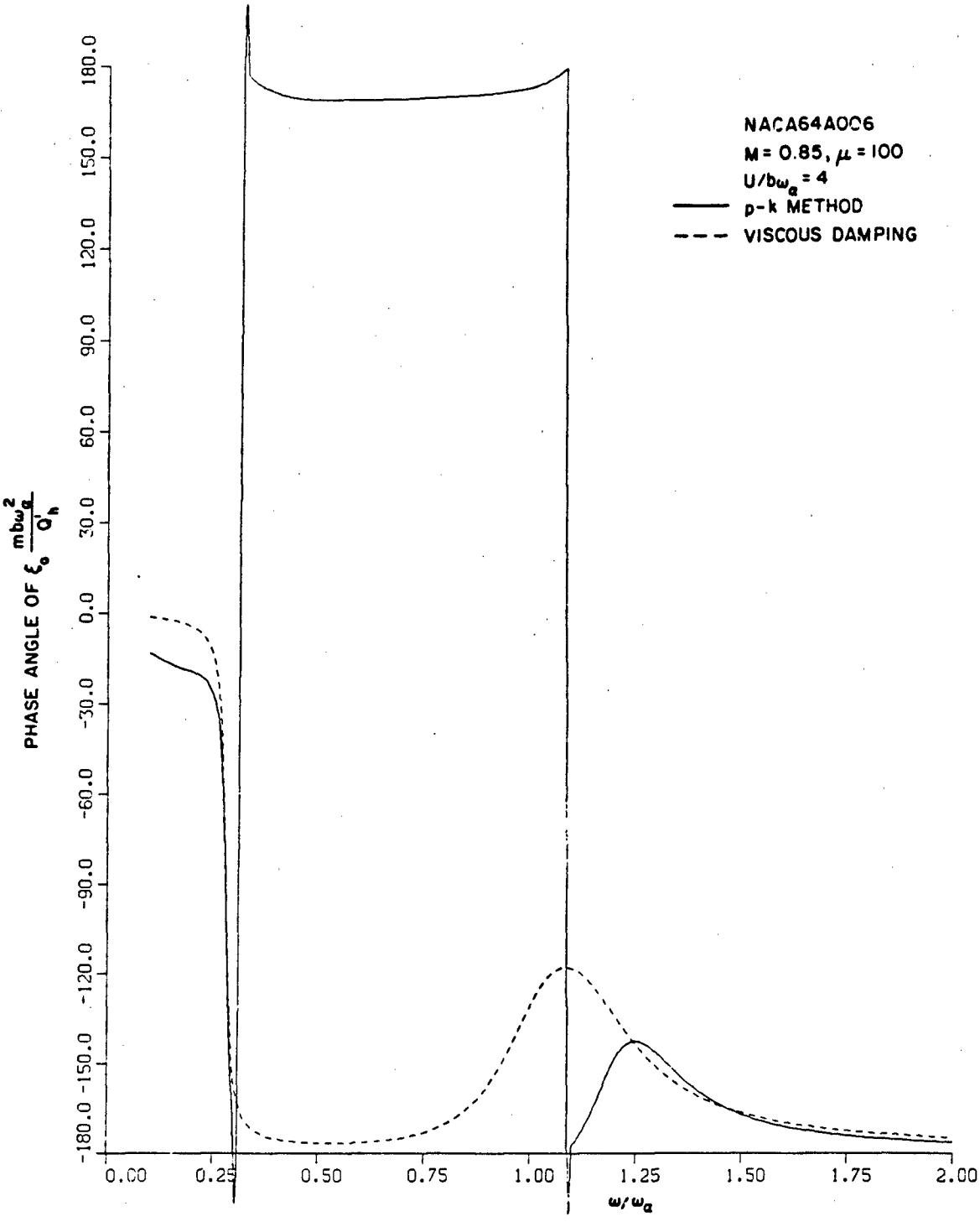

FIG. 37: COMPARISON OF PHASE ANGLE OF DISPLACEMENT RESPONSE BETWEEN VISCOUS DAMPING AND p-k METHODS FOR AN EXTERNALLY APPLIED SINUSOIDAL FORCE

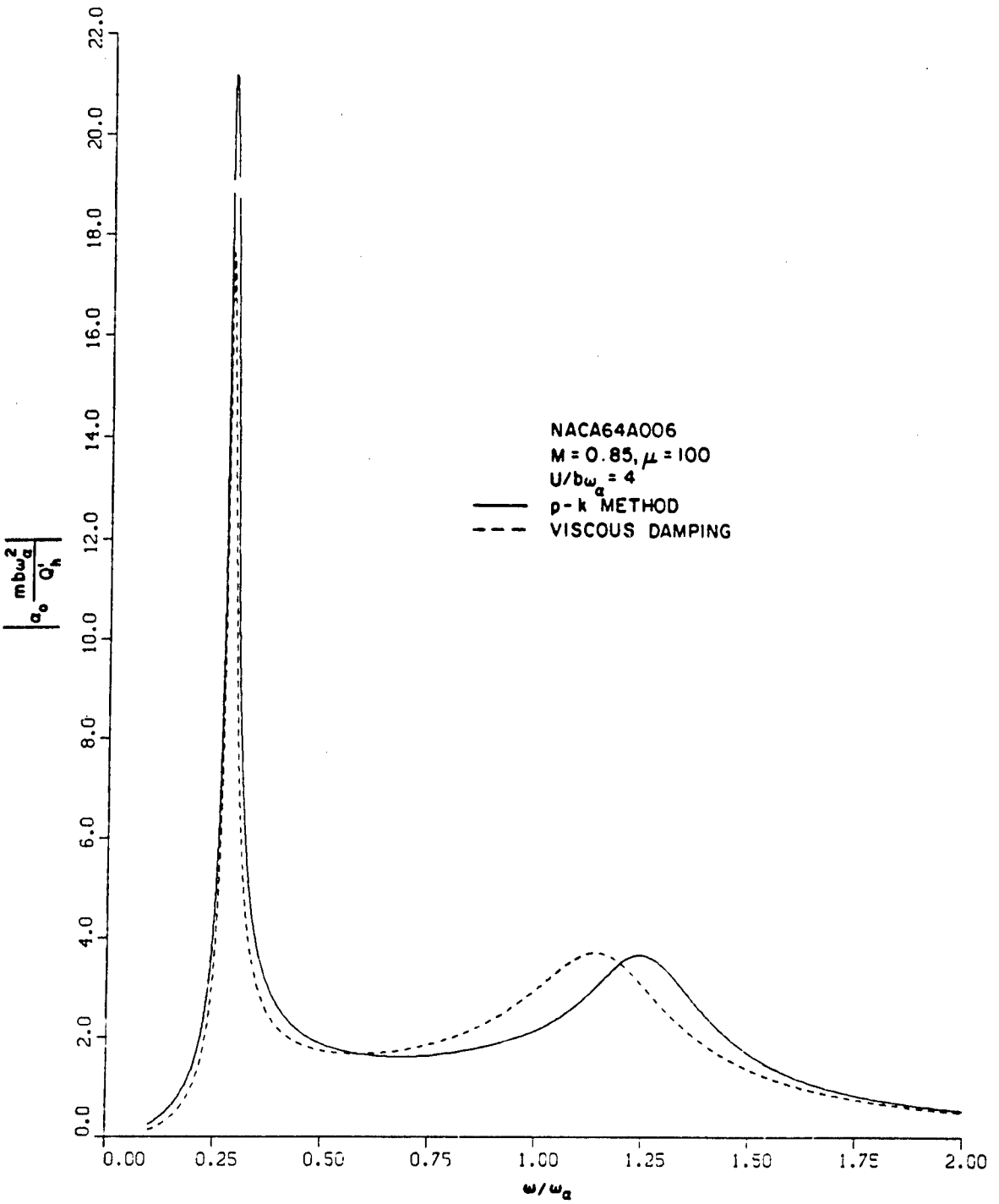

FIG. 38: COMPARISON OF AMPLITUDE OF PITCH RESPONSE BETWEEN VISCOUS DAMPING AND p-k METHODS FOR AN EXTERNALLY APPLIED SINUSOIDAL FORCE

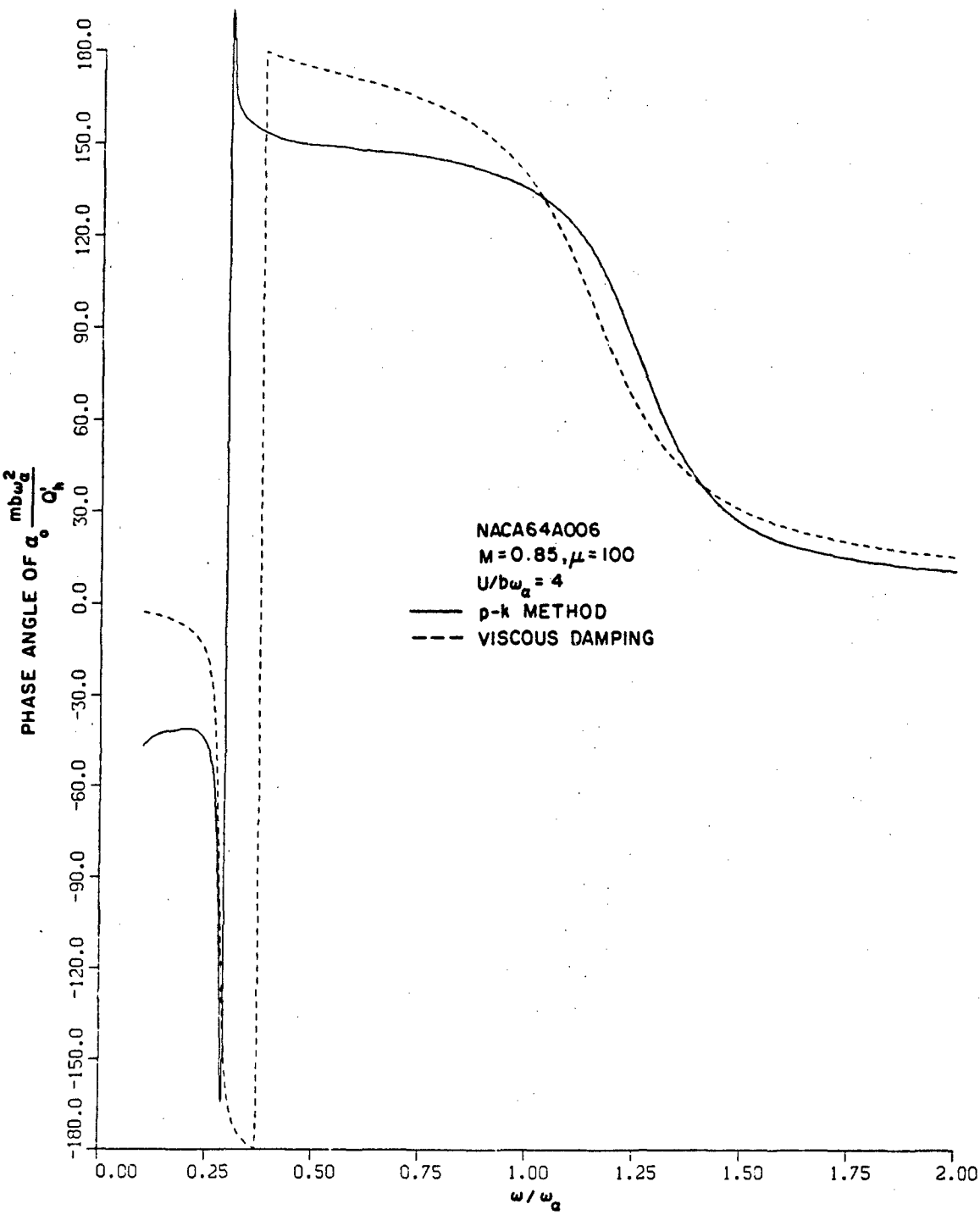

FIG. 39: COMPARISON OF PHASE ANGLE OF PITCH RESPONSE BETWEEN VISCOUS DAMPING AND p-k METHODS FOR AN EXTERNALLY APPLIED SINUSOIDAL FORCE

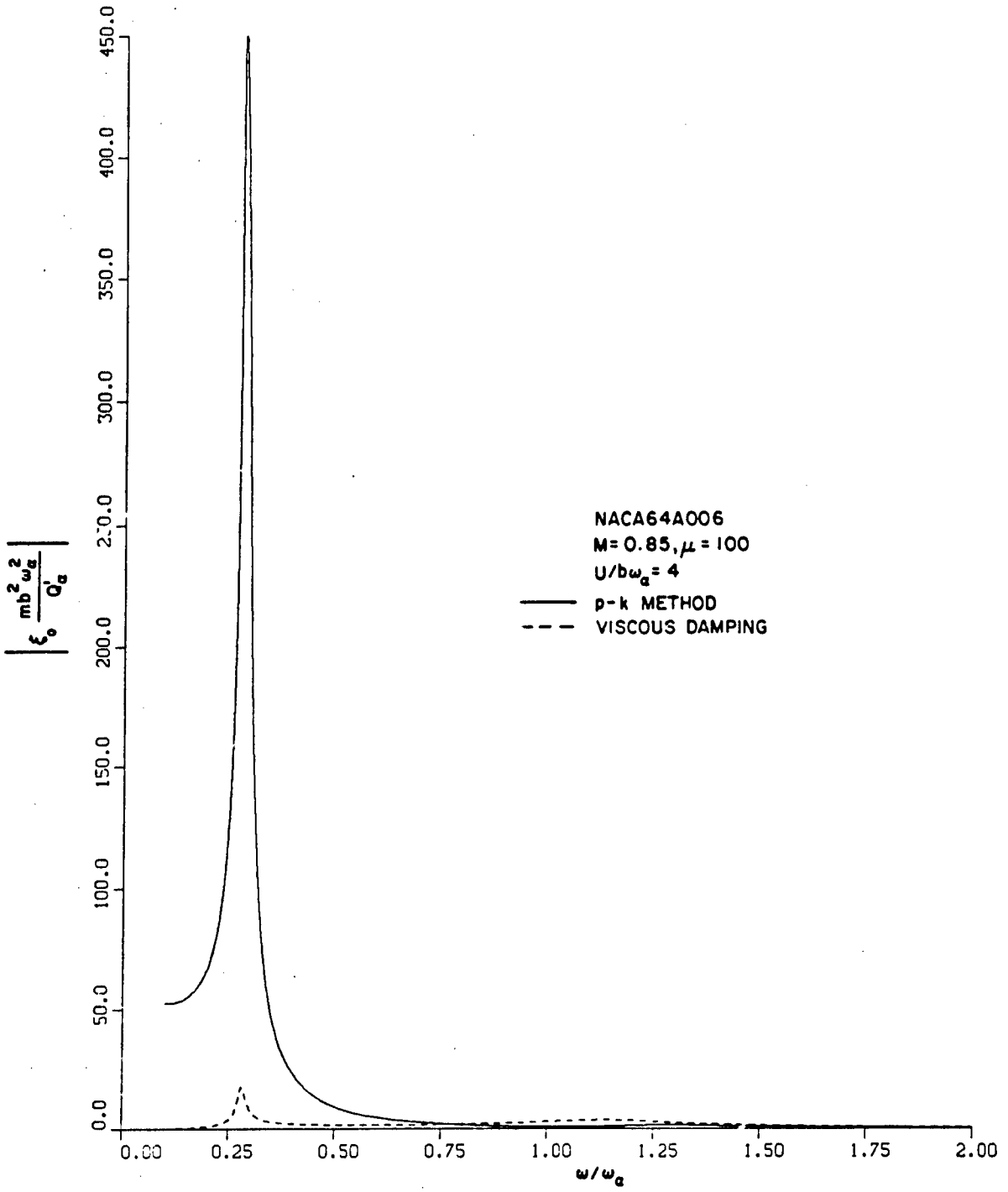

FIG. 40: COMPARISON OF AMPLITUDE OF DISPLACEMENT RESPONSE BETWEEN VISCOUS DAMPING AND p-k METHODS FOR AN EXTERNALLY APPLIED SINUSOIDAL MOMENT AT ELASTIC AXIS

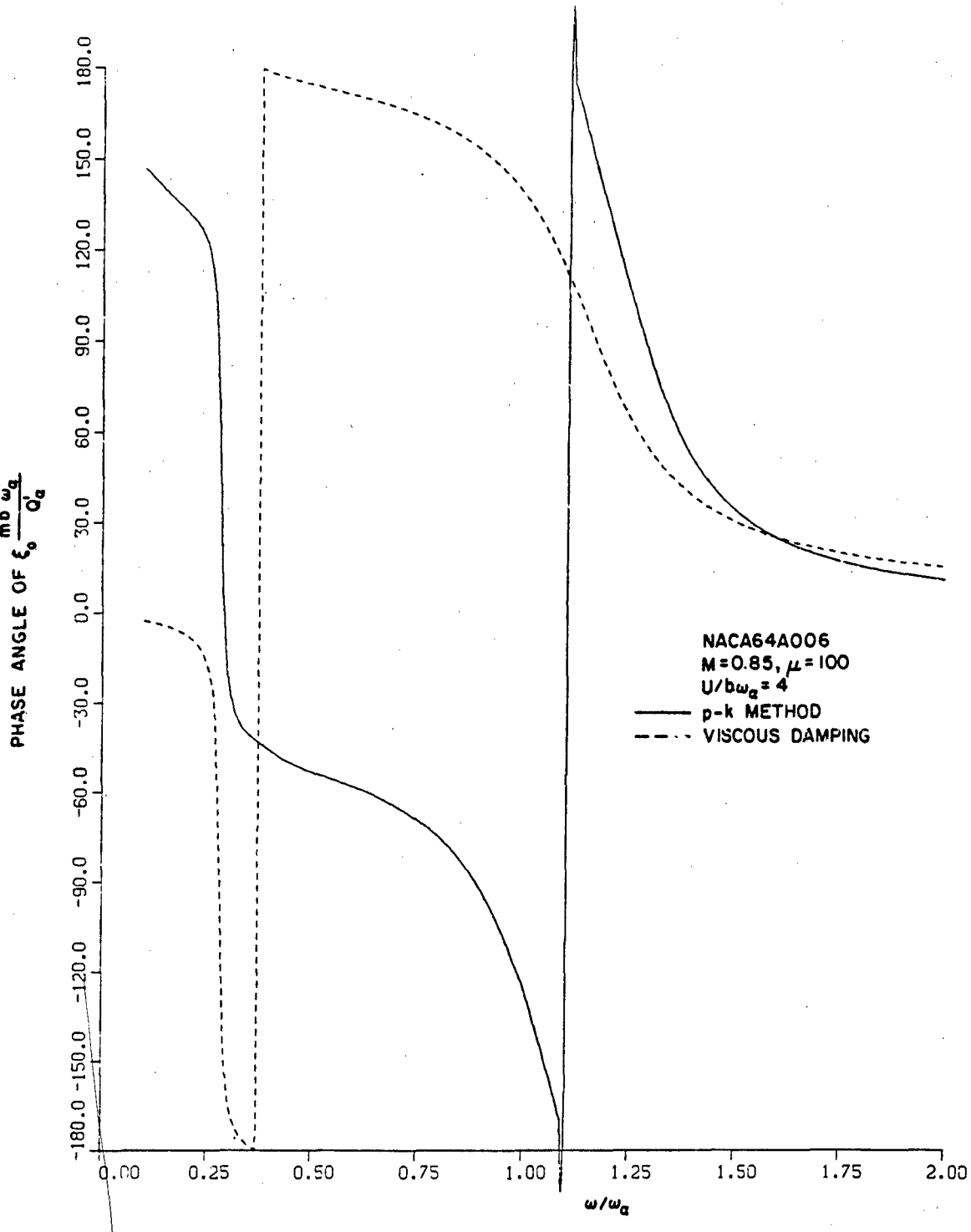

FIG. 41: COMPARISON OF PHASE ANGLE OF DISPLACEMENT RESPONSE BETWEEN VISCOUS DAMPING AND p-k METHODS FOR AN EXTERNALLY APPLIED SINUSOIDAL MOMENT AT ELASTIC AXIS

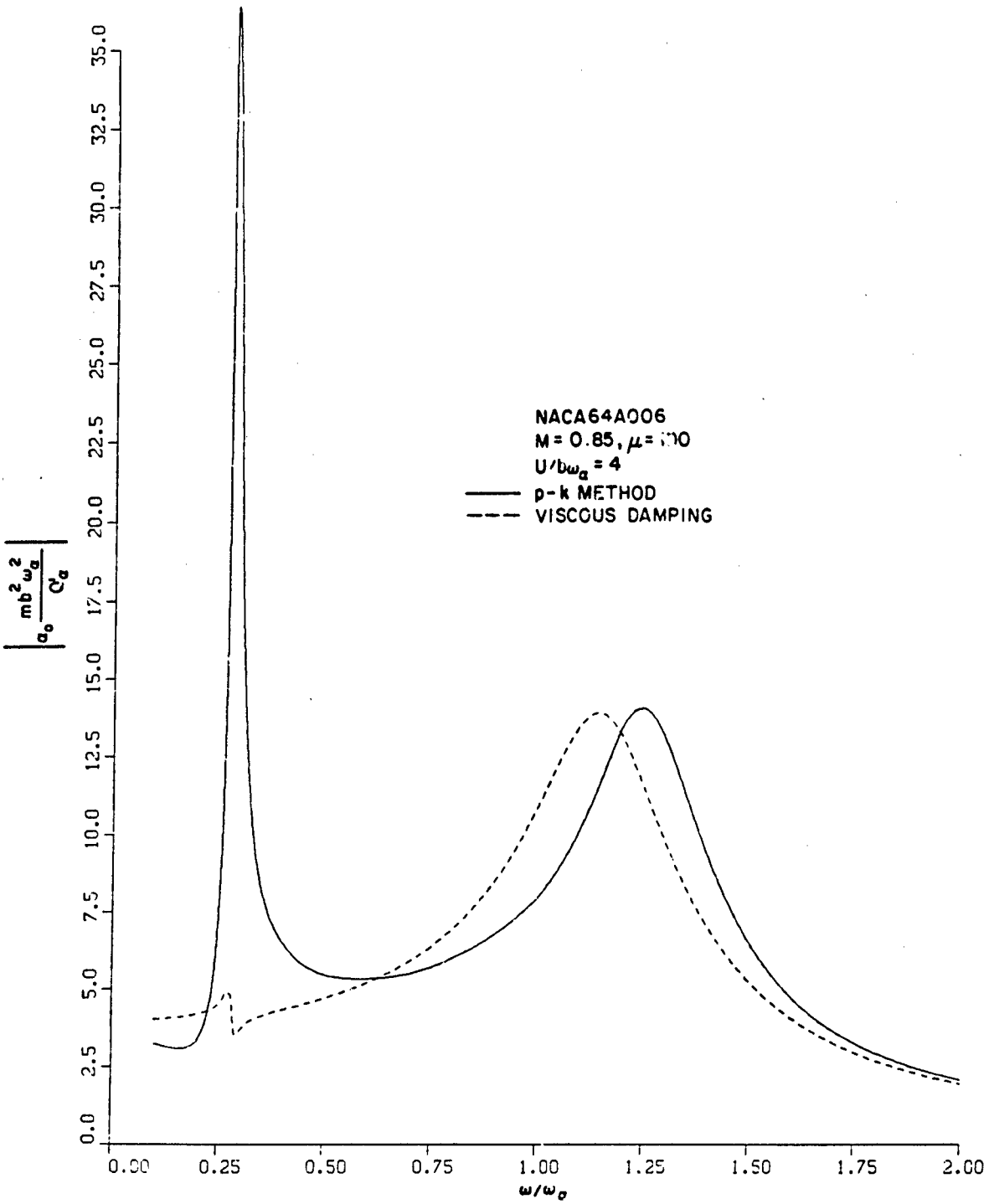

FIG. 42: COMPARISON OF AMPLITUDE OF PITCH RESPONSE BETWEEN VISCOUS DAMPING AND p-k METHODS FOR AN EXTERNALLY APPLIED SINUSOIDAL MOMENT AT ELASTIC AXIS

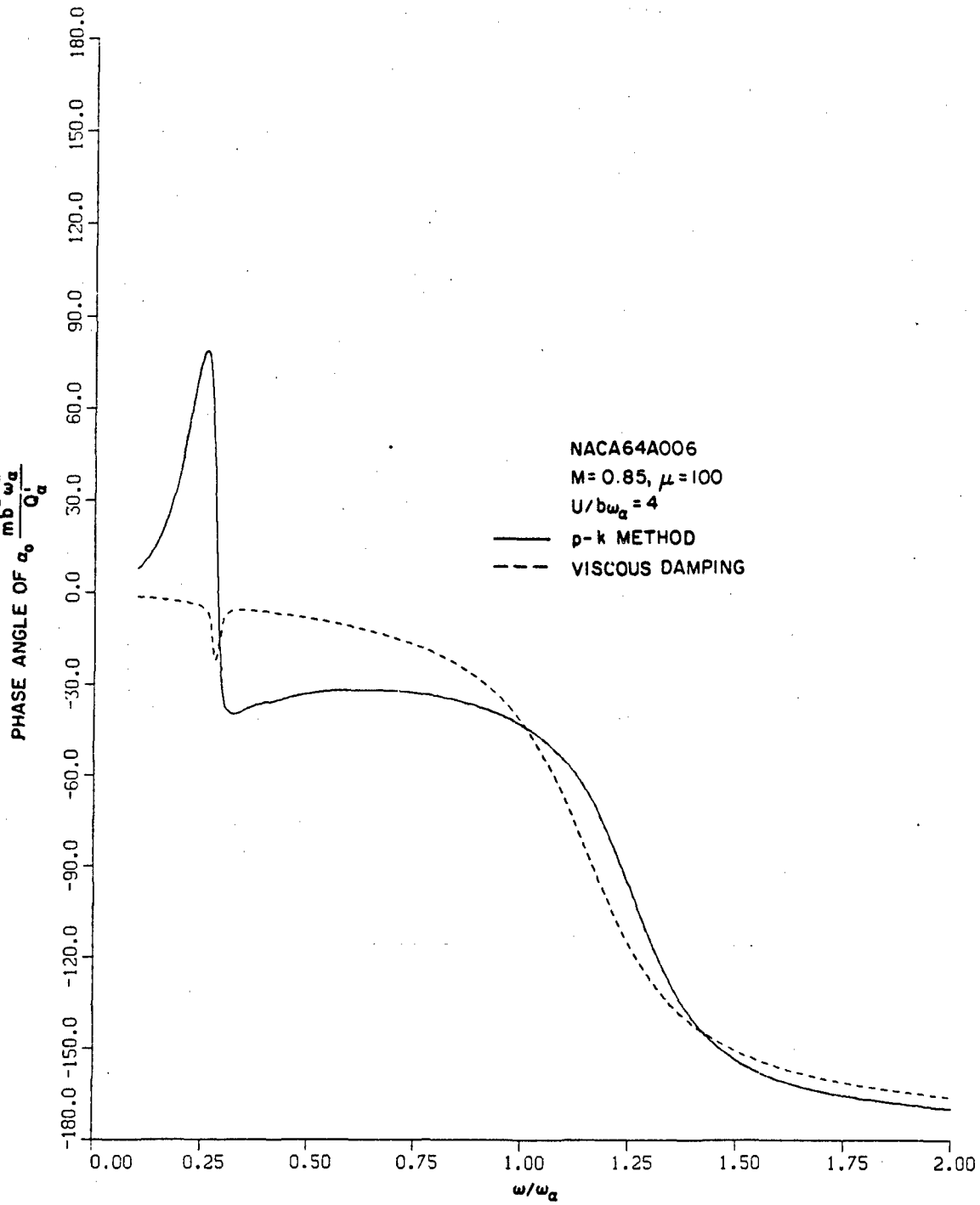

FIG. 43: COMPARISON OF PHASE ANGLE OF PITCH RESPONSE BETWEEN VISCOUS DAMPING AND p-k METHODS FOR AN EXTERNALLY APPLIED SINUSOIDAL MOMENT AT ELASTIC AXIS

REPORT DOCUMENTATION PAGE / PAGE DE DOCUMENTATION DE RAPPORT

REPORT/RAPPORT	REPORT/RAPPORT
LR-615 (1a)	NRC No. 23959 (1b)
REPORT SECURITY CLASSIFICATION / CLASSIFICATION DE SÉCURITÉ DE RAPPORT: Unclassified (2)	DISTRIBUTION (LIMITATIONS): Unlimited (3)

TITLE/SUBTITLE/TITRE/SOUS-TITRE (4)

A Study of Transonic Flutter of a Two-Dimensional Airfoil Using the U-g and p-k Methods

AUTHOR(S)/AUTEUR(S) (5)

B.H.K. Lee

SERIES/SÉRIE (6)

Aeronautical Report

CORPORATE AUTHOR/PERFORMING AGENCY/AUTEUR D'ENTREPRISE/AGENCE D'EXÉCUTION (7)

National Research Council Canada
National Aeronautical Establishment — High Speed Laboratory

SPONSORING AGENCY/AGENCE DE SUBVENTION (8)

DATE (9)	FILE/DOSSIER (10)	LAB. ORDER / COMMANDE DU LAB. (11)	PAGES (12a)	FIGS/DIAGRAMMES (12b)
84-11			69	43

NOTES (13)

DESCRIPTORS (KEY WORDS)/MOTS-CLÉS (14)

1. Transonic Aerodynamics
2. Aerofoils (Transonic)
3. Transonic Flutter

SUMMARY/SOMMAIRE (15)

Transonic flutter of a NACA64A006 airfoil undergoing plunging and pitching oscillations is studied using the U-g and p-k methods. The aerodynamic coefficients are calculated using an improved version of an ONERA unsteady transonic aerodynamics code which include the second time derivative term of the velocity potential in the governing equation. Comparisons with LTRAN2-NLR show good agreement up to and in some cases exceeding k_c = 0.4, except for the pitching moment curves at the transonic dip Mach number of 0.85. All flutter results are presented for M = 0.85. The p-k method gives flutter speeds identical to those from the U-g method. Subcritical damping ratios using the U-g method with Frueh's and Miller's damping formula are quite close to those obtained from the p-k method, especially for large values of the airfoil-air mass ratio. Response of the airfoil to externally applied forces and moments is studied using the p-k method and a viscous damping model for coupled motions.

END

FILMED

4-85

DTIC